universität wien

MASTERARBEIT / MASTER'S THESIS

Titel der Masterarbeit / Title of the Master's Thesis

„Insulin and insulin receptor splice variants and the development of hepatocellular carcinoma“

verfasst von / submitted by

Elisabeth Polster, BSc

angestrebter akademischer Grad / in partial fulfilment of the requirements for the degree of

Master of Science (MSc)

Wien, 2022 / Vienna, 2022

Studienkennzahl lt. Studienblatt / degree programme code as it appears on the student record sheet:	UA 066 834
Studienrichtung lt. Studienblatt / degree programme as it appears on the student record sheet:	Masterstudium Molekulare Biologie
Betreut von / Supervisor:	Ao.Univ.-Prof.in Dr.in Bettina Grasl-Kraupp

Acknowledgements

First of all, I want to thank Univ.-Prof.in Dr.in Bettina Grasl-Kraupp for giving me the opportunity to work on this project for my master thesis.

I want to thank Birgit Mir-Karner and Helga Koudelka for their general support and their helpfulness.

I want to thank my colleagues, especially Christina Papst and Paula Schwarz, who supported me emotionally and always had a sympathetic ear for me. I am extremely thankful to you for your special and warm friendship.

Further, I want to thank my family and my friends for their constant emotional support throughout my university years. You always believed in me and lifted me up.

And most importantly I want to thank my beloved boyfriend, Adrian. You always encouraged me, cheered me up and believed in me. I will be forever grateful and will always carry you in my heart.

Ich habe mich bemüht, sämtliche Inhaber*innen der Bildrechte ausfindig zu machen und ihre Zustimmung zur Verwendung der Bilder in dieser Arbeit eingeholt. Sollte dennoch eine Urheberrechtsverletzung bekannt werden, ersuche ich um Meldung bei mir.

Table of contents

I. Abstract

The development of hepatocellular carcinoma (HCC) is often associated with hyperinsulinemia which suggests an important role of insulin in hepatocarcinogenesis. The present thesis examined the effect of the hormone and the role of insulin-receptor splice variants A and B for the development of a malignant phenotype.

The expression data of insulin-regulated genes were obtained by whole-genome gene expression analyses of rat HCC-prestages and were compared to published expression data of human HCC-prestages. Differentiated dHepaRG™ and undifferentiated HepaRG™ cells served as cell culture models and were treated with insulin. By means of lentiviral gene transfer insulin-receptor-A and -B overexpressing cell lines were established. The hormonal effect on the metabolic gene expression was explored by RT-qPCR and on the malignant phenotype by tests for clonogenicity and migration. Western Blot was performed to detect the nuclear transfer of pyruvate kinase M2 (PKM2).

Several insulin-regulated genes in carbohydrate-, cholesterol-, and fatty acid metabolism and the pentose-phosphate pathway showed overexpression in rat and human HCC-prestages. Insulin induced several of these genes especially in HepaRG™ and partly increased the expression of cancer-specific isoenzymes dHepaRG™. Overexpression of insulin-receptor-B led to enhanced colony formation and cell migration, whereas insulin-receptor-A had no effect. Further, insulin treatment promoted the nuclear transfer of PKM2 in dHepaRG™ and HepaRG™, which might explain the elevated expression of some metabolic genes.

The results indicate that insulin might contribute to hepatocarcinogenesis due to effects on metabolic gene expression and stimulation of PKM2 translocation to the nucleus. Insulin-receptor-B may mediate the development of a malignant phenotype.

II. Introduction

II.1 Hepatocellular Carcinoma (HCC)

Liver cancer occupies place four in the ranking of cancer-related deaths worldwide and ranks sixth with regard to new cases per year (Craig *et al.,* 2020). Hepatocellular carcinoma (HCC) is the most frequent form of primary liver cancer and typically evolves from hepatocytes in a chronically diseased liver (Craig *et al.,* 2020). In the western world HBV (hepatitis B virus) and HCV (hepatitis C virus) infection as well as alcohol abuse and nonalcoholic fatty liver disease (NAFLD) are the major causes (Craig *et al.,* 2020). Type-2 diabetes mellitus (T2DM) appears to be another independent risk factor of HCC development which is linked to insulin resistance and hyperinsulinemia (Li *et al*., 2017). In the following chapters the physiological functions of insulin and its role as possible trigger for HCC development will be outlined.

II.2 Insulin

Insulin is an anabolic peptide hormone, which regulates the metabolism of carbohydrates, lipids and proteins in liver, skeletal muscle and adipose tissue. Cells, which are sensitive to insulin, anchor insulin receptors in their membranes where the hormone may bind to provide a signal for the cell (Chettouh *et al.,* 2015; Leclercq *et al.,* 2007; Schulze *et al.,* 2019; Wilcox, 2005). A major target of insulin is the liver where it controls glucose metabolism by promoting glycolysis, glucose storage as glycogen, protein synthesis, lipogenesis and by inhibiting gluconeogenesis. But also processes such as synthesis and storage of fat, protein synthesis, cell growth, cell proliferation, survival and differentiation are regulated by insulin (Chettouh *et al.,* 2015; Leclercq *et al.,* 2007; Schulze *et al.,* 2019; Wilcox, 2005). Insulin also plays a crucial role as growth factor in hepatocytes by promoting cell division and survival by suppressing apoptosis (Chettouh *et al.,* 2015). More details on the role of insulin in hepatocyte metabolism and cell cycle are given in chapters II.5.1 and II.6.

In humans insulin is encoded by a gene (*INS*) which is located on chromosome 11 and transcriptionally regulated by upstream enhancer elements (Tokarz *et al.*, 2018). In response to glucose, insulin gene expression in the pancreatic β-cells of the islets of Langerhans is activated. Insulin is translated into preproinsulin protein and during

transition through the rough endoplasmatic reticulum and the trans-Golgi network it is processed to proinsulin. After further processing in the trans-Golgi network mature insulin, coupled with Zn^{2+} as hexamer, is secreted in secretory granules (Tokarz *et al.*, 2018). Insulin is a dipeptide containing 51 amino acids and has a molecular weight of 5802. It is composed of A and B chains which are linked by disulphide bridges. (Schulze *et al.,* 2019). The hormone is released to the venous blood stream and delivered from the pancreas to the liver in discrete pulses every ~ 5 min. During fasting the amplitude of these pulses is 0.5 – 1 nmol/liter whereas after a meal it may rise to ~ 5 nmol/liter (Song *et al.,* 2000).

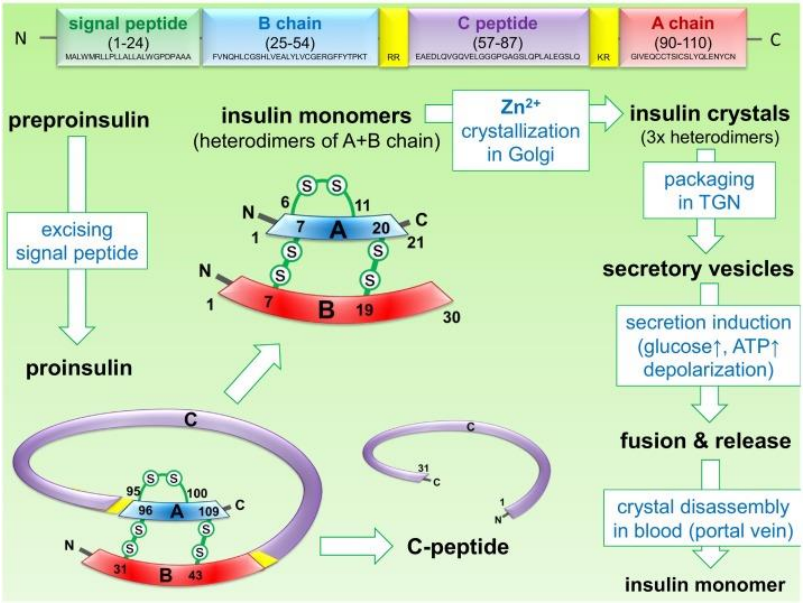

Figure 1. Insulin maturation and secretion pathway. (Reprinted from Vakilian, Tahamtani & Ghaedi, 2019)

II.3 Insulin Receptor (IR)

As member of the receptor tyrosine kinase family (RTK) the insulin receptor is a transmembrane multi-subunit glycoprotein which is anchored on the surface of cells and binds insulin as well as pro-insulin (Belfiore et al., 2009). It is encoded by a single gene on chromosome 19 with 22 exons and 21 introns spanning 120 kb. Alternative splicing of the 12 amino acid long exon 11 of the IR pre-mRNA generates two different

insulin receptor isoforms, IR-A (lacking exon 11) and IR-B (including exon 11) (Belfiore et al., 2009).

The insulin receptor is a hetero-tetramer, built as disulfide-linked covalent dimer with two extracellular α-subunits with ligand-binding domains and two transmembrane β-subunits containing the intracellular RTK domain. (De Meyts *et al.,* 2008)

II.3.1 Regulation of IR Isoform generation

High expression of IR is found in adipose tissue whereas in liver, heart and lung tissue the expression is around 30% of that in adipose tissue (Belfiore *et al.*, 2017). Transcription of the InsR gene is regulated by transcription factors, such as Sp1, hepatocyte-specific transcription factor of the insulin receptor gene (HTFIR), IR nuclear factors I and II (IRNF-I and IRNF-II), high-mobility group protein A1 or HMGA1 (Payankaulam *et al.,* 2019).

The expression of IR isoforms is differently distributed in organs and changes during lifetime. Although IR-A is highly expressed in adult life, IR-B is predominant in liver, muscle, kidney and adipose tissue which are all targets of insulin. Accordingly, in the liver 80% of IR expression is occupied by isoform B (Belfiore *et al.,* 2017). Generally, in tissues with predominantly metabolic effects of insulin (liver, skeletal muscle, adipose tissue and kidney) IR-B/IR-A mRNA ratio is higher compared to tissues where insulin acts as mitogen, such as fetal and cancer cells with high levels of IR-A mRNA (Westermeier *et al.,* 2015).

The exact mechanism in IR exon 11 splicing is not completely solved. Some splicing enhancers and factors are known that regulate the process, but the interplay involved in regulation of tissue-specific or developmental-related exon 11 skipping remains unclear (Belfiore *et al.,* 2017). Studies of Malakar *et al.,* (2016) showed, that insulin induced exon 11 inclusion in human and mouse pancreatic β-cells via Ras-MAPK/ERK signaling pathway and up-regulation of splicing factor serine/arginine-rich splicing factor 1 (SRSF1).

II.3.2 Differences in IR-A/B properties

The IR isoforms differ with regard to their ligand binding affinity. IR-A binds both insulin and IGF-2 with a higher affinity than IR-B (Belfiore *et al.,* 2017). Differences regarding

signaling have been noticed in neonatal hepatocytes which express IR-A, but not IR-B. These cells showed a high basal glucose uptake which does not correlate with insulin stimulation (Belfiore *et al.,* 2017). Neonatal hepatocytes expressing IR-B alone showed increased apoptosis compared to those expressing only IR-A. Hepatocytes with both IR isoforms were protected from apoptosis. Studies also showed that cells with IR-A isoform alone preferentially undergo proliferation when IGF-II was bound to the receptor but activate glucose uptake upon insulin binding (Belfiore *et al.,* 2017).

II.3.3 IR interaction with IGF receptors

The signaling pathways, induced by insulin and IGF-1 and 2 (Insulin like growth factor 1), are highly similar but the biological processes they regulate are still strikingly distinct (Belfiore *et al.,* 2017; Cai *et al.,* 2017). The corresponding receptors IR-A, IR-B and IGF-1 receptor can be activated by insulin and IGF-1 and 2 whereas IR-A has higher affinity for IGF-2 compared to IR-B. Further complexity is added by the fact that IR-A, IR-B and IGF-1 and 2 receptors show a high degree of homology and are able to heterodimerize which enhances cell responsiveness to IGFs (Belfiore *et al.,* 2017; Cai *et al.,* 2017).

II.3.4 Insulin Receptor Signaling Pathway

The insulin receptor is activated upon binding of insulin which leads to conformational change and autophosphorylation of tyrosine residues. Signaling proteins, such as IRS 1-6 (Insulin receptor substrate) and Shc (Src homology 2 domain containing) bind to these phosphorylated sites which is the starting point of the various intracellular signaling cascades (Chettouh *et al.,* 2015; De Meyts *et al.*, 2016). The main components in this network are the phosphatidylinositol 3-kinase (PI3K)/AKT and the Raf/Ras/MEK/MAPK (mitogen activated protein kinase) pathways. While the first pathway regulates metabolic effects of insulin and is activated only by IRS, the second one is involved in gene expression regulation by insulin. The PI3K and the MAPK pathways together impact on cell growth and differentiation (Chettouh *et al.,* 2015; De Meyts *et al.*, 2016).

II.3.4.1 The PI3K Signaling Pathway

Binding of the regulatory subunit of PI3K to IRS1 and 2 activates the pathway followed by phosphorylation of phosphatidylinositol 4,5-bisphosphate (PIP2) and generating phosphatidylinositol-3,4,5-triphosphate (PIP3). Then, PDK (phosphoinositide-dependent protein kinase) gets phosphorylated and activated which in consequence phosphorylates and activates protein kinase B (AKT/PKB) (Chettouh *et al.,* 2015; De Meyts *et al.* 2016)**.** Phosphorylated AKT is important for the regulation of glucose metabolism as well as cell size, proliferation and cell survival (Arcidiacono *et al.,* 2012). AKT/PKB activates three critical substrates with important functions: mTOR (mammalian target of rapamycin), FoxO (forkhead box-containing protein, O subfamily) and GSK3 (glycogen synthase kinase 3). By activating mTOR (especially mTORC1) protein translation and cell growth are promoted. AKT regulates gene regulation via phosphorylation of FOXO transcription factors which have an impact on cell metabolism, differentiation, apoptosis as well as cell cycle arrest and DNA repair (Arcidiacono *et al.,* 2012). FoxO1 is inhibited by AKT mediated phosphorylation which regulates gluconeogenic and adipogenic genes (Titchenell *et al.,* 2015). GSK3 inhibits glycogen synthase and is inhibited by activated AKT/PKB. Lipid metabolism is also regulated by AKT/PKB via sterol regulatory element-binding proteins (SREBP) which increases cholesterol and fatty acid accumulation (Huang *et al.,* 2018).

II.3.4.2 The MAPK-ERK Signaling Pathway

The adapter protein Grb2 binds to IRS and Shc which leads to phosphorylation and activation of the serine/threonine kinases Raf/MEK/ERK1-2. Phosphorylated ERK1-2 translocates to the nucleus to phosphorylate and activate various transcription factors which induce gene expression and regulate cell proliferation, differentiation, apoptosis and transcription. (Guo *et al.,* 2020). Furthermore mitogen (MAPK)- and stress activated protein kinases are phosphorylated by ERK1-2 as well (De Meyts *et al.,* 2016).

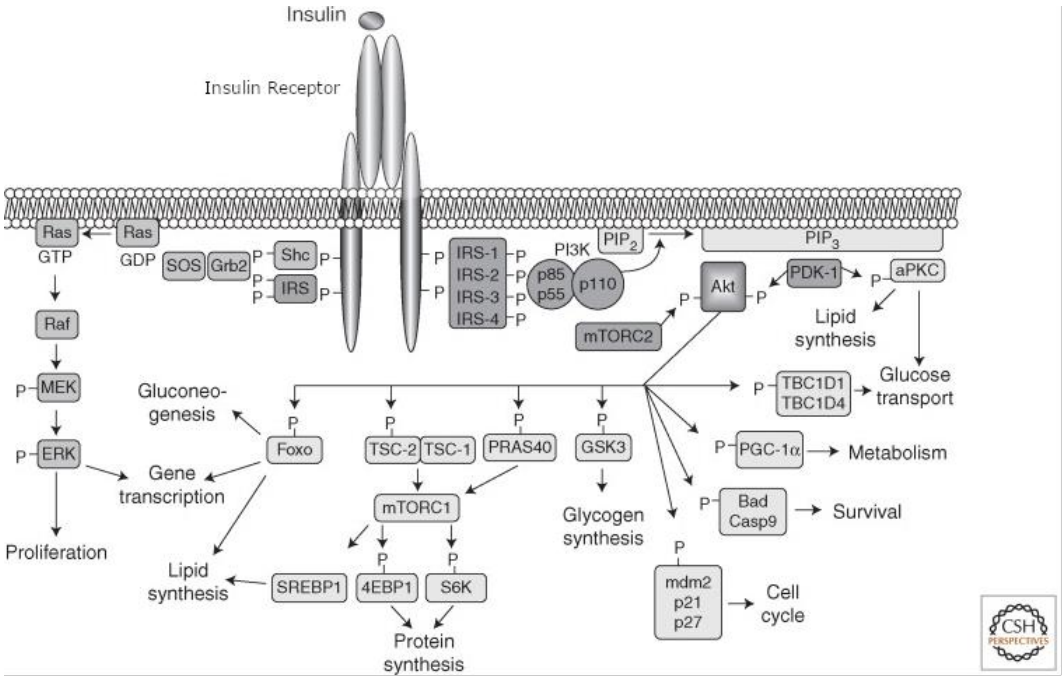

Figure 2. Insulin receptor signaling pathway. (Reprinted from Boucher J. *et al*., 2014)

II.4 Metabolic Effects of Insulin

Insulin plays important roles in carbohydrate and protein metabolism. Furthermore, it induces lipogenesis and protein synthesis and inhibits lipolysis and protein degradation (Edgerton *et al.,* 2017).

Insulin's function in glucose metabolism is implemented by two signaling pathways, insulin-mediated glucose uptake and glucose-stimulated insulin secretion. The first pathway is activated upon binding of insulin to its receptor (INSR) and thereby activating a signaling cascade (Vargas *et al.,* 2021). Thereby insulin causes an increased glucose uptake by cells in skeletal muscle and adipose tissue whereas in hepatocytes the glucose generation is suppressed by an insulin-mediated decrease of gluconeogenesis and increase of glycogenesis. (Edgerton *et al.,* 2017).

In skeletal muscles and adipose tissues three glucose transporters (GLUT1, GLUT3 and GLUT4) are responsible for glucose uptake. Insulin increases the uptake by inducing the translocation of GLUT4 from intracellular space into the cell membrane. It also stimulates hexokinase and 6-phosphofructokinase which enhance glycolysis in muscle cells. Insulin also increases the gene expression of glucokinase and pyruvate kinase which are crucial glycolysis enzymes (Qaid and Abdelrahman, 2016).

Lipid metabolism is regulated by insulin as well as it increases the expression of important enzymes in adipocytes such as fatty acid synthase (FAS), pyruvate dehydrogenase (PDH) and acetyl-CoA-carboxylase (ACC) (Vargas *et al.,* 2021). Lipogenesis is a process of fat synthesis and is promoted by insulin which induces a higher uptake of triglycerides into adipose tissue and muscle. On the other hand insulin inhibits the degradation of fat to fatty acid and triacylglycerol, called lipolysis. In consequence fatty acid is stored in adipose tissue and fatty acid oxidation is decreased in muscle and liver (Qaid and Abdelrahman, 2016).

In glycogenesis glycogen is synthesized from carbohydrates which is then stored in the liver and muscles. Insulin stimulates glycogen synthesis from glucose in the liver by increasing substrate-specific activity of protein phosphatase I (PPI) on glycogen particles (Qaid and Abdelrahman, 2016; Vargas *et al.,* 2021).

In the liver, kidney, brain, testes and erythrocytes non-carbohydrates such as pyruvate, lactate, glycerol, alanine and glutamine are converted to glucose (Qaid and Abdelrahman, 2016). Insulin inhibits gluconeogenesis by directly inhibiting the gene expression of the metabolic enzymes phosphoenolpyruvate carboxylase (PEPCK), fructose-1,6-bisphosphatase (FBP) and glucose-6-phosphatase (G6PC) which control rate limiting steps (Vargas *et al.,* 2021).

Figure 3. Metabolic Effects of Insulin. (Reprinted from Qaid and Abdelrahman, 2016)

II.5 Regulation of the Hepatocyte Cell Cycle

The liver is a tissue which is able to regenerate after injuries or resections by proliferation of highly differentiated hepatocytes which is unique among adult tissues (Greenbaum *et al.,* 2004). Three stages can be described during liver regeneration: a priming phase, describing the reentering of hepatocytes from G0 into the G1 phase of cell cycle, a proliferation phase during which hepatocytes progress, and a termination phase which stops cell proliferation. This process is enabled by the fact that hepatocytes are not terminally differentiated but are in a proliferative quiescence (G0 phase) and can reenter the cell cycle upon stimulation (Nowatari *et al.,* 2012).

Crucial factors for the priming phase are hepatocyte growth factor (HGF), transforming growth factor alpha (TGFα), nuclear factor kB (NFkB), signal transducer and activator of transcription 3 (STAT3), activator protein-1 (AP-1), mitogen-activated protein kinase (MAPK)/extracellular signal-regulated protein kinase (ERK), glucagon and insulin (Nowatari *et al.,* 2012; Taub *et al.,* 2004).

The stimulus for differentiated cells to reenter cell cycle and start liver regeneration are the proinflammatory cytokines tumor necrosis factor (TNFα) and interleukin 6 (IL-6) which are produced by liver Kupffer cells (nonparenchymal cells). Transcription factors and signal transduction pathways, such as NFkB, STAT3, MAPK/ERK, PI3K/Akt, AP-1 and CCAAT/enhancer-binding-protein-β are immediately activated and promote expression of “immediate early genes” and hepatocyte proliferation. The cells respond to the growth factors by passing the G1 phase of the cell cycle and reaching the “restriction point” where mitogens no longer control the progression of mitosis. During the proliferation phase hepatocyte growth factor (HGF) and epidermal growth factor (EGF) are responsible for the replication process (Greenbaum *et al.,* 2004; Nowatari *et al.,* 2012). Kupffer cells contribute to the accumulation of platelets which play a role in stimulating or accelerating hepatocyte proliferation (Nowatari *et al.,* 2012).

The progression in the G1/S phase is controlled by a family of transcription factors called E2F the members of which either have anti- or pro-proliferative properties (Greenbaum *et al.,* 2004). The G1/S transition is also regulated by cyclin dependent kinase 2 (Cdk2) which interacts with cyclin C in early G1 phase (Corlu and Loyer, 2012). During early and late G1 phase cyclin-cdk complexes are activated. Especially D- and E-type cyclins associate with Cdk2, Cdk4 and Cdk6 and release repressive (anti-proliferative) E2F/pocket protein complexes by phosphorylating the repressive pocked protein, retinoblastoma protein (pRb). The release of E2F transcription factors

in late G1 activates transcription of genes required for the progression in late G1 phase. (Greenbaum *et al.,* 2004; Corlu & Loyer, 2012). In the liver cyclin D1 is overexpressed to induce replication and progress through the G1/S restriction point (Greenbaum *et al.*, 2004). The entry into and progression in S phase and centrosome duplication depends on Cdk2 and Cdk1 (Corlu & Loyer, 2012).

Crucial factors in the termination phase are transforming growth factor beta1 (TGFβ1) produced by platelets and activins. (Corlu & Loyer, 2012).

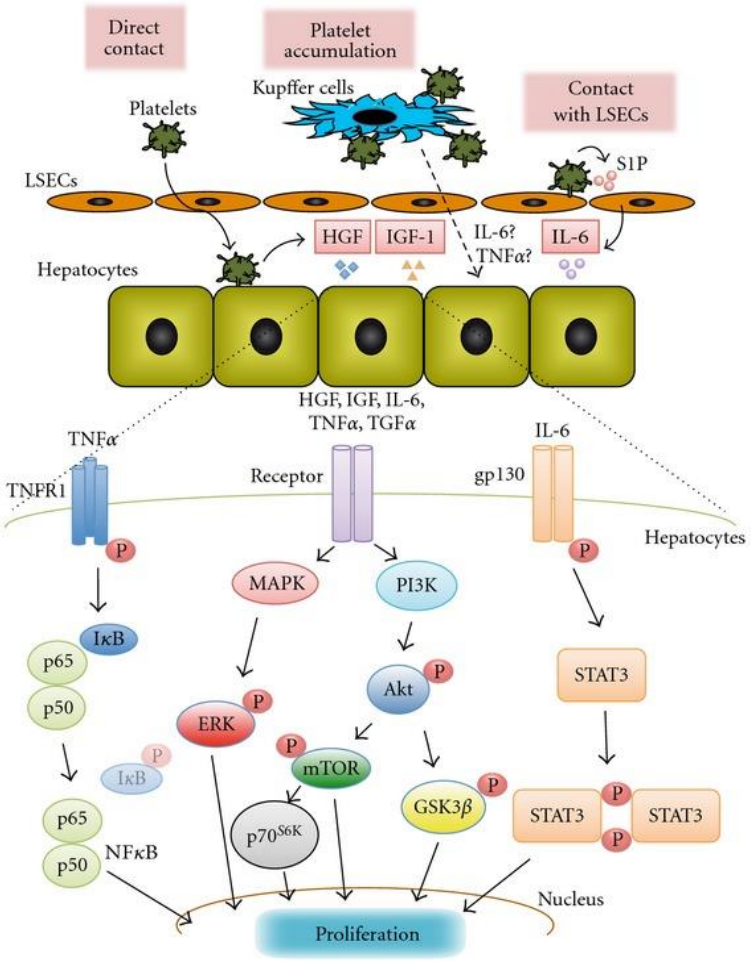

Figure 4. Signaling pathways and factors involved in hepatic cell cycle regulation. (Reprinted from Nowatari, Fukunaga and Ohkohchi, 2012)

II.5.1 Insulin and Cell Cycle Regulation of Hepatocytes

Insulin plays a crucial role as growth factor by pushing hepatocytes through the G1/S and G2/M phases of the cell cycle and cytokinesis and suppressing cell death by apoptosis. Terminal differentiation in hepatocytes is controlled by insulin as well via regulation of tetraploidization (Chettouh *et al.,* 2015). The peptide hormone influences signaling pathways, cytokines and growth factors which play crucial roles in liver generation. The activation of insulin receptors (IR) by insulin results in the activation of the PI3K-PKB-mTOR pathway which increases the survival and proliferation of hepatocytes (Abu Rmilah *et al.,* 2020).

Studies by Amaya *et al.* (2013) with the SkHep-1 human hepatoma cell line observed another mechanism by which insulin impacts hepatocyte regeneration. An insulin treatment of 5 minutes led to the internalization of IR via endosomes from the plasma membrane to the cytoplasm and the translocation into the nucleus. Next the enzyme phospholipase C is activated which catalyzes the hydrolysis of phosphatidylinositol 4,5-bisphosphate into diacylglycerol which in turn activates inositol 1,4,5-triphosphate ($InsP_3$). $InsP_3$ subsequently initiates nuclear and cytosolic Ca^{2+} signals by binding to its receptor which is located on a ligand-gated Ca^{2+} channel. These studies showed that insulin leads to a higher expression of nuclear and cytosolic $InsP_3$ which results in elevated Ca^{2+} signals (Amaya *et al.,* 2013). It turned out that insulin-induced liver regeneration and cell proliferation may depend on Ca^{2+} signals which are induced only by nuclear $InsP_3$. (Abu Rmilah *et al.,* 2020).

II.6 Altered metabolism in HCC

To enable proliferation of malignant cells they need a constant supply of energy and macromolecules. This requires an alteration of metabolic pathways which is one of the hallmarks of cancer cells (Wang *et al.,* 2016).

II.6.1 Reprogrammed glucose metabolism and the Warburg effect

Glucose metabolism is a major task of hepatocytes. Glycolysis metabolizes glucose to generate energy and glycogenesis stores excess glucose in the form of glycogen. In

hepatocellular carcinoma these important pathways are dysregulated. The Warburg effect describes the change in cancer cells from the more energy-efficient oxidative phosphorylation pathway towards aerobic glycolysis, a quick energy source with enhanced glucose uptake and lactate production for accelerated growth and proliferation (Tenen *et al.,* 2021; Wang *et al.,* 2016).

A high glucose uptake in HCC occurs via upregulating GLUT1 and GLUT2 isoforms. This alteration becomes apparent in the upregulation of crucial glycolysis enzymes such as hexokinase 1 (HK1), glucose-6-phosphate isomerase (GPI), aldolase A (AldoA), glyceraldehyde-3-phosphate dehydrogenase (GAPDH), phosphoglycerate kinase (PGK1), phosphoglycerate mutase 1 (PGAM1), enolase 1 (ENO1) and pyruvate kinase liver and red blood cells (PKLR) (Tenen *et al.,* 2021).

Another important alteration in glycolysis of HCC cells concerns the conversion of phosphoenolpyruvate to pyruvate by the pyruvate kinase (PK). PK exists in four splice isoforms with PKL prevalent in normal liver. Studies showed that in HCC expression of the PKM2 isoform is upregulated. In HCC cells glycolysis mainly produces lactate since lactate dehydrogenase (LDH) is overexpressed and catalyzes the conversion of pyruvate to lactate instead of acetyl-coenzyme A (acetyl-CoA) even in the presence of oxygen (De Matteis *et al.,* 2018; Tenen *et al.,* 2021).

On the other hand, expression of gluconeogenesis enzymes such as glucose-6-phosphatase (G6PC) and fructose-1,6-bisphosphatase (FBP1) is decreased (Khan *et al.,* 2015; Tenen *et al.,* 2021; Yang *et al.,* 2017).

These alterations result in a higher rate of glycolysis generating pyruvate that is either converted into lactate or enters the tricarboxylic acid (TCA) cycle (De Matteis *et al.,* 2018). The TCA cycle uses pyruvate from glycolysis to produce reduced nicotinamide adenine dinucleotide (NADH) and reduced flavin adenine dinucleotide ($FADH_2$). Succinate, fumarate and malate are metabolic intermediates in this cycle which are reduced in HCC. Pyruvate dehydrogenase kinase 4 (PDK4) which regulates pyruvate dehydrogenase complex (PDC), a multi-enzyme complex that catalyzes the oxidative decarboxylation of pyruvate, is downregulated as well (Tenen *et al.,* 2021).

II.6.2 Pentose-phosphate Pathway

For the synthesis of nucleotides, the pentose-phosphate pathway (PPP) turns glucose-6-phosphate to ribose-5-phosphate which is the precursor of DNA and RNA (Tenen *et*

al., 2021). In HCC the pentose-phosphate pathway is highly activated and nearly all enzymes are transcriptionally upregulated e.g. glucose-6-phosphate dehydrogenase (G6PD) which is the rate limiting enzyme of PPP and ribose-5-phosphate isomerase (RPI). High expression of G6PD is associated with migration and invasion, chemoresistance, metastasis, higher tumor grade of HCC (Tenen *et al.,* 2021).

II.6.3 Lipid metabolism

In HCC lipid metabolism is dysregulated to support tumorigenesis by providing lipids for membrane formation, energy generation and post-translational modification. Fatty acid synthesis is increased since fatty acids are a source of energy that enable cancer cells to proliferate (Tenen *et al.,* 2021; Wang *et al.,* 2016). Enzymes which catalyze fatty-acid biosynthesis such as fatty-acid synthase (FASN), acetyl-CoA carboxylase (ACC), ATP citrate lyase (ACLY), stearoyl-CoA desaturase (SCD1), 3-hydroxy-3-methylglutaryl-CoA reductase (HMGCR) and transcription factors for adipogenesis, such as sterol regulatory element-binding protein (SREBP1), are transcriptionally upregulated for enhanced cholesterol synthesis (De Matteis *et al.,* 2018; Tenen *et al.,* 2021) Studies observed that the AKT/mTORC pathway induces gene-expression alterations and post-transcriptional modifications which increase lipogenesis and carcinogenesis (Tenen *et al.,* 2021).

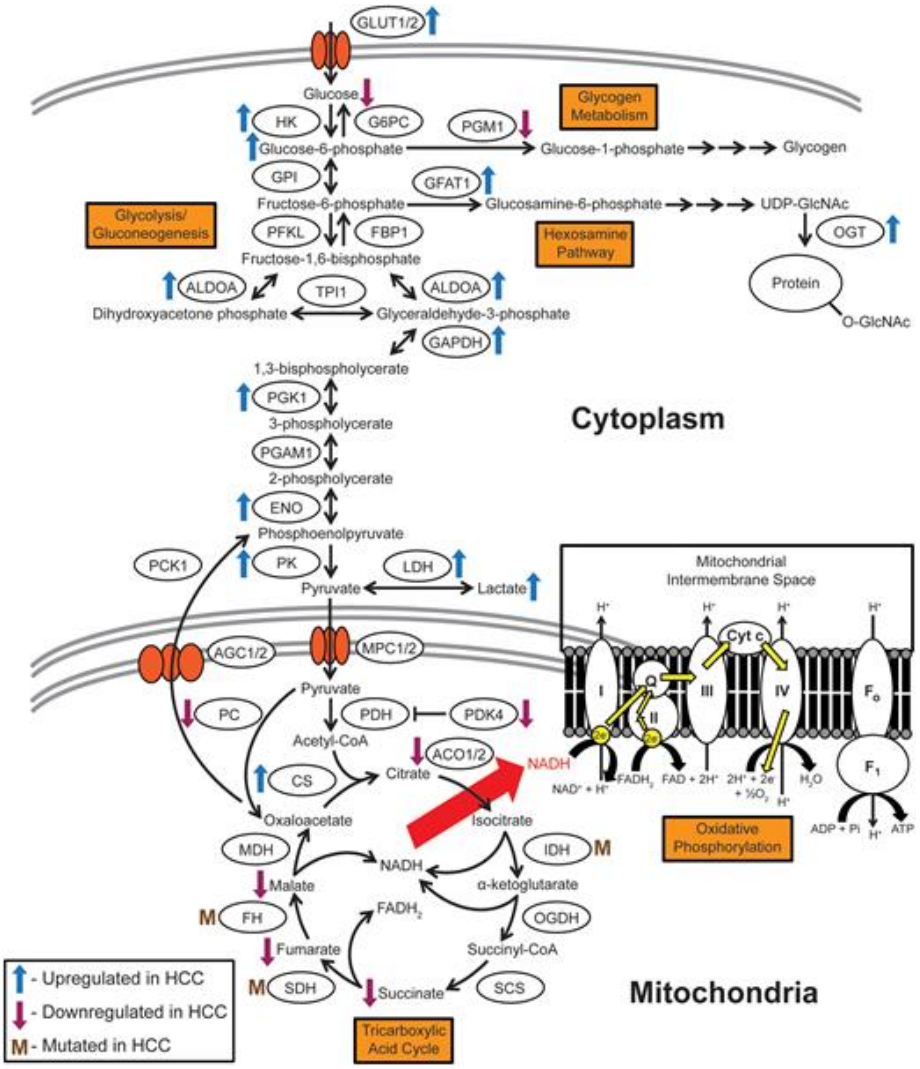

Figure 5. Metabolism alterations in HCC. (Reprinted from Tenen *et al.,* 2021)

II.7 Insulin as Risk Factor for HCC

Studies showed a link between insulin resistance and elevated cancer risk and that hyperinsulinemia plays an important role in tumor promotion and progression in insulin-resistant patients (Arcidiacono *et al.,* 2012), which is outlined in the following chapters.

II.7.1 Insulin Resistance, Hyperinsulinemia, Obesity and T2D

Insulin resistance is often associated with central obesity, dyslipidemia and systemic hypertension which are components of the metabolic syndrome. As a very heterogenous disorder insulin resistance may be due to lifestyle as well as genetic factors (Arcidiacono *et al*., 2012). The main causes are obesity as a result of overeating

and a defect of the insulin receptor (INSR) function. As a result, pancreatic beta cells overproduce insulin to counteract insulin resistance. Accordingly, chronic hyperinsulinemia is a hallmark of insulin resistance and a key feature of obesity and type 2 diabetes (T2D) in which high levels of insulin circulate in the blood relative to the glucose levels (Arcidiacono *et al*., 2012).

Studies observed that insulin-resistant patients are at higher risk of developing cancer in the liver but also breast, colorectum and pancreas (Arcidiacono *et al.,* 2012). Some mechanisms are illustrated in Fig. 6. Insulin positively impacts on the production and activity of insulin-like growth factor 1 (IGF1) which is able to promote cell proliferation. Studies showed that removing of the IGF1 receptor or reducing IGF1 concentration reduced cancer growth (Jee *et al.,* 2005). It has also been documented that chronic hyperinsulinemia in insulin resistant patients reduces hepatic production of insulin-like growth factor binding proteins 1 (IGFBP-1) and 2 (IGFBP-2) which increases the bioactivity of IGF-1 and the risk of developing tumors (Arcidiacono *et al.,* 2012).
Since insulin has the ability to reduce sex hormone-binding globulin (SHGB) the bioavailability of estrogen is positively affected and breast cancer risk increases (Arcidiacono *et al.,* 2012).
Insulin may promote cancer formation also by abnormally stimulating cellular signaling cascades which affects cell metabolism and enhances cell proliferation. (Arcidiacono *et al.,* 2012; Chettouh *et al.,* 2015; Jee *et al.,* 2005).
Insulin resistance is often associated with obesity, which is considered a low-grade inflammatory state characterized by an overproduction of free fatty acids, interleukin-6 (IL-6), adiponectin, leptin, tumor necrosis factor alpha (TNFα), plasminogen activator inhibitor-1 and monocyte chemoattractant protein (MCP-1) (Arcidiacono *et al.,* 2012).
Also increased oxidative stress is associated with obesity and T2D which contribute to a higher cancer risk. Reactive oxygen species (ROS) are overproduced and activate PI3K/Akt signaling pathway which may cause genetic modifications and DNA damage resulting in tumor formation and progression. NFκB as an important hub in coordinating immunity, inflammation and cell survival cross-talks with ROS and can induce aerobic glycolysis and lactate production (Arcidiacono *et al.,* 2012).

As an anti-inflammatory hormone insulin controls inflammation and pro-inflammatory transcription factors such as nuclear factor-kappa B (NFκB), activating protein-1 (AP-1), matrix metalloproteinase-9 (MMP-9), tissue factor (TF) and plasminogen activator

inhibitor-1 (PAI-1). Furthermore, insulin controls the inflammatory markers IL-1β, IL-6, macrophage migration inhibition factor (MIF) and tumor necrosis factor-alpha (TNF-α). Insulin resistance interrupts these activities in target tissues such as skeletal muscle, liver and adipose tissue which may result in the activation of genes that can enhance inflammatory processes (Arcidiacono *et al.,* 2012; Jee *et al.,* 2005).

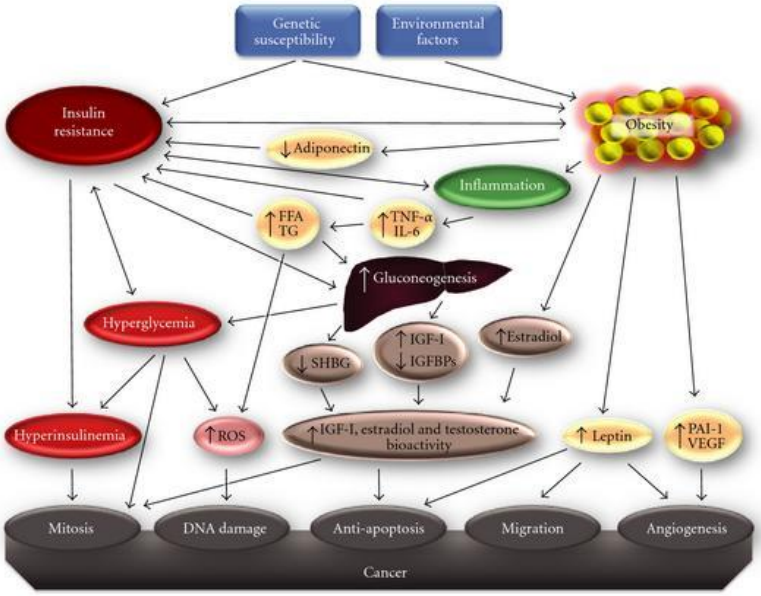

Figure 6. Mechanisms that link insulin resistance and cancer. (Reprinted from Arcidiacono *et al*., 2012)

II.8 Pyruvate kinase (PK)

Pyruvate kinase as a glycolytic enzyme is an important key player in regulating cell metabolism since it catalyzes the conversion of phosphoenolpyruvate (PEP) and adenosine diphosphate (ADP) to pyruvate and adenosine triphosphate (ATP) (Yang *et al.,* 2020). The protein exists in four isoforms in mammals: PKL, expressed in liver, kidney and early fetal tissues; PKR, expressed in erythrocytes; PKM1, expressed in adult muscle, brain, bladder cells and in adult fibroblasts; and PKM2 which is expressed in all proliferating cells especially tumor and embryonic tissues. (Yamada and Noguchi, 1999; Yang *et al.,* 2013; Zahra *et al.,* 2020).

Luo *et al.,* (2012) showed that PKM2 is highly expressed in human cancer cells and Iqbal *et al.,* (2013) observed that insulin up-regulates PKM2 gene (*PKM2*) expression. Based on these observations this kinase is considered as a critical link between insulin signaling and hepatocarcinogenesis. In addition, PKM2 may also be a key regulator of the Warburg effect, since its downregulation or replacement with PKM1 results in the reversal of the Warburg effect and reduced tumor formation in nude mouse xenografts (Li *et al.,* 2018).

PKL	PKR	PKM1	PKM2
• Hepatocytes • Intestine • Pancreas • Kidney	• Erythrocytes	• Heart • Skeletal muscle • Smooth muscle • Brain • Adrenal medulla • Mature sperm	• Tumor cells • Embryonic tissue • Testis • Ovaries • Adrenal cortex • Pancreatic islet cells • Thymus • Kidney distal tubule cells • Leucocytes

Figure 7. Tissue distribution of pyruvate kinase isoenzymes. (Reprinted from Zahra *et al.,* 2020)

II.8.1 PK gene expression

In mammalians the *PKL* and *PKM* genes code for the four PK isoenzymes, whereas *PKL* codes for PKR and L isoenzyme and *PKM* codes for PKM1 and M2 isoenzymes (Yamada and Noguchi, 1999). The *PKL* gene consists of 12 exons and 11 introns with tissue-specific promotors whereas the first two exons are specific for R and L isoenzymes. The *PKM* gene also consists of 12 exons and 11 introns with exons 9 and 10 being specific for M1- and M2- isoforms. Alternative splicing from a common primary transcript, mediated by members of the heterogenous nuclear ribonucleoprotein (hnRNP) family, produces the two isoenzymes (Wong *et al.*, 2013). In skeletal muscle,

heart and brain exclusively exon 9 is prevalent while exon 10 is present in other adult tissues and tumor cells.

Experiments of Yamada and Noguchi (1999) showed that *PKL* gene expression was increased in rats on high-glucose diet but was decreased in diabetic rat. Insulin administration to diabetic rats resulted in higher levels of PKL mRNA due to enhanced gene transcription (Yamada and Noguchi, 1999).

II.8.2 PKM2

PKM2 is exclusively expressed in embryonic and tumor cells and is replaced by tissue-specific PKM1, PKL or PKR when development is proceeding. In cancer cells PKM2 is highly expressed while other isoenzymes are decreased. To reach a higher amount of the M2 isoform cancer cells are able to predominantly splice the M2 form than the M1 via c-Myc-mediated upregulation of two members of the hnRNP family (Wong *et al.,* 2013). The M2 isoform is important for maintaining the metabolism of cancer cells (Zahra *et al.,* 2020). A shift from PKM2 to PKM1 expression in cancer cells results in a change from aerobic glycolysis to aerobic oxidation of glucose and a decreased ability to proliferate, metastasize and invade (Zhang *et al.,* 2019).

PKM2 is the only isoenzyme type which exists in two forms, namely as a highly active tetramer form and a dimer form with low activity. The ratio between tetramer and dimer depends on environmental factors, oncogenes, tumor suppressor genes and intermediate metabolites (Zhang *et al.,* 2019).

The change from one form to the other is allosterically regulated by endogenous and exogenous activators and inhibitors such as reactive oxygen species (ROS) which regulate the activity of some proteins via oxidation. The tetramer form leads to a higher production of ATP by catalyzing the conversion of phosphoenolpyruvate (PEP) to pyruvate. In cancer cells the tetramer is modified post-translationally leading to the formation of the PKM2 dimer which results in inhibiting the conversion of PEP. The dimer stimulates glycolytic enzymes of the pentose phosphate pathway (PPP) and synthesis of NADPH which suppresses ROS production and is needed for nucleotide biosynthesis. These changes promote further cancer progression (Zahra *et al.,* 2020).

II.8.3 Dimeric PKM2 and nucleus transfer

The low-activity PKM2 dimer is mainly present in the absence of environmental stress and can translocate from the cytoplasm to the nucleus where it acts as transcriptional co-activator of genes associated with tumor cell growth, metastasis and cell death (Zhang *et al.,* 2019). For the nuclear translocation exon 10 of PKM2 recruits extracellular signal-regulated kinase 2 (ERK2) which phosphorylates Ser37 of

PKM2 and recruits peptidyl-prolyl cis-trans isomerase (PIN1) to form a PKM2/PIN1 complex. This complex seems to be necessary to enable the entry of PKM2 into the nucleus. Studies in cancer cells showed that IGF-1 stimulates AKT which phosphorylates PKM2 at S202 residue resulting in its transfer into the nucleus. In the nucleus PKM2 dimer acts as protein tyrosine kinase and promotes transcriptional activities of hypoxia inducible factor-1α (HIF-1α), β-catenin (β-cat), insulin, signal transducers and activators of transcription 3 (STAT3) and octamer binding transcription factor (Oct 4) to promote cell growth and proliferation. PKM2 contributes to β-catenin-mediated expression and transactivation of cyclin D and c-myc thereby enhancing cell proliferation and cell-cycle progression (Wong *et al.,* 2013; Zahra *et al.,* 2020; Zhang *et al.,* 2019).

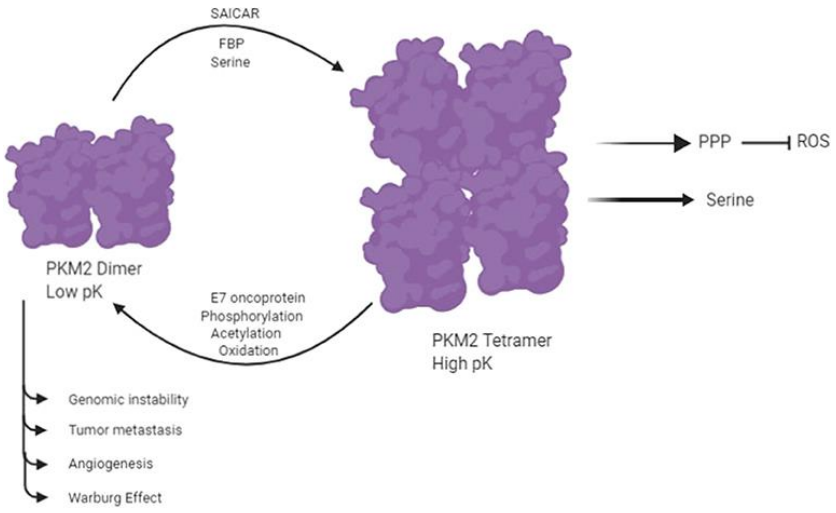

Figure 8. PKM2 dimer and tetramer formation regulation. (Reprinted from Zahra *et al.,* 2020)

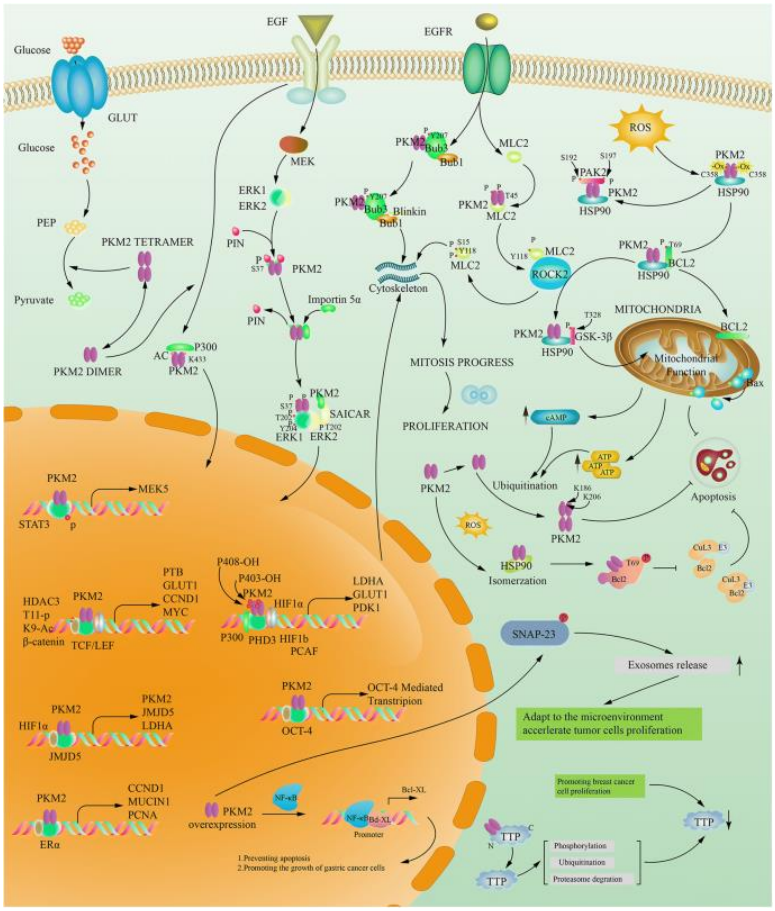

Figure 9. PKM2 protein interactions and pathways. (Reprinted from Zhang *et al.,* 2019)

II.8.4 Insulin regulates PKM2 activity and expression

Studies of Li *et al.* (2013) observed that insulin dependent glucose consumption and expression of mTOR, HIF-1α and PKM2 in HepG2 cells and that PKM2 is involved in insulin-induced glucose metabolism. Iqbal *et al.* (2013) showed that after 8 hours of insulin treatment PKM2 expression reached its maximum whereas insulin reduced the PKM2 activity to ~ 70% after 15 minutes of insulin treatment (100nM) in HepG2 cells. A significant decrease of activity was already reached with 1nM insulin and a maximum decrease was observed with 100nM insulin which was constant over a time span of 15 minutes to 8 hours (Iqbal *et al.,* 2013). Insulin up-regulated PKM2 protein expression and simultaneously decreased enzyme activity promoted aerobic glycolysis and macromolecular synthesis. In cancer cells PKM2 protein expression promotes aerobic glycolysis with high glucose uptake and lactate production even in presence of oxygen (Iqbal *et al.,* 2013). HepG2 cells treated with insulin showed the same characteristics compared to PKM2-silenced, insulin treated cells indicating that insulin regulates these

processes through upregulation of PKM2 expression. This upregulation of expression was induced by insulin via PI3K/mTOR mediated HIF-1α induction (Iqbal *et al.,* 2013).

Another characteristic of cancer cells, induced by the insulin-suppressed PKM2 activity, is the accumulation of glycolytic intermediates which are required for tumor growth. To be specific, upon insulin treatment PKM2 activity decreased as a result of tetramer dissociation into the dimer form. Co-incidentally insulin increased the production of ROS by ~60% inhibiting PKM2 activity by cysteine oxidation. A correlation between the elevated ROS production, increasing insulin concentrations and the decrease in PKM2 activity was observed; these alterations were followed by accumulation of glycolytic intermediates and NADPH (Iqbal *et al.,* 2013; Prakasam *et al.,* 2018).

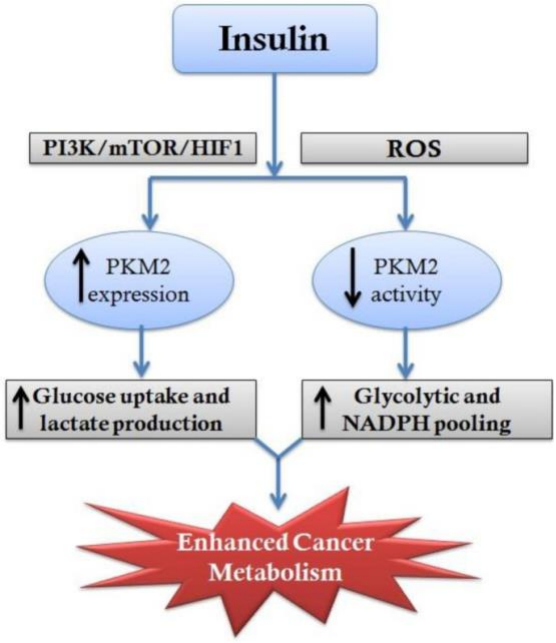

Figure 10. Insulin regulates PKM2 expression and activity. (Reprinted from Iqbal *et al.,* 2013)

II.8.5 PKM2 in HCC and the Warburg effect

In cancer cells pyruvate produced by glycolysis is converted to lactate via anaerobic glycolysis (Warburg effect) while in normal cells pyruvate is used in the mitochondrial oxidative respiratory chain for oxidative phosphorylation (Zhao *et al.,* 2016). Pyruvate kinase M2 turned out to be crucial for the Warburg effect in tumor cells. Its expression and low enzymatic activity are responsible for the glycolytic phenotype of cancer cells.

In HCC PKM2 is highly expressed and crucial for cell proliferation which is reduced when PKM2 is knocked down in vitro resulting in a decreased lactate production (Zhao *et al.,* 2016). Studies of Li *et al.* (2020) proved that PKM2 promotes HCC growth and metastasis in vitro and in vivo and that this enzyme may serve as a metabolic biomarker for predicting the prognosis of HCC patients.

II.9 Hepatocarcinogenesis and Cell Culture Models

In hepatocarcinogenesis genetic alterations in mature hepatocytes may cause mutations in critical cancer-related genes. In case of severe genetic or other types of damage to hepatocytes, cells will undergo necrosis followed by regenerative liver growth. Repeated necrosis of liver tissue will result in a chronic liver disease and progredient scarring of the organ (cirrhosis) (Pons *et al.,* 2005). Under this strong regenerative growth pressure liver nodules are formed, which may harbor hepatocytes with genetic and epigenetic changes and which may start to grow and acquire preneoplastic properties (Libbrecht *et al.,* 2005). Over time some of the lesions may turn into neoplastic liver nodules and HCC (Pons *et al.,* 2005).

Another origin of HCC could be the hepatocellular adenoma (HCA) which is a rare benign liver tumor resulting from benign proliferations of mature hepatocytes without the background of cirrhosis. It has five subtypes: HNF1A inactivated HCA, β-catenin mutated HCA, inflammatory HCA, sonic hedgehog HCA and HCA with no specific features, with β-catenin mutated HCA having the highest risk of malignant transformation into HCC (Beaufrère & Paradis, 2021, Nault *et al.,* 2013).

Since insulin may impact on different stages of hepatocarcinogenesis, different cell culture models were used which are comparable to unchanged and preneoplastic cell stages and enable in vitro studies. For this purpose, the HepaRG™ cell line was used, which was established from an Edmond grade I liver tumor associated with a chronic hepatitis C virus infection. The cell line is a human bipotent progenitor cell line characterized by its ability to differentiate into biliary-like cells and hepatocyte-like cells, which are well distinguishable under the microscope (dHepaRG™); dHepaRG™ cells show similar properties as mature human hepatocytes (Marion *et al.,* 2010). For

the present study dHepaRG^{TM} and HepaRG^{TM} cells were used as model to investigate the effect of insulin on the transition of mature hepatocytes to preneoplastic hepatocytes.

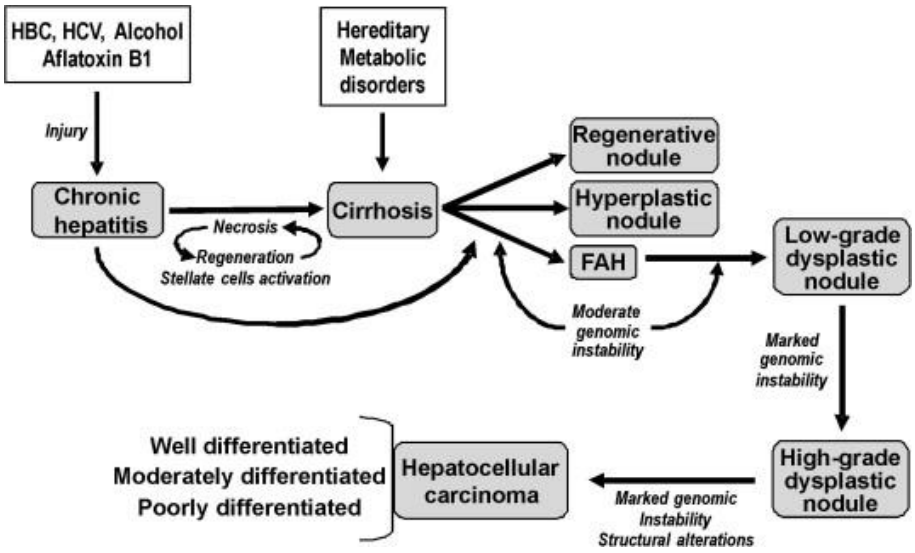

Figure 11. The multistep process of hepatic carcinogenesis. (Reprinted from Frau *et al.,* 2010)

II.10 Aim of the study

The aims of this study were to study whether

(i) premalignant hepatocytes show alterations in the transcriptome and in isoenzyme patterns, which may be due to the action of insulin. For this purpose, we analyzed transcriptome patterns of metabolic genes of rats. Literature search was performed to find genes which are under influence of insulin and also deregulated in liver cancer. The data were then compared with data of human HCA.

(ii) insulin may promote the development of hepatocellular carcinoma by investigating the effect of the hormone on cell proliferation and migration in cell models for unaltered and premalignant hepatocytes.

(iii) insulin induces the nuclear transfer of pyruvate kinase M2 (PKM2) in cell models for unaltered and premalignant hepatocytes as well as in hepatocarcinoma cell lines.

III. Materials

III.1 Devices

Device	Supplier	Model
Autoclave	CertoClav	Multicontrol
Centrifuge	Eppendorf	54515-R
Centrifuge	Heraeus	Megafuge 40R
Fluorescence Microscope	Nikon	
Gel electrophoresis cell	Bio-Rad	Mini-PROTEAN Tetra Cell (# 1658002EDU)
Incubator	Thermo Scientific	HeraCell 150i
Microscope	Nikon	Ti Eclipse
Nanodrop	Thermo Scientific	Nanodrop 1000
pH Meter	Thermo Scientific	Orion™ 3-Star Benchtop pH Meter
Photometer (plate reader)	TECAN	Infinite 2000 Pro
Thermo Cycler (RT-qPCR)	Bio-Rad	CFX96 TouchTM
Wet electroblotting sytem	Bio-Rad	Mini Trans-Blot Transfer Cell (# 1703930)
X-Ray Film Processor	Protec	Optimax

Table 1. Devices

III.2 Substances

Substance	Supplier	Product Number
6-well plates, Surface Treated, sterile	VWR	734-2323
96-well Cell Clear Flat Bottom TC-treated Culture Microplate	Falcon	353075
40% Acrylamid	Bio-Rad	1610140
Agar	Sigma-Aldrich	A1296
APS	Sigma-Aldrich	A3678
Amersham ECL-Prime Western Blotting Detection Reagent	GE Healthcare	RPN 2232
Bio-Rad Protein Assay Dye Reagent Concentrate	Bio-Rad	5000006
Bovine Serum Albumin (BSA)	Sigma-Aldrich	A6003
BRAND® counting chamber BLAUBRAND® Neubauer improved	Merck	BR717805
Chloroform	Merck	1024452500
CL-XPosure™ Film	VWR	PIER34089
Dexamethasone (100 mg)	Sigma-Aldrich	D4902
di-Natriumhydrogenphospha t-Dihydrat	Merck	1065801000
Diethyl Pyrocarbonate (DEPC)	Sigma-Aldrich	472301
DMSO	Sigma-Aldrich	472301
dNTP Mix, 10mM (1ml)	Fermentas Freezer	R0192
Dulbecco's Modified Eagle's Medium (DMEM)	Sigma-Aldrich	D5648
Ethanol 99,5%	AustrAlco	7025

FCS (Fetal Calf Serum)	Biowest	S1400
FCS (HyClone FetalClone II Serum)	Life Sciences GE Healthcare	SH30066.03
Folic acid	Sigma-Aldrich	F8758
Formaldehyde 37-40% with 10% Methanol	Merck	K35855803
Gentamycin Sulfate	Serva	22185
Gibco GlutaMAX™	Thermo Scientific	35050061
Gibco™, William's E Medium	Thermo Scientific	22551-022
Glycine for electrophoresis, ≥99%	Sigma-Aldrich	G8898-1KG
goat anti-rabbit Ig/HRP	Dako	P0448
goat anti-mouse Ig/HRP	Dako	P0447
Hard-Shell® 96-Well PCR Plates, low profile, thin wall, skirted, white/clear	Bio-Rad	SP9601
Hydrochloric acid fuming 37% for analysis EMSURE®	Merck	1003171000
Insulin (recombinant human) min. 27.5 IU/mg	Serva	26360.01
Isopropanol 99,5%	Acros Organics	1841130025
L-Glutamine	Sigma-Aldrich	G-5763
Lamin B1 Antibody (B-10)	Santa Cruz	Sc-374015
Lipofectamine™ 2000 Transfection Reagent	Thermo Fisher	11668027
Luna® Universal qPCR Master Mix, 1000 runs	NEB	M3003X
MEM Non-essential Amino Acid Solution (100x)	Sigma-Aldrich	M7145
Microseal ‘B’ PCR Plate Sealing Film	Bio-Rad	MSB1001

Millex GP Syringe Driven Filter Unit (0,22µm)	Merck	SLGP033RB
Monoclonal mouse anti-β-Actin antibody	Sigma-Aldrich	A-5441
Natriumchlorid BioXtra ≥99.5% (AT)	Sigma-Aldrich	S7653
Natriumdihydrogenphosphat-Monohydrat for analysis EMSURE®	Merck	1063461000
Natriumhydrogencarbonat	Merck	106329
Natriumpyruvat	Sigma-Aldrich	P2256
NE-PER™ Nuclear and Cytoplasmic Extraction Reagents	Thermo Fisher	78833
PageRuler Prestained Protein Ladder 2x250µL	Fermentas Freezer	26616
Penicillin/Streptomycin 100X	VWR	K952-100ML
peq-GOLD- Trifast	VWR PeqLab	30-2020
PKM2 (D78A4) XP® Rabbit mAB	Cell Signaling	4053
Polybrene Transfection Reagent	Sigma-Aldrich	TR-1003-G
Puromycin	Thermo Fisher	A1113803
Random Hexamer Primer	Fermentas Freezer	SO142
RevertAid Reverse Transcriptase (200 U/µL)	Fermentas Freezer	EP0442
RiboLock™ RNase Inhibitor	Fermentas Freezer	EO0381
RNase A	Qiagen	19101
RNA – Solv Reagent	Omega	17457FC10
RPMI-1640 Medium 10x	Sigma-Aldrich	R1145
SDS	Merck	822050

Skim Milk Powder	Sigma-Aldrich	70166
T-25 CytoOne® Flask, TC-Treated, Vented	Starlab	CC7682-4825
T-75 CytoOne® Flask, TC-Treated, Vented	Starlab	CC7682-4875
TEMED	Sigma-Aldrich	T8133
Trizma® base BioUltra, ≥ 99.8% (T)	Sigma-Aldrich	93349
Tube, 50 mL, PP, Screw Cap	Greiner Bio-One	227261
Tween® 20 for synthesis	Merck	8221840500

Table 2. Substances

III.2.1 Human Primer for RT-qPCR

Target Gene	Direction (F=forward; R=reverse)	Sequence (5' - 3')
β-Aktin (NM_001101.5)	F	GCACTCTTCCAGCCTTCCTT
	R	CGCTCAGGAGGACCAATGAT
ACADL (NM_001608)	F	AGTTGCGGTCACAAATC
	R	CTGGCAACCGTATATCTTC
ACLY (NM_001096.3)	F	GATCATGTGTTACGCTATC
	R	CCCGGCAAATCTTATATTC
ACSL5 (NM_203379.2)	F	AAACCAAACCAGCCCTAC
	R	GCAAAGATGCCGACAAAC
ALDOA (NM_001243177.4)	F	TGGCCCGTTATGCCAGTATC
	R	CAGCGCTTCAAGTCATGGTC
ALDOB (NM_000035)	F	TATGGCCACCGTAACAGCTC
	R	GAGTGGCATCCTCTTCACTC
ASNS (NM_001673.5)	F	TGAGGATTCCAATCTGATAC
	R	TTGCCATCATTGCATCATCAAC
ELOVL6 (NM_024090.3)	F	GTCGGCACCTAATGAATAAAC
	R	AGCACCGAATATACTGAAGAC
G6PD (NM_001360016.2)	F	CTGACATCCGCAAACAGAG
	R	ACATAGGAGTTGCGGGCAAAG
	F	AAGGGCATCCTTCTCAAC

GCK (NM_000162.5)	R	CCATTGCCACCACATCCATTTC
SLC2A1 (NM_006516)	F	CAGCAGCAAGAAGCTGAC
	R	GTAGAACTCCTCGATCAC
GLUT2 (NM_000340.2)	F	ATTGGGACCATCTCATATAC
	R	GAGCAATTTCACCGATATAC
GYS2 (NM_021957.4)	F	CCAGCATGCCAGACACCTGAC
	R	TGAGGACTGGAGGCCTGAGAC
HK1 (NM_000188.3)	F	CCCTAAATGCTGGGAAAC
	R	GGAAGAGGAATCCCTTCTTG
HMGCR (NM_000859.3)	F	CCAGAGCAAGCACATTAG
	R	ATCGAGGGTAAACGTAGG
HMGCS1 (NM_001098272.3)	F	ACAACTAATGCATGCTATGG
	R	GTGGCATATACAGCAATATCTC
INSR-A (NM_001079817.3)	F	TTTTCGTCCCCAGGCCATC
	R	GTCACATTCCCAACATCGCC
INSR-B (NM_000208.4)	F	CCCCAGAAAAACCTCTTCAGG
	R	GTCACATTCCCAACATCGCC
LDHA (NM_005566.4)	F	TGTATGGAGTGGAATGAATG
	R	ATGTGTAGCCTTTGAGTTTG
LDHB (NM_002300.8)	F	GGCAACAGTTCCAAACAATAAG
	R	ACAAGAGCAAGTTCATCAG
PHGDH (NM_006623.4)	F	CTGACCCTGCAATGCTGCCTAC
	R	GCAAGGAGGAGATGCCCATGAC
PKLR (NM_000298.6)	F	CGCCCTGGACACCAAGGGAC
	R	CAGCACCTGGGAGCCCTTCAC
PKM2 (NM_001012642.3)	F	CCTCTCTTTTCTGCTGGGGAG
	R	ACTGAAGGGGGCAACCTGTA
	F	TCTCTTTTCTGCTGGGGAGGG
	R	CTGAAGGGGGCAACCTGTA
RPIA (NM_144563)	F	CAGCGAATAGCTGAAAGG
	R	CCTGAAATCAGCGATCAC
TKT (NM_001064.4)	F	GCCGCCAATACAAAGGGTATC
	R	ACCTGGTCATCCTTGCTCTTC

Table 3. Human Primer for RT-qPCR

III.3 Media

III.3.1 Williams Growth Medium (GM)

Substance	Volume
Williamsmedium	442,5 ml
10 % FCS Fetaclone II #SH30066.03	50 ml
Penicillin/Streptomycin (50 U/ml)	500 µl
Glutamax (2mM)	5 ml
Insulin (5 µg/ml)	1 ml
Dexamethason (50 µM)	500 µl
Gentamicin (80 µg/ml)	500 µl

Table 4. Williams Growth Medium (GM)

III.3.2 Williams Differentiation Medium (DM)

Substance	Volume
Williamsmedium	433,5 ml
10 % FCS Fetaclone II #SH30066.03	50 ml
1,8 % DMSO	9 ml
Penicillin/Streptomycin (50 U/ml)	500 µl
Glutamax (2mM)	5 ml
Insulin (5 µg/ml)	1 ml
Dexamethason (50 µM)	500 µl
Gentamicin (80 µg/ml)	500 µl

Table 5. Williams Differentiation Medium (DM)

III.3.3 Williams Starving Medium (SM)

Substance	Volume
Williamsmedium	483,5 ml
1,8 % DMSO	9 ml
Penicillin/Streptomycin (50U/ml)	500 µl
Glutamax (2mM)	5 ml
Insulin (5 µg/ml)	1 ml
Dexamethason (50 µM)	500 µl
Gentamicin (80 µg/ml)	500 µl

Table 6. Williams Starving Medium (SM)

DNP10 Medium

DMEM

10% FBS (100 µL/mL)

1% MEM (10 µL/mL)

1mM Natriumpyruvat (500mM Stock)

DNP0 Medium

Components of DNP10 Medium, without FBS.

III.4 Buffer and Solutions

10x PBS (Phosphate Buffered Saline)

58.6 g NaCl

11.5 g Na_2HPO_4

26.2 g $NaH_2PO_4*H_2O$

The Ingredients were dissolved in 800 mL ddH_2O and the pH was adjusted to 7.4. Afterwards the solution was filled up to 1 L with ddH_2O, autoclaved and stored at room temperature.

10x PBST

1 L PBS was substituted with 500 µL Tween20.

10x Running Buffer

30 g Trisma Base

144 g Glycin

10 g SDS

Filled up to 1 L with Aqua bidest and stored at room temperature

2.5x Transfer Buffer

15 g 125 mM Trisma Base

72 g 960 mM Glycin

250 g 25% Methanol

Filled up to 2 L with Aqua bidest and sotred at -4°C.

5x Laemmli Sample Buffer

300 mM Tris/HCl (pH 6.8)

60% Glycerol

10% SDS

0.025% Bromphenolblau

930 µL aliquotes were made and 70 µL β-mercaptoethanol were added per vial. The aliquotes were stored at -20°C.

100x β-mercaptoethanol (0.1 mM)

200 mL PBS (1x)

144 µL β-mercaptoethanol (14 M)

β-mercaptoethanol was added to PBS. The solution was sterile filtrated, aliquoted and stored at -20°C. After first usage it was kept at 4°C.

1x PBST

PBS substituted with 0.05% Tween 20.

3% milk powder

3g milk powder dissolved in 100 mL PBST.

Trypsin-EDTA (0.1% Trypsin, 0.01% EDTA)

80 g	NaCl
10 g	Glucose-Monohydrate
4 g	KCl
8.4 g	$NaHCO_3$
1 g	EDTA
100 mg	Phenol red
10 g	Trypsin (Gibco)

After adding all ingredients, the solution was filled up to 10 L with ddH_2O and was sterile filtered with a filter of 0.22 µm pore width. It can then be stored at -20°C and after thawing it the solution is kept at 4°C.

Insulin

A 30 mM HCl solution was prepared with 6 mL 0.1 M HCl filled up to 14 mL with ddH_2O. 50 mg insulin were then dissolved in 20 mL of this solution to obtain a 2.5 mg/mL stock solution, which was stored at -20°C.

Dexamethasone

10 mg dexamethasone (Sigma, D4902) were dissolved in 0.5 mL EtOH. Afterwards the solution was sterile filtered (filter with 0.22 µm pore width) and stored at -20°C.

III.5 Plasmids

For virus assembly and production three plasmids were needed: a packaging plasmid, an envelope plasmid and a vector with the desired sequence. The packaging as well as the envelope plasmid were designed with addgene and the vector for the overexpression of the genes of interest were designed by GeneCopoeia. The packaging plasmid pCMV delta R8.2 (Fig. 12) carries a SV40 promoter, which maintains transgene expression stably during long-time culture. The pCMV-VSV-G envelope plasmid (Fig. 13) and the vectors (Fig. 14) for the overexpression of InsR-A and InsR-B sequence carry a CMV promoter, which yields the highest transgene expression levels and the highest transfection efficiency. (Wang X.-Y., *et al.* 2016) For selection of positive cells all vectors (Fig. 14) carry a puromycin resistance cassette and an eGFP sequence.

Vector Name	Size (bp)	Catalog No.:	Source
INSR-A vector	12725	EX-Y4304-Lv205	GeneCopoeia™
INSR-B vector	12761	EX-Y4566-Lv205	GeneCopoeia™
EC vector	8567	EX-NEG-LV205	GeneCopoeia™
pCMV delta R8.2	8128	12263	Addgene
pCMV-VSV-G	6363	8454	Addgene

Table 7. Plasmids

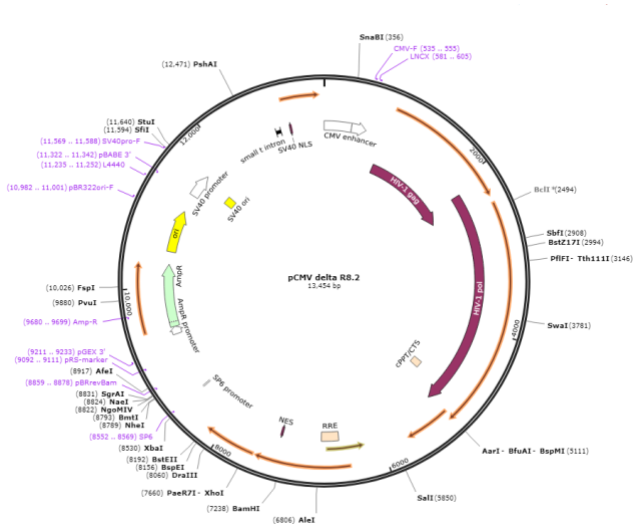

Figure 12. pCMV delta R8.2 plasmid

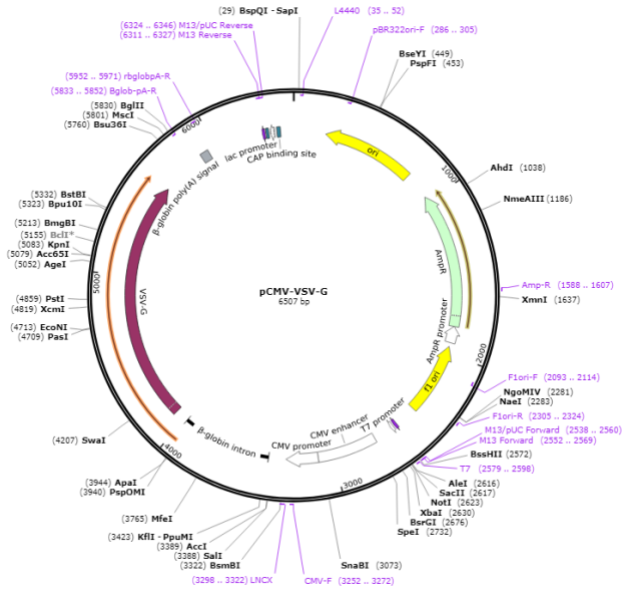

Figure 13. pCMV-VSV-G plasmid

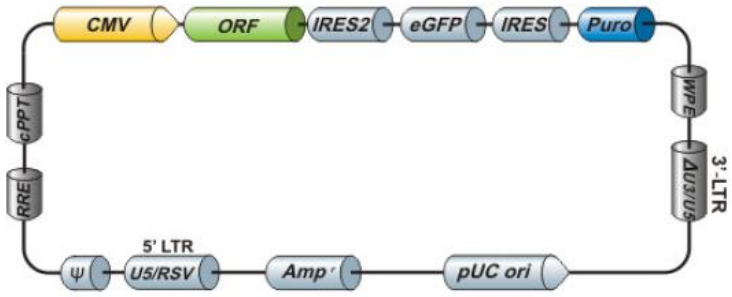

Figure 14. INSR-A/INSR-B vector.

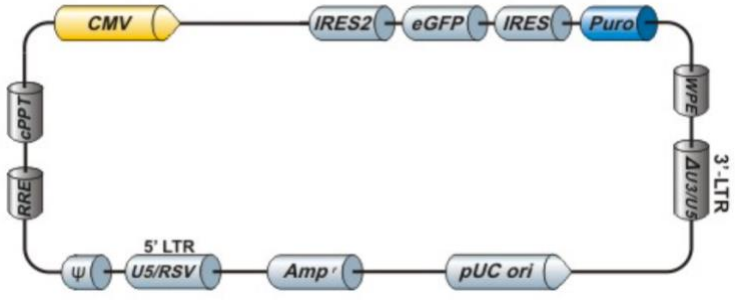

Figure 15. EC vector

IV. Methods

IV.1 Cell Culture

IV.1.1 Cell Lines

HepaRG™ cell line

The hepatic stem cell line HepaRG™ was provided by Biopredic International. Cells were cultivated in T-75 flasks with 10mL of growth medium (see Materials). Once a week the medium was changed.

HCC-1.2 cell line

The hepatocellular carcinoma cell line HCC-1.2 (RRID:CVCL_0C53) was established at the Institute of Cancer Research at the Medical University of Vienna *(*Sagmeister *et al.,* 2008). The cells were cultivated in T-75 flasks with 10mL of R10 medium (see Materials). Once a week the medium was changed.

Plate Size	Volume
T-75 flask	10 mL
T-25 flask	5 mL
6-well	1,5 mL
12-well	1 mL
24-well	500 µL

Table 8. Amount of medium used depending on plate size.

IV.2 Splitting of cells

Cultured cells reaching confluence need to be split. For this purpose, cells were treated with trypsin to detach them from the surface of the flask/well. The medium was aspirated and cells were washed gently with 3 mL trypsin (for T-75 flasks) or PBS to get rid of the serum. Afterwards 3 mL trypsin (for T-75 flasks) were added and cells were incubated at 37°C for around 3 minutes. The trypsin reaction was stopped by 7 mL of WE10 medium (see materials). The cell suspension was aspirated and transferred into a 50 ml Falcon tube in which the cells were centrifuged at 800 rpm for 5 minutes. The supernatant was aspirated, the cell pellet was re-suspended well in 10

mL medium (R10 for HCC and GM for HepaRG™) and cells were counted with a hemocytometer (BRAND® counting chamber BLAUBRAND® Neubauer improved). The chamber grid consists of four rectangles one in each corner. 10 µL of cell suspension was pipetted onto the chamber and cells which are inside the four rectangles were counted under the microscope. Next the mean of the four values was estimated and multiplied by 10^4 to obtain the cell number per ml.

The cells were split at a certain ratio appropriate for the size of the flask or well. HepaRG™ and HCC-1.2 cells were split once a week. For T-75 flasks HepaRG™ cells were seeded at a density of 2 x 10^6 cells in 10 ml GM. HCC-1.2 cells were seeded at a density of around 5 x 10^5 cells in 10 ml R10 medium. After 7 days when HepaRG™ cells were confluent and HCC-1.2 were 80% confluent they were split 1:10 and seeded into a new flask or well.

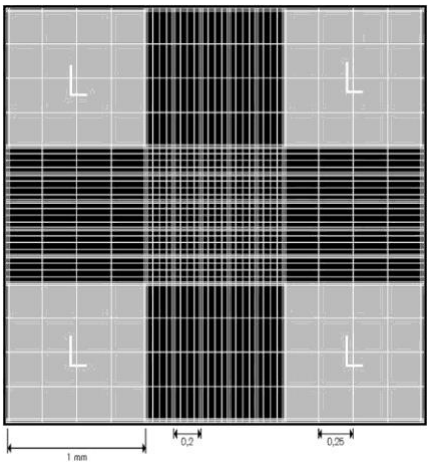

Figure 16. Cell counting chamber grid. (Source online available at: https://www.sigmaaldrich.com/catalog/product/aldrich/br717810?lang=de&region=AT [Accessed 09 April 2022])

IV.3 Freezing of cells

First, cells were detached from the surface of the flask or the well. Then the cell number was determined with the help of a hemocytometer. The cell pellet was put on ice and was re-suspended in medium with 10% DMSO. The cell suspension was then transferred to cryotubes with a final cell number of around 2 x10^6 cells per tube. The tubes were immediately stored at -80°C and after one week the frozen cells were transferred to a liquid nitrogen storage.

IV.4 Thawing of cells

First, a tube with 9 mL of warm growth medium was prepared. Then the cells were removed from liquid nitrogen storage and placed into a 37°C water bath to thaw very fast while pivoting the tube until there was just a small bit of ice left in the tube. The tube was then wiped with 70°C ethanol and put into the laminar flow. Then the cells were transferred into the tube with pre-warmed growth medium and centrifuged for 5 min at 800 rpm. Afterwards the supernatant was removed, the cell pellet was re-suspended in 6 mL of growth medium and the cell suspension was pipetted into a T-25 tube which was then stored in the 37°C-incubator. The next day medium was changed.

IV.5 Differentiation of HepaRG™ cells

For differentiation of the HepaRG™ cell line 2.0 x 10^5 cells were seeded in 1.5 mL GM per well of a 6-well plate. They grew in GM for two weeks, then the medium was changed to DM (GM with 1.8% DMSO) for further two weeks with a medium change each week. After four weeks, HepaRG™ cells were finally differentiated into cholangiocyte-like and hepatocyte-like dHepaRG™ cells and ready to use.

IV.6 Growth Curve/Doubling Time

To estimate the doubling time of HepaRG™ cells after transduction 2 x 10^6 cells were seeded onto a T-75 flask. The cell number was determined after 7 days with a hemocytometer. To calculate the doubling time the following formula was used: dT =T x [ln2/ln(Xe/Xb)] whereas T is the incubation time in any units. Xb is the cell number at the beginning of the incubation time. Xe is the cell number at the end of the incubation time.

IV.7 Lentivirus Production

For the production of the desired lentiviruses HEK293FT cells were used which were transfected with a packaging (pCMV delta R8.2) and an envelope plasmid (pCMV-VSV-G) and three different vectors for three different conditions: one vector containing the INSR-A sequence (GeneCopoeia™; #EX-Y4304-LV205) , another vector with the

INSR-B sequence (GeneCopoeia™; #EX-Y4566-LV205) and a control vector with no sequence added (EC vector). For selection all vectors carry a puromycin resistance cassette.

1.5 x 10^6 HEK293FT cells were seeded in 5mL DNP10 medium in a T-25 flask. After two days the cells were confluent and ready for lipofection of the virus plasmids with the help of lipofectamine™ 2000 Transfection Reagent (Thermo Fisher; #11668027). First the medium of the HEK293FT cells was changed to a volume of 4mL DNP10. Afterwards the plasmids were prepared. For each transfer plasmid two Eppendorf tubes were prepared, one to prepare the lipofectamine (Table 9, Tube A) and one to prepare the plasmids (Tube B). For the lipofectamine preparation 500 µL serum-free medium (DNP0) and 25 µL lipofectamine were added dropwise to tube A and incubated for 5 min at room temperature.

Tube A	
Component	**Volume**
Serum-free medium (DNP0)	500 µL
Lipofectamine™ 2000 Transfection Reagent	25 µL (added dropwise)

Tube B	
Component	**Amount**
transfer plasmid (INSR-A vector, INSR-B vector or EC vector)	5 µg
pCMV delta R8.2	3.75 µg
pCMV-VSV-G	1.25 µg
add serum-free medium (DNP0) to a volume of 500 µL	

Table 9. Lentivirus production. Tube A and B are prepared. Afterwards the content of tube B is added to tube A dropwise and incubated for 20 min at room temperature.

The content of tube B was then added dropwise to tube A and incubated for 20 min at room temperature. This content was then added dropwise to the HEK cells cultivated in the T-25 flask and incubated in an S2 safety lab. After 24 h the medium was changed using approximately 5.5 mL DNP10 and the transduced cells were seeded at a density of 350,000 (HepaRG™ cells) and 60,000 (hepatocarcinoma cells) per well of a 6-well plate.

IV.7.1 Transduction

After 72 hours the medium changed its color to yellow and cells were examined under a fluorescence microscope to see if they show green fluorescence. The lentivirus was then ready for harvesting. For this purpose, the medium was removed and transferred into a 50 mL falcon which was then centrifuged for 5 min at 500 g. The supernatant was aspirated and filtered into a new Falcon with a 0.45 µm PES filter. If not used immediately the supernatant was frozen in liquid nitrogen and stored at -80°C until later use.

Previous to transduction of the cells their medium was changed and polybrene was added at a final concentration of 8 µg/mL per well. Then the virus was added with different dilutions per well (see Figure 17) and cells w between IR isoforms ere incubated in a 37°C-incubator for 24 hours. Selection was performed with medium (GM or R10) supplemented with puromycin (2µg/mL for HepaRG™ and 1µg/mL for HCC), an antibiotic which eliminates all cells with insufficient virus transfection. For further cultivation medium contained puromycin. As soon as the cells were confluent they were split and could be kept outside the S2 virus lab.

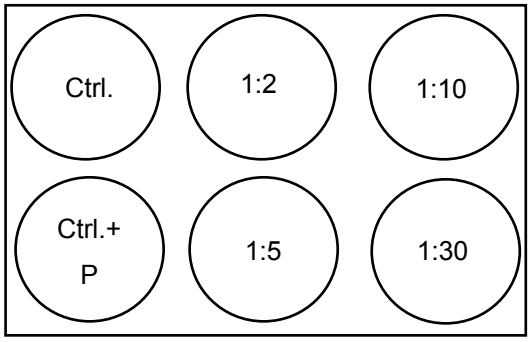

Figure 17. 6-well plate for transduction. In each of the wells cells are transfected with a different virus concentration, i.e., 1:2, 1:5, 1:10 and 1:30 dilutions in a total volume of 1.5mL. Two wells are used as control with no virus added, one well with growth medium and puromycin (Ctrl.+ P) the other one with growth medium only (Ctrl.).

IV.8 Quantitative Real Time Polymerase Chain Reaction (RT-qPCR)

IV.8.1 Insulin Treatment of Cells

HepaRG™ cells were seeded at 2.0 x 10^5 and HCC-1.2 cells at 2.0 x 10^5 cells in 1.5 mL of *GM* per well of a 6-well plate. After five days the cells had reached confluency to withdraw the serum (starvation). The cells were washed twice with serum free medium and 1.5 mL Starvation Medium (SM) without insulin, i.e. SM for HepaRG™ cells or R0 for HCC-1.2 cells. After 72 hours the cells were treated with insulin by adding 1.5 mL of SM or R0 medium, substituted with 2nM, 50nM, 200nM and 1µM insulin or no insulin as control group. After 24 h RNA was isolated and transcribed into cDNA. The expression levels of our genes of interest were determined via RT-qPCR.

IV.8.2 Cell Lysis and RNA Isolation

The following steps were all performed under the fume hood, with filter tips and on ice. The medium was removed and cells were washed with 1x PBS or serum free medium. To lyse the cells 300µl peq-GOLD-TriFast™ was added to each well of a 6-well plate with passing the cell lysate several times through the pipette. The cell lysate was transferred in a reaction tube (Eppendorf tube) which was vortexed for 15 sec and stored at -80°C or immediately used for further RNA isolation.

For RNA isolation via phase separation 60 µL chloroform was added to the defrosted samples followed by 15 sec of shaking. The samples were incubated at room temperature for 10 min followed by a 10 min centrifugation step with 12.000 g at 4°C to separate the homogenate into three phases. The upper aqueous phase which exclusively contained the RNA was carefully (without disturbing the other phases) transferred into a new 2 mL reaction tube. The interphase and the lower organic phase which contain DNA and proteins were discarded. For precipitating the RNA 150 µL -20°C cold isopropanol was added to the sample and mixed with a Vortexer. To fell the RNA the samples were incubated at -80°C overnight.
The next day the samples were centrifuged for 10 min at 12.000 g and 4°C and the supernatant was discarded. The precipitated RNA pellet was washed with 300 µL 70% and -20°C cold ethanol and shortly vortexed until the pellet lost contact with the bottom of the reaction tube. After centrifugation for 8 min at 14.000 g and 4°C the supernatant was discarded, and the pellet was air-dried for about 15 min. The RNA

pellet was re-suspended in 20 µL RNase-free DEPC H_2O and RNA concentration was measured via NanoDrop™ 1000 Spectrophotometer (Thermo Scientific). The RNA samples were stored at -80°C.

IV.8.3 cDNA Synthesis

All following steps were performed on ice and exclusively filter tips were used. RNA was reversely transcribed into cDNA by using the RevertAid First Strand cDNA Synthesis Kit (Thermo Scientific; #K1621); 500 ng RNA were diluted in 15 µL DEPC H_2O and 0.625 µL hexamer-primer were added. After briefly vortexing the samples they were spun down and then incubated at 70°C for 2 min in a thermo-cycler (Applied Biosystems, C 1000). The samples were immediately returned back on ice and first strand cDNA synthesis reaction mixture was prepared as shown in Table 10. A volume of 25 µL was obtained after adding the mixture to the RNA sample. The solution was mixed by gentle pipetting, incubated at 42°C for 60 min and heated to 94°C for 5 min. The samples were then kept at 4°C in the thermo cycler. After adding 50 µL DEPC H_2O the cDNA solution was transferred into a new 0.5 mL reaction tube, briefly vortexed and spun down quickly. cDNA was stored at -20°C.

Components	**Volume**
5X Reaction Buffer	5 µL
10 mM dNTP Mix	1.56 µL
RiboLock Rnase Inhibitor (20 U/µL)	0.625 µL
DEPC H_2O	1.19 µL
RevertAid M-MuLV RT (200 U/µL)	1.0 µL
Total volume	**9.375 µL**

Table 10. Components for synthesis of cDNA. Components are obtained from RevertAid First Strand cDNA Synthesis Kit (Thermo Scientific; #K1621).

IV.8.4 Quantitative Real-Time PCR

To determine transcript expression levels (CT values) of specific target genes quantitative real-time polymerase chain reaction (RT-qPCR) was performed. For this purpose a master mix for duplicate analysis of cDNA samples was prepared, using

SYBR Green-based Luna® Universal qPCR Master Mix (NEB; #M3003), DEPC H_2O, primer forward (20 µM), primer reverse (20 µM) and the cDNA sample to detect. The exact volumes are listed in Table 11. The mix was briefly vortexed and quickly spun down. For each cDNA sample two wells of a 96-well plate (Bio-Rad; Hard-Shell® 96-Well PCR Plates, low profile, thin wall, skirted, white/clear #HSP9601) were filled with 12 µL of the mixture. Afterwards the plate was sealed with adhesive, optical Microseal 'B' PCR Plate Sealing Film (Bio-Rad; #MSB1001) and put into the Real-Time PCR Detection System (Bio-Rad; Thermo Cycler (RT-qPCR) CFX Touch TM) where it ran through a specific cycling protocol (see Table 12).

Reagent	**Volume (for two wells)**
Luna® Universal qPCR Master Mix	12.5 µL
DEPC H_2O	8.5 µL
Primer forward (20 µM)	1.0 µL
Primer reverse (20 µM)	1.0 µL
cDNA sample	2.0 µL
Total volume	**25 µL** (12 µL/well)

Table 11. Components for Quantitative RT-qPCR reaction.

Stage	**Temperature**	**Duration**	**Cycles**
Preheating	50°C	20 sec	
Initial denaturation	95°C	10 min	
Denaturation	95°C	15 sec	39 x
Annealing & Extension	60°C	1 min	
Melting curve	60°C - 95°C	5 sec at 60°C; 5 min + 0.5°C per cycle	

Table 12. Cycling protocol for RT-qPCR cycler.

IV.8.5 ΔCT value Analysis

The cDNA samples were analyzed by the CFX Maestro™ Software for CFX Real-Time PCR Instruments (version 1.1; Bio Rad; #12004110) which determined the cycle thresholds (CT values). To obtain the mRNA expression levels of the genes of interest the ΔCT value was calculated. The CT values of the human β-actin gene were used as reference value since the expression level of ß-actin is considered to be stable and not to change between experimental samples. For normalization (graphed as ΔCT) the CT value of β-actin was subtracted from the CT value of the specific gene of interest. ΔΔCT were calculated by subtracting the ΔCT value of the control group from the experimental sample. With the comparative CT method by Schmittgen and Livak, (2001) the relative expression was calculated ($2^{-\Delta\Delta CT}$). To calculate isoform ratios the following formula of Harvey and Cheng, (2016) was used: $2^{-\Delta CT}$ whereas ΔCT = ΔCT of isoform 1 - ΔCT of isoform 2.

IV.8.6 Primer Design

Oligonucleotide primer were designed using NCBI Primer Blast (Ye *et al.,* 2012) and produced and purchased from Eurogentec. Primers used are listed in Table 3.

IV.9 Nuclear Extraction and Western Blot

IV.9.1 Insulin Treatment of HepaRG™ and HCC-1.2

HepaRG™, dHepaRG™ and transfected HepaRG™ cells were seeded onto 6-well plates at a density of 2 x 10^5 cells per well. HCC-1.2 were seeded at a density of 6 x 10^4 cells per well. Five days later insulin treatment was performed as described in chapter IV.8.1 with three treatment durations, i.e. 3h, 6h and 24h.

IV.9.2 Harvesting cells

The cell lines were first washed with around 400 µL trypsin per well and then incubated with 400 µL of fresh trypsin for 5 min in the incubator. To stop trypsinization 1 mL WE10 or R10 was added per well and re-suspended. The cell suspension was transferred to a 15 mL Falcon™ tube and cells with the same treatment were pooled. The cells were

centrifuged at 200 g for 5 min at 23°C using an acceleration (ACC) and deceleration (DEC) of 1. Afterwards the supernatant was removed and the pellet was re-suspended in 1 mL PBS, transferred in a new reaction tube (Eppendorf) and put on ice.

IV.9.3 Nuclear and Cytoplasmic protein Extraction

For protein extraction the nuclear and cytoplasmic extraction kit was used. The re-suspended pellet was centrifuged for 3 min at 500 g and 4°C. The supernatant was removed properly, and the volume of the pellet was estimated to calculate the required buffer volumes (see Table 13). First the cytoplasmic proteins were extracted with CER1 and CER2 buffer. The pellets were re-suspended in ice-cold CER1 buffer supplemented with protease inhibitors (PI). After 15 sec of vortexing the samples were incubated on ice for 10 min and CER2 buffer was added. The samples were again vortexed for 15 sec and incubated on ice for 1 min followed by another 15 sec vortexing step.

	Volume	**Volume of PI**
Pellet	15 µL	
CER1	150 µL	1.5 µL
CER2	8.25 µL	
NER	75 µL	0.75 µL

Table 13. Volumes used per 15µl sample for nuclear and cytoplasmic extraction.

The samples were centrifuged for 5 min at full speed and 4°C. The supernatant which contained the cytoplasmic extract was pipetted into a new reaction tube and stored at -80°C.

For nuclear extraction the pellet was re-suspended in 75 µL ice-cold NER buffer supplemented with 0.75 µL protease inhibitor. The sample was vortexed for 15 sec and incubated on ice for 10 min which was repeated five times in a row. After centrifugation for 10 min at full speed and 4°C the supernatant containing the nuclear fraction was pipetted into a new reaction tube and stored at -80°C.

IV.9.4 Bradford Protein Assay

To measure the protein concentration of the extracts Bradford Protein Assay was performed. A BSA dilution series with 12 dilutions served as standard curve whereas NER buffer and UPW were used as negative control (see Table 14). The protein extraction samples were diluted 1:10 with UPW (ultrapure water). Dilution series and samples were added as duplicates with a volume of 10 µL per well of a clear, flat bottom 96-well plate (Falcon® 96-well Cell Clear Flat Bottom TC-treated Culture Microplate; #353075). 100 µL of a 1:5 dilution of Bio-Rad Protein Assay Dye Reagent Concentrate (Bio-Rad; #5000006) with water was added to each well. The absorbance was measured at 595 nm using the Tecan plate reader (Infinite 2000 Pro)

	UPW (µL)	BSA (µL)	NER buffer (µL)
1	9	0	1
2	8,75	0,25	1
3	8,5	0,5	1
4	8,25	0,75	1
5	8	1	1
6	7,5	1,5	1
7	7	2	1
8	6,5	2,5	1
9	6	3	1
10	5	4	1
11	4	5	1
12	3	6	1

Table 14. BSA dilution series.

IV.9.5 SDS-PAGE

To separate the proteins according to their size and charge, SDS-PAGE (Polyacrylamidgele) was performed. In table 15 components are listed, required for one SDS- PAGE. The gel was prepared in a frame (Bio-Rad; Mini-PROTEAN® Casting Frame; #1653304) between to glass plates (Bio Rad; Mini-PROTEAN® Spacer Plates with 1.0 mm Integrated Spacers; #1653311). First the separating gel was prepared

(see Table 15), filled between the two glass plates and topped with 70% ethanol for anaerobic polymerization. After 1.5 hours ethanol was removed with filter paper, the already prepared stocking gel (see Table 15.) was poured between the plates and a comb (Bio-Rad; Mini PROTEAN® Comb, 10 well, 1.0 mm, 44 µl; #1653359) was inserted to form sample pockets. After 45 min of polymerization the comb was removed and the SDS-PAGE was added into a tank (Bio-Rad Buffer Tank and Lid #1658040), filled with 1x running buffer (see chapter III.4).

The protein samples were diluted to reach a final concentration of 20 µg in 20 µl UPW. Two µL of 5x Laemmli sample buffer was added and samples were heated at 95°C for 5 min. Twenty-two µL of the samples and 5 µL marker (1 Kb Plus DNA Ladder; Thermo Scientific; #10787018) were loaded onto the gel. The protein samples were separated in a Bio-Rad Mini-PROTEAN Tetra Cell (Bio-Rad; #1658002EDU) at 60 V for 30 min following 1.5 hours at 120 V.

10% Separating Gel	
Components	Volume
Acrylamid/Bis (40%)	1.50 mL
1.5 M Tris (pH 8.8)	1.25 mL
10% SDS	50 µL
H_2O	2.15 mL
10% APS	100 µL
TEMED	10 µL

4% Stocking Gel	
Components	Volume
Acrylamid/Bis (40%)	250 µL
1,5M Tris (pH 6.8)	313 µL
10% SDS	25 µL
H_2O	1.9 mL
10% APS	50 µL
TEMED	5 µL

Table 15. Gels for SDS-PAGE

IV.9.6 Western Blot

To transfer the separated protein bands from to gel onto a 0.45 µm nitrocellulose membrane a Bio-Rad wet electroblotting system (Bio-Rad Mini Trans-Blot Electrophoretic Transfer Cell; #1703930) was used. The sandwich assembly is pictured in Fig. 18, the nitrocellulose membrane was activated by methanol. Two 3mm

filter papers were used on each side and the transfer was performed in 2.5x transfer buffer, overnight at 28 V.

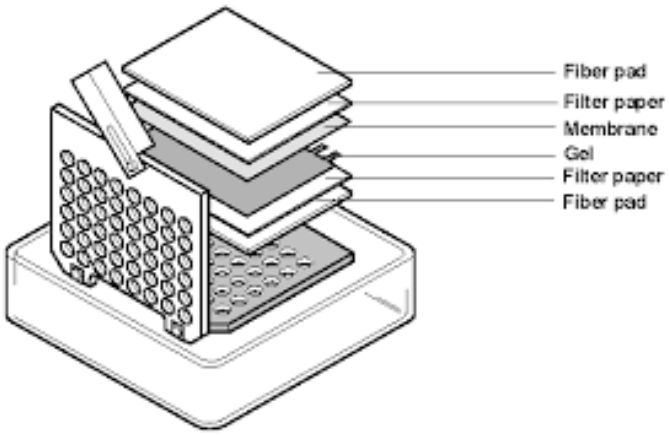

Figure 19 Sandwich assembly. (Reprinted from Theriault, 2016)

IV.9.7 Immunoblotting

The nitrocellulose membrane with the plotted proteins was washed with 1x PBST for 15 min, blocked with blocking buffer (3% skim milk powder diluted in PBST) for 2 hours and washed in 1x PBST for 10 min. PKM2 protein (~ 60 kDa) was detected using a primary antibody against PKM2 (Cell Signaling; #4053). The antibody was diluted 1:1000 in 3% milk powder and stored at -20°C. For detection the membrane was incubated with the primary antibody at 4°C over night in a centrifuge tube. The membrane was then washed with 1x PBST for 10 min, then with 3% blocking buffer for 10 min and again with 1x PBST for 10 min. Afterwards the membrane was incubated with the secondary antibody goat anti-rabbit immunoglobulins/HRP (Dako; #P0448) coupled to horseradish peroxidase (HRP). 1 µL of the secondary antibody was diluted in 15 mL blocking buffer and added to the membrane for 2 hours. The membrane was again washed as in the step before. Amersham ECL-Prime Western Blotting Detection Reagent (GE Healthcare; #RPN 2232) was used to detect proteins of interest. The two detection solutions were mixed together 1:1 (for one membrane 1 mL is needed in total) and the membrane was incubated with this mixture for 5 min. In the dark chamber, CL-XPosure™ Film (VWR; #PIER34089) was placed on the membrane for a few seconds which was then developed by the Protec Optimax X-Ray Film Processor.

As loading control anti-β-actin (Sigma; #A-5441) antibody (mouse) and lamin-B1 (Santa Cruz; #Sc-374015) antibody (mouse) were used. β-actin is detectable at ~ 45 kDA and lamin-B1 at ~ 68 kDA. Goat anti-mouse immunoglobulins/HRP (Dako; #P0447), coupled to horseradish peroxidase (HRP) was used as secondary antibody. Immunoblotting was performed as already described.

Detected membranes were stored in a closed box at 4°C.

IV.10 Clonogenicity Assay

Cells were seeded (in duplicates) in 1.5 mL GM medium onto 6-well plates at different low cell densities. After one day cells were washed with serum free medium and GM with different FCS concentrations was added (see Fig. 16). The next 5 weeks cells were kept in the incubator and medium was changed once a week. For analysis the medium was removed, cells were washed with 1x PBS, fixed with a methanol-aceton solution (1:1) for 5 min and washed again with 1x PBS. For staining crystal violet (1:1000 in 1x PBS) was added to the cells for 5 min and afterwards washed with aqua bidest.
To investigate growth and size of colonies pictures were taken and analyzed with Lucia G 4.6 software.

1200 cells GM 10% FCS	2000 cells GM 10% FCS	1200 cells GM 3% FCS
1200 cells GM 10% FCS	2000 cells GM 10% FCS	1200 cells GM 3% FCS

2000 cells GM 3% FCS	1200 cells GM 1% FCS	2000 cells GM 1% FCS
2000 cells GM 3% FCS	1200 cells GM 1% FCS	2000 cells GM 1% FCS

Table 16. Setup of clonogenicity assay. Each box is one well of a 6-well plate.

IV.11 Scratch Assay

Cell migration is a major ability of cancer cells and a requirement for metastasis. To determine if the InsR-A and InsR-B transduction of HepaRG^{TM} cells together with different insulin concentrations impact on migration a scratch assay was performed. For this purpose, cells were seeded in five wells of a 6-well plate with a density of 2.0 x 10^5 cells per well in GM supplemented with 2 µg/ml puromycin. After one week medium was removed and cells were washed twice with SM medium and starved for 72 hours. The cell layer was then gently scratched with a 1000µL tip and the medium was replaced by SM medium with different insulin concentrations (0nM, 2nM, 50nM, 200nM, 1µM insulin). A picture of the scratch was taken under the microscope after 0h, 24 h, 28 h and 72 h of incubation. The area of the scratch was determined by Image J program at each time point and relative alterations were calculated.

V. Results

V.1 Analysis of gene expression in PNL and HCA

One of the main questions in the present work was the effect of insulin on the gene expression in liver preneoplastic lesions (PNL) and hepatocellular adenoma (HCA) which are prestages of hepatocellular carcinoma (HCC). Therefore, data from a detailed literature search focused on the (i) identification of genes, which are modified directly or indirectly by insulin at the transcriptional or post-transcriptional level in hepatocytes, whole liver or liver-relevant experimental models and (ii) the question whether these genes are deregulated also in human PNL and HCA samples. The data from the literature search were compared with gene expression data on rat PNL and rat HCA. These lesions, which were generated by a two-stage initiation-promotion protocol in male Wistar rats, were subjected to whole genome expression analyses by the help of a rat Affymetrix GeneChip (Riegler *et al* 2015; Nejabat *et al*., 2017). The outcome is shown in Table 18.

To be more specific, based on published data >80 genes were identified which are directly or indirectly regulated by insulin in unaltered rat, human and rat hepatocytes, whole liver or liver-relevant experimental models (see table 18). About two third of these genes are regulated proedomintly transcriptionally by insulin whereas the regulation of about one third of these >80 genes occur predominatly at a post-transcriptional level. Indirect gene regulation by insulin subsumes involvement of other pathways such as MEK/ERK, mTOR and PI3K/AKT that can be affected by the hormone. A direct regulation means that insulin can directly influence enzymes or factors such as transcription factors by regulating their activity or their binding to insulin-response elements, respectively.

The literature search showed that the genes which are regulated by insulin are all part of important pathways which are crucial for metabolism, survival and/or growth of cells. Genes such as HK1, GPI, PFKL, ALDOA, GAPDH, PGAM1, ENO1 and PKLR are important key players in glycolysis and are upregulated by insulin in rat hepatocytes whereas G6PC is downregulated. Insulin also impacts on GLUT4 and GLUT8 expression which encode transport proteins for glucose. Furthermore, genes encoding crucial enzymes of cholesterol synthesis (HMGCS1 and HMGCR) are overexpressed

in hepatocytes under influence of insulin. FASN, ELOVL6 and SCD1 which are involved in lipid synthesis and genes of the pentose-phosphate pathway (G6PD, RPIA, TKT) are expressed at higher levels under insulin. Two further enzymes are changed by insulin, i.e. ACSL5, being crucial for acetyl-CoA production, and CPT1A preparing for β-oxidation. The TCA cycle is also influenced by insulin which is indicated by a transcriptional downregulation of two important enzymes, PDK2 and PDK4. Insulin acts on the biosynthesis of two amino acids, L-serine and asparagine, by effecting the gene expression of PHGDH and ASNS. LDHB which converts pyruvate into lactate is another enzyme which shows altered gene expression levels under insulin.

Published data show that insulin regulates the gene expressions of crucial cell cycle regulatory proteins (CCNB1, CCND1, CDK2, CDK4) and chromatin structure modulators as NUCKS1. Transcription factors (ATF3, FOXA2, USF2), co-activators (FAMB3) and translation regulators (YBX1, CPEB1, RPS6KB1) are regulated by insulin as well. Moreover, components of the IR signaling pathway are transcriptionally affected by insulin, such as INSR, IRS2, INSIG1, INSIG2, GSK3A/B, NCK1, SREBP and PRKCI. The IGF and leptin pathways are two further signaling cascades with some of their components being transcriptionally influenced by insulin, such as IGF1, IGF2, IGF1R, IGFBP1, IGFBP3, IGF2BP3 and LEP, LEPR. Membrane proteins including SORT1, receptors (DDR1, GHR, MFSD2, FXR), transporters (SLC2A2, SLC2A4, SLC2A8 and SLC25A22) and scaffold proteins (CAV1) are transcriptionally regulated by the hormone. Expression of protease inhibitors SERPINB1a and SERPINA12 and of ENPP1 and PHD3 are influenced by insulin as well.

Fig. 19 illustrates the insulin-induced alterations in crucial pathways in the liver leading to shifts in the carbohydrate metabolism, pentose-phosphate pathway and the synthesis of cholesterol, fatty acids and amino acids.

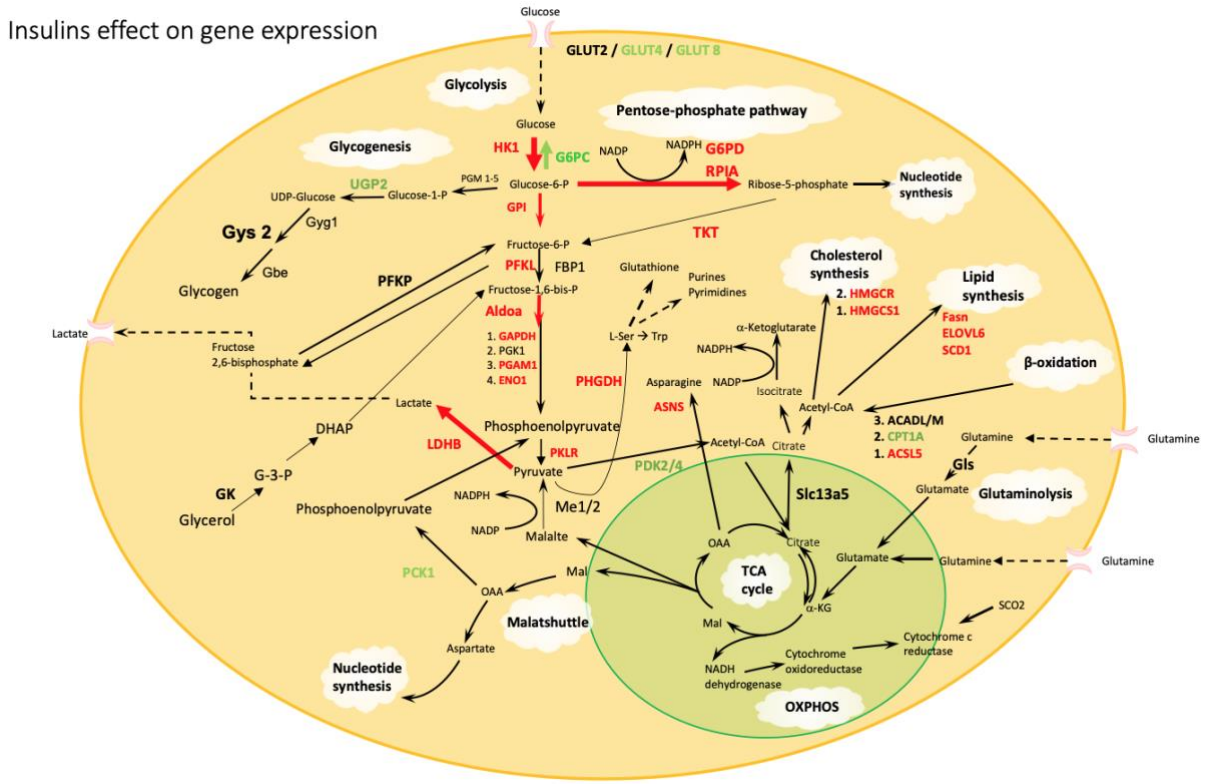

Figure 19. Effects of insulin on gene expression in unaltered hepatocytes, whole liver or liver-relevant models. The yellow circle depicts an unaltered hepatocyte cell with the green circle being the mitochondrion. Upregulated genes by insulin are colored in red, whereas downregulated genes are marked in green. For further details please see table 18 in the appendix.

Figs. 20 and 21 show that many genes, which are under partial control of insulin in the liver, are altered in the rat HCC prestages, PNL and HCA. As example, the glucose transporters GLUT4 and GLUT8 and the genes G6PC and FBP1 are transcriptionally downregulated, while the glycolysis genes HK1 and ALDOA and some genes of the pentose-phosphate pathway, namely G6PD and TKT, are upregulated. PDK4, which connects glycolysis and the TCA cycle, is downregulated in both PNL and HCA. Upregulations are seen for PHGDH and ASNS, enzymes of L-serine and asparagine biosynthesis, respectively. ELOVL6, SCD1 (lipid synthesis) and HMGCR (cholesterol synthesis) are expressed at higher levels whereas CPT1A (β-oxidation) is downregulated. The lipid synthesis enzyme FASN is another transcriptionally upregulated gene in HCA. PCK1 which regulates gluconeogenesis is transcriptionally downregulated in both, PNL and HCA.

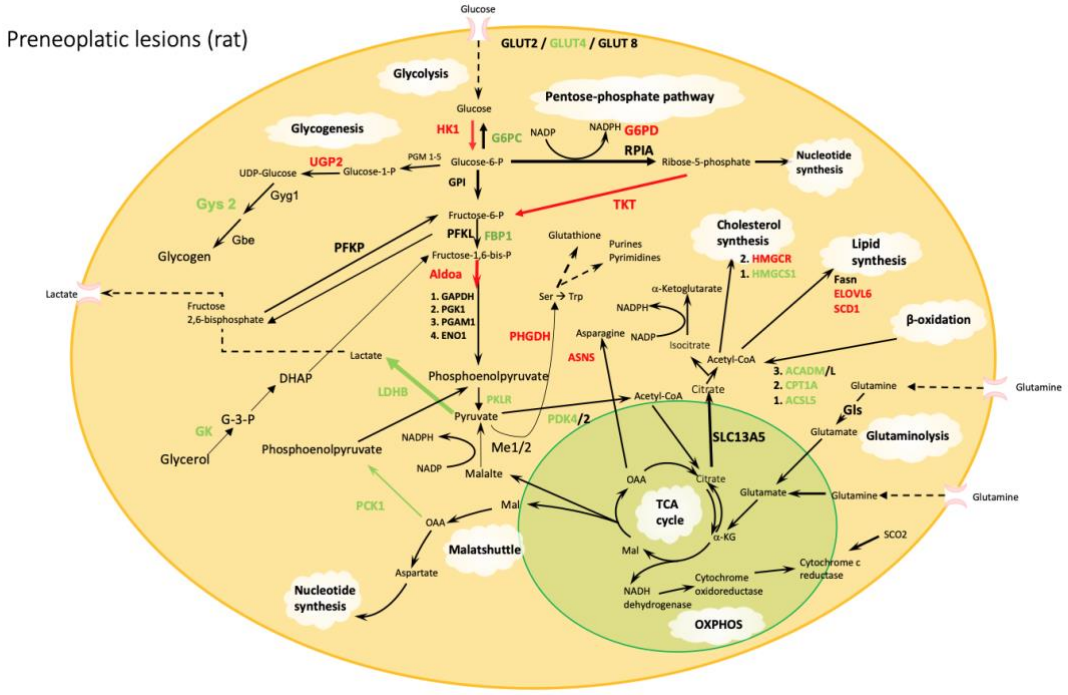

Figure 20. Illustration of the gene expression alterations in a rat PNL cell. The yellow circle depicts a PNL cell with the green circle being the mitochondrion. Upregulated genes (compared to unaltered hepatocytes) are colored red, whereas downregulated genes are colored green. For further details please see table 18 in the appendix.

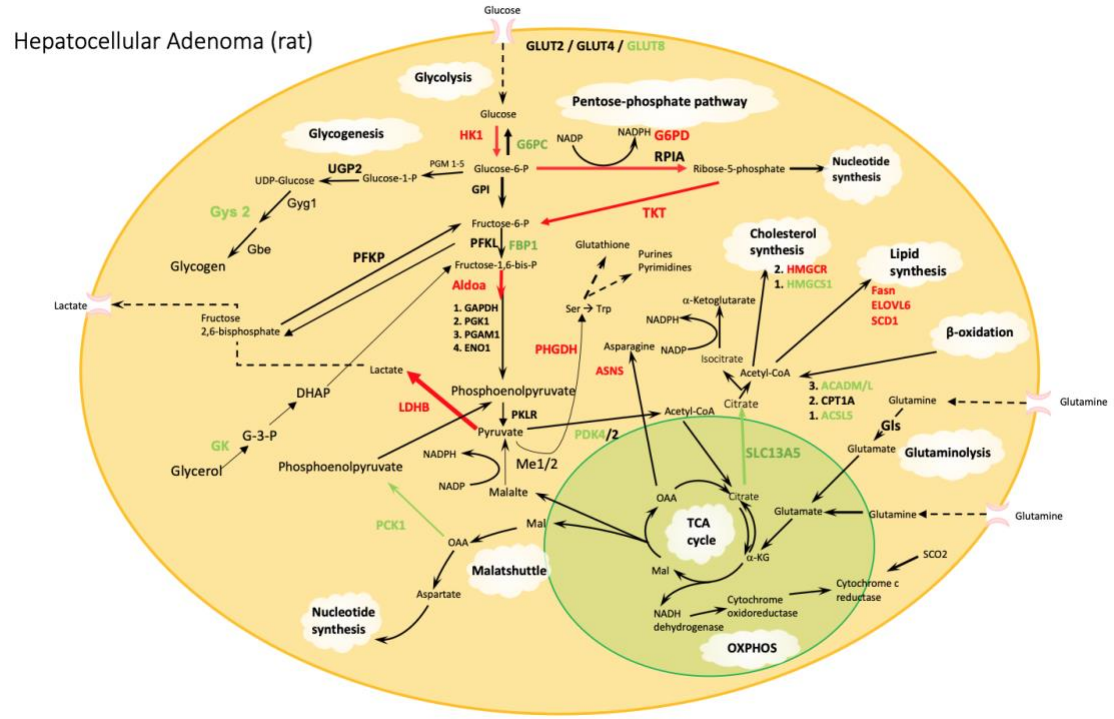

Figure 21. Illustration of the gene expression alterations in rat hepatocellular adenoma. The yellow circle depicts an HCA cell with the green circle being the mitochondrion. Upregulated genes (compared to unaltered hepatocytes) are colored red, whereas downregulated genes are colored green. For further details please see table 18 in the appendix.

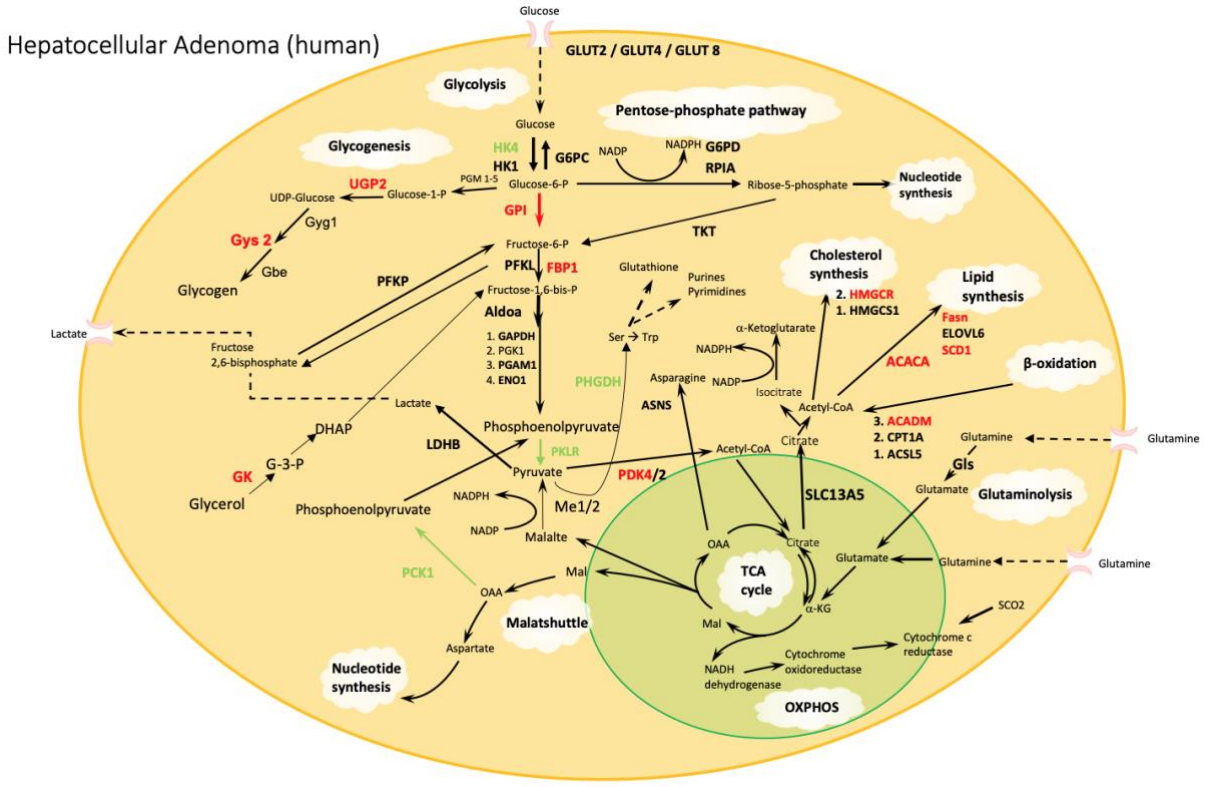

Figure 22. Illustration of the gene expression alterations in human hepatocellular adenoma cell. The yellow circle depicts an HCA cell with the green circle being the mitochondrion. Upregulated genes (compared to unaltered hepatocytes) are colored red, whereas downregulated genes are colored green. For further details please see table 18 in the appendix.

A comparison of the expression profile of insulin-regulated genes in rat and human HCA reveal highly analogous alterations in both species, i.e. more or less the same pathways were affected in a highly similar way (Fig. 22).

The upregulation of many insulin-induced genes in liver cancer prestages indicate that the lesions may show a kind of insulin-specific signature and might be “over-responsive” to the metabolic effects of insulin, e.g., the pentose phosphate pathway enzymes G6PD and TKT (connects the PPP with glycolysis), which are inducible by insulin and fundamental in tumors cells, are overexpressed in cancer prestages. Insulin may also promote the Warburg effect since crucial genes of glycolysis are changed by the hormone. To provide an example, glycolysis may be enhanced by overexpression of HK1, ALDOA/B and/or GPI and concomitant suppression of gluconeogenic enzymes, such as G6PC. Further, the glucose metabolism is predominantly shifted towards pyruvate and lactate production as indicated by an increased expression of LDHB.

All these changes are inducible by insulin, are observed at higher levels in cancer prestages than in the surrounding liver and may contribute to the development of HCC.

V.2 HepaRG™ cell line as cell culture model for HCC prestages

As already described in chapter II.9. the HepaRG™ cell line was used as cell culture model. The cell line is a human bipotent progenitor cell line characterized by its ability to differentiate into biliary-like and hepatocyte-like cells, which are well distinguishable under the microscope (dHepaRG™). The hepatocyte-like subpopulation in the differentiated dHepaRG™ cells show similar properties as mature human hepatocytes and undifferentiated HepaRG™ cell lines served as surrogate for HCC prestages (PNL, HCA). For the present study dHepaRG™ and HepaRG™ cells were used to investigate the effect of insulin and to draw indirect conclusions on the possible impact of insulin on the transition of mature hepatocytes to preneoplastic hepatocytes.

For differentiation of the HepaRG™ cell line 2.0 x 10^5 cells were seeded in 1.5 mL GM per well of a 6-well plate. They grew in GM for two weeks, then the medium was changed to DM (GM with 1.8% DMSO) for further two weeks with a medium change each week. After four weeks, dHepaRG™ cells had completed differentiation into cholangiocyte-like (biliary-like epithelial cells) and hepatocyte-like dHepaRG™ cells and were ready to use.

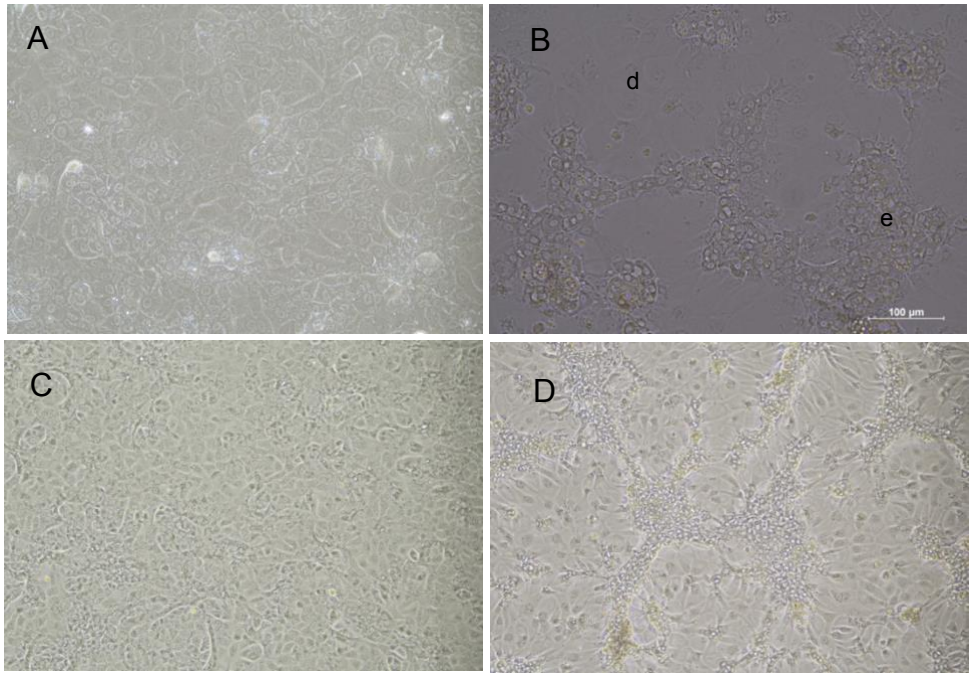

Figure 23. Inverse light microscope image of differentiated and undifferentiated HepaRG™ cells. Differentiated dHepaRG™ (**A**, **C**) and undifferentiated HepaRG™ (**B**, **D**). In **D** hepatocyte-like cells and cholangiocyte-like cells are indicated by "d" and "e" respectively. Magnificiation: x 20 in (**A**, **B**) and x 10 in (**C**, **D**).

V.3 The state of differentiation and the expression level of metabolic enzymes

dHepaRG™ and HepaRG™ cells were used to study the expression of metabolic enzymes at the differentiated and undifferentiated state. We analyzed mRNA expression of genes involved in glycolysis, glycogenesis, pentose-phosphate-pathway, lipid synthesis, cholesterol synthesis and beta-oxidation.

The basal expression levels (ΔCt values) of some important metabolic genes were compared between dHepaRG™ and HepaRG™ cells (see Fig. 24). A high ΔCt value indicates a low mRNA expression and vice versa. Overall, all genes of the four metabolic pathways (carbohydrate metabolism, pentosephosphate metabolism, cholesterol/fatty acid metabolism, amino acid metabolism) tended to be expressed at higher levels in dHepaRG™ cells than in HepaRG™ cells, which indicates a lower metabolic capacity in the dedifferentiated state.

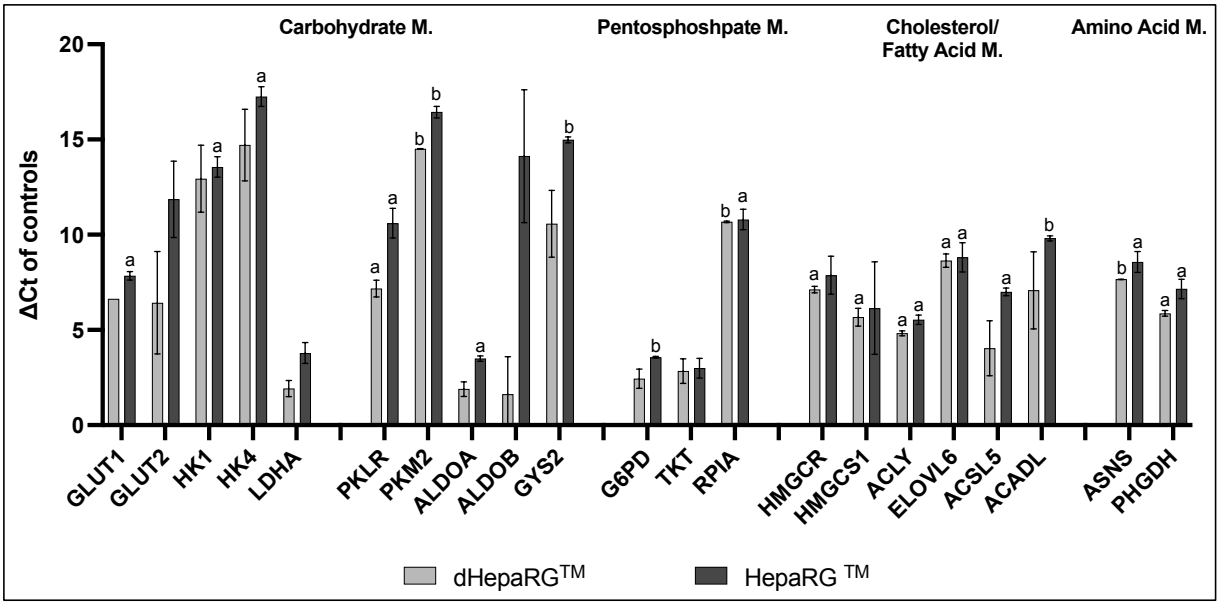

Figure 24. Basal gene expression of important metabolic genes involved in carbohydrate, pentose-phosphate, cholesterol/fatty acid and amino acid metabolism in dHepaRG™ and HepaRG™ cells. dHepaRG™ and HepaRG™ cells were seeded and after 5 days they were starved for 72 hours in serum- and insulin-free medium. RNA was extracted and transcribed into cDNA to determine mRNA by RT-qPCR. The housekeeping gene β-actin served to normalize expression levels. The ΔCt value of dHepaRG™ and HepaRG™ were calculated and depicted. Data are based on one or two independent experiments and are expressed as mean ± SEM. The statistical significance of the data was analysed by the One-Sample t-test. a: $p<0.05$, b: $p<0.01$. Abbreviation of the enzymes are as follows: glucose transporter 1 (GLUT1), glucose transporter 2 (GLUT2), hexokinase 1 (HK1), hexokinase 4 (HK4), lactate dehydrogenase A (LDHA), pyruvate kinase L/R (PKLR), pyruvate kinase M (PKM2), aldolase (ALDOA), aldolase B (ALDOB), glycogen synthase 2 (GYS2), glucose-6-phosphate dehydrogenase (G6PD), transketolase (TKT), ribose-5-phosphate isomerase (RPIA), HMG-CoA reductase (HMGCR), 3-Hydroxy-3-Methylglutaryl-CoA Synthase 1 (HMGCS1), ATP citrate lyase (ACLY), ELOVL fatty acid elongase 6 (ELOVL6), acyl-CoA Synthetase 5 (ACSL5), acyl-CoA dehydrogenase long chain (ACADL), asparagine synthetase (ASNS), phosphoglycerate dehydrogenase (PHGDH).

V.4 Effect of insulin on mRNA expression

Metabolic reprogramming of the carbohydrate metabolism is a hallmark of cancer cells (Yu *et al.,* 2017). The question was addressed whether insulin impacts on the expression of crucial genes of the carbohydrate metabolism in dHepaRG™ and HepaRG™.

GLUT1 and GLUT2 are transmembrane carrier proteins which transport glucose from the blood into liver cells. The GLUT1 mRNA expression appeared to be positively influenced by insulin since a concentration of 50nM induced an approximately 1,7-fold increased expression in dHepaRG™ cells, which remained elevated at 200nM and 1µM. In HepaRG™ cells GLUT1 transcription level reached the highest value at 200nM

insulin (approximately 1,5-fold increased). In HepaRG™ cells mRNA expression of GLUT2 was elevated with rising insulin concentrations in the medium, reaching the highest level at 1µM of insulin. In dHepaRG™ cells the opposite effect was seen, i.e., the mRNA expression decreased with rising insulin concentrations compared to conditions without insulin (see Fig. 25).

HK1 catalyzes the rate-limiting and first step of glycolysis. The diagram in fig. 25 shows that in dHepaRG™ cells the expression was increased after insulin treatment, with the highest expression at 200nM insulin. In HepaRG™ cells HK1 expression did not change significantly up to 200nM but was increased approximately 3-fold with 1µM insulin.

In analogy to HK1, HK4 (GCK) catalyzes the first step of glycolysis. Furthermore, it may increase or decrease glycogen synthesis depending on glucose levels. In dHepaRG™ cells the transcription dropped at all insulin concentrations but was elevated only at 200nM. On the other hand, HK4 expression was slightly elevated in HepaRG™ cells by insulin displaying the highest mRNA levels at 50nM insulin.

LDHA is an isoenzyme which catalyzes the conversion of the glycolysis product pyruvate into lactate. The RT-qPCR data of dHepaRG™ cells show that LDHA expression dropped after insulin treatment. The results of HepaRG™ cells show that LDHA levels were elevated steadily with rising insulin concentrations.

PKLR is expressed mainly in the liver, while PKM2 occurs predominantly in embryonic development and cancer cells. The enzymes catalyze the last step in glycolysis, namely the production of pyruvate and ATP. The RT-qPCR results of PKLR show expression changes with no specific trend in dHepaRG™ and HepaRG™ cells. In dHepaRG™ cells PKM2 transcription tended to dropp under insulin, whereas in HepaRG™ the expression was upregulated with rising insulin concentrations.

ALDOA and ALDOB are both involved in glycolysis. The RT-qPCR results show that in dHepaRG™ cells insulin caused a slight decrease of ALDOA mRNA expression at almost all concentrations. In HepaRG™ cells ALDOA gene expression was increased at higher insulin concentrations. In dHepaRG™ cells mRNA levels of ALDOB fell with

increasing insulin concentrations, while the expression was more or less unchanged in HepaRG™ cells.

GYS2 is expressed exclusively in the liver and is important for glycogen storage. The RT-qPCR results show that in dHepaRG™ an insulin concentration of 200nM led to a sharp increase of GYS2 expression. In HepaRG™ insulin positively affected the mRNA expression reaching the highest expression at 1µM insulin.

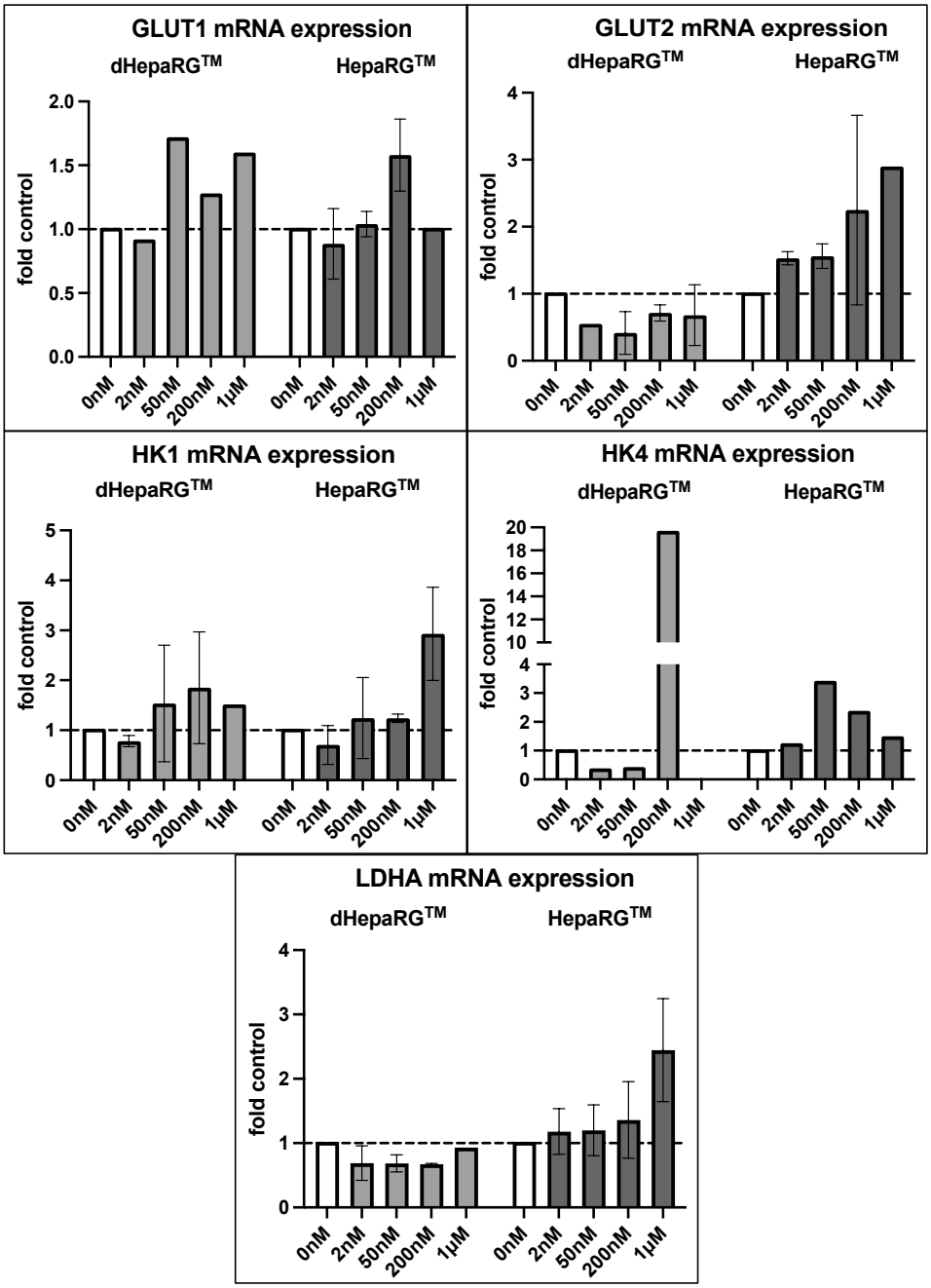

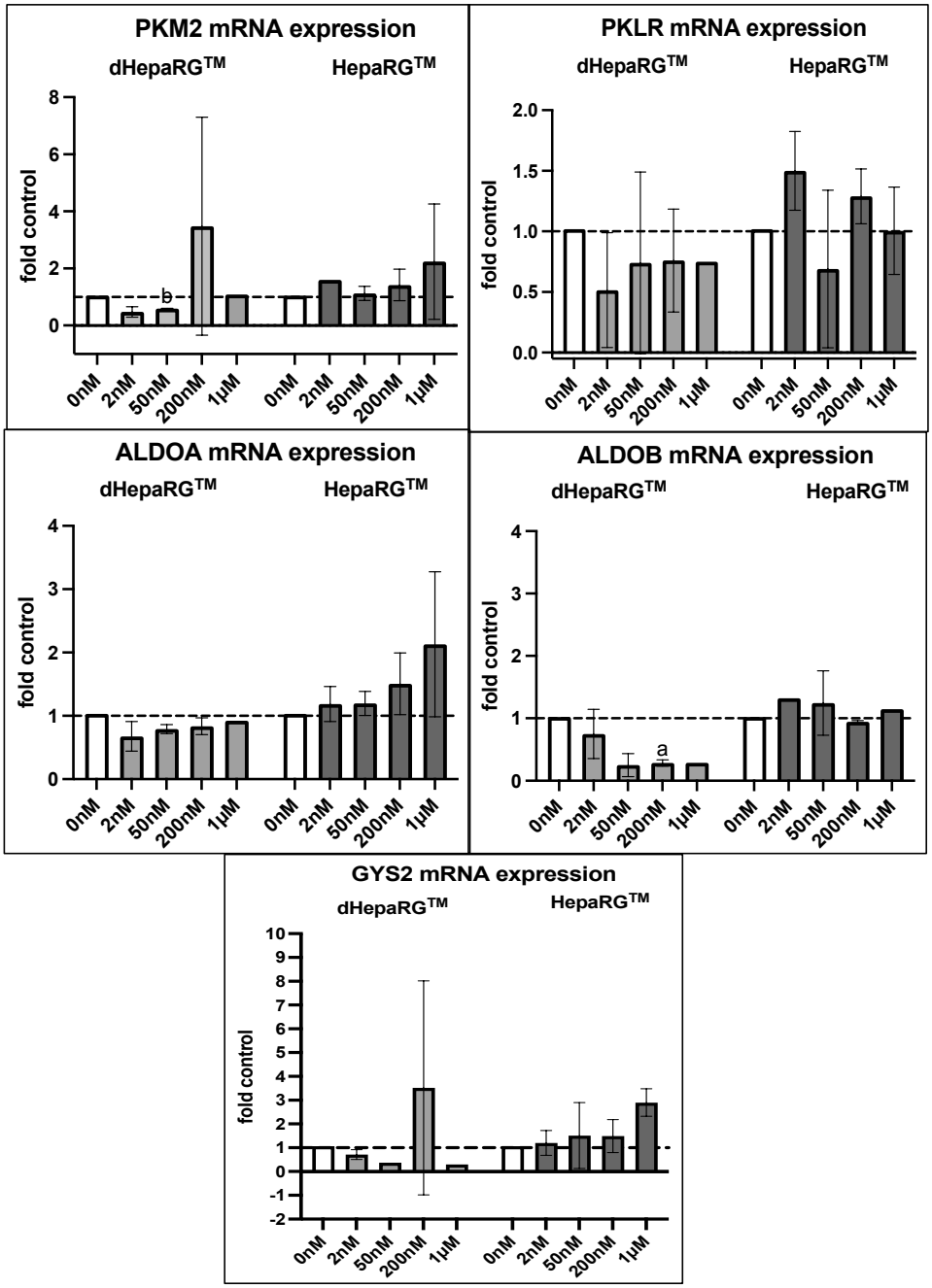

Figure 25. Effect of insulin on mRNA expression of genes involved in carbohydrate metabolism. dHepaRG™ and HepaRG™ cells were seeded and after 5 days they were starved for 72 hours in serum- and insulin-free medium. Then, the cells were treated with 0nM, 2nM, 50nM, 200nM or 1µM of insulin for 24 hours. RNA was extracted and transcribed into cDNA to determine mRNA by RT-qPCR. The housekeeping gene β-actin served to normalize expression levels. Symbols: white bars: serum- and insulin free; light grey bars: serum- free and insulin treatment. The data are normalized by expression values obtained at 0nM insulin (control), are based on one or two independent experiments, and are expressed as mean ± SEM. The statistical significance of the data was analyzed by the One-Sample t-test. a: $p<0.05$, b: $p<0.01$.

To conclude, the data indicate that insulin might have enhanced glycolysis and glycogenesis especially in HepaRG™ cells as indicated by an increased expression of GLUT2, HK1, ALDOA and GYS2. In dHepaRG™ cells the mRNA expression of HK1 was positively affected by insulin.

The pentose phosphate pathway is another critical pathway for liver cancer since it contributes to a higher nucleotide synthesis thus supporting indirectly growth of tumor cells. (Ciou *et al.,* 2015). To study whether insulin exerts effects on this pathway, RT-qPCR analysis served to determine the transcript levels of crucial pathway-components, such as G6PD, TKT and RPIA (see Fig. 26).

G6PD is the rate limiting enzyme in the pentose phosphate pathway. In both, dHepaRG™ and HepaRG™ cells G6PD expression was elevated together with increasing insulin concentrations. TKT catalyzes the reaction connecting the pentose phosphate pathway with glycolysis. In dHepaRG™ and HepaRG™ insulin positively affected TKT expression. RPIA catalyzes the conversion between ribose-5-phosphate and ribulose-5-phophate. In dHepaRG™ the expression remained nearly unchanged by insulin treatment. The RT-qPCR results of HepaRG™ give evidence that with rising insulin concentrations the mRNA expression was elevated as well.

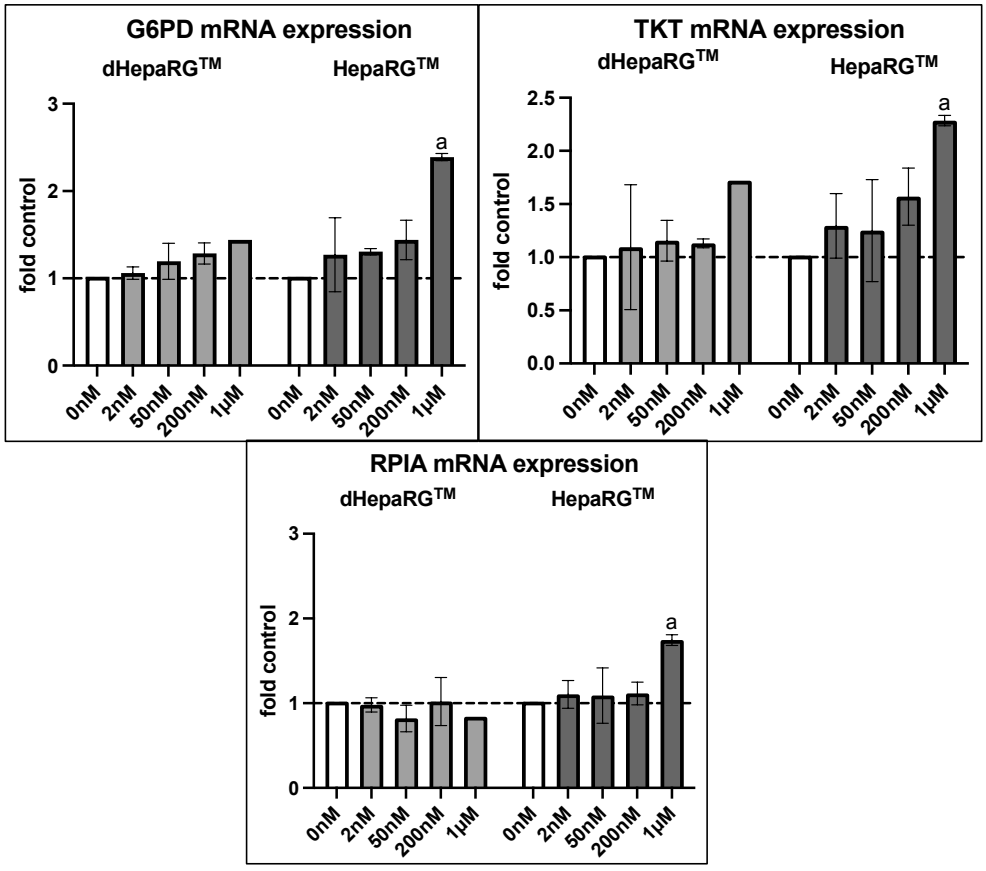

Figure 26. Effect of insulin on mRNA expression of genes of the pentose phosphate pathway. dHepaRG™ and HepaRG™ cells were seeded and after 5 days they were starved for 72 hours in serum- and insulin-free medium. Then, the cells were treated with 0nM, 2nM, 50nM, 200nM or 1µM insulin for 24 hours. RNA was extracted and transcribed into cDNA to determine mRNA by RT-qPCR. The housekeeping gene β-actin served to normalize expression levels. Symbols: white bars: serum- and insulin free; light grey bars: serum- free and insulin treatment; dark grey bars: serum-free and highest insulin concentration. The data are normalized by expression values obtained at 0nM insulin (control),

are based on one or two independent experiments and are expressed as mean ± SEM. The statistical significance of the data was analyzed by the One-Sample t-test. a: $p<0.05$, b: $p<0.01$.

To conclude, the data indicate that insulin may enhance the pentose phosphate pathway which is suggested by an upregulation of G6PD and TKT in dHepaRG™ and HepaRG™ and of RPIA in HepaRG™ cells.

Cholesterol and fatty acid metabolism are pathways which play a critical role in membrane synthesis and lipid signaling and are thus contributing to proliferation of cancer cells (Yang *et al.,* 2020). To study the effect of insulin on these metabolic pathways the gene expression of HMGCR, HMGCS1, ACLY, ACSL5, ACADL and ELOVL6 was analyzed, as shown in fig. 27.

The enzyme HMGCR is the rate-controlling enzyme of the cholesterol biosynthesis. The RT-qPCR data show that in both, dHepaRG™ and HepaRG™ cells, insulin clearly led to an increased HMGCR expression.
HMGCS1 is involved in acetyl-CoA metabolic process, the farnesyl diphosphate biosynthetic process as well as the mevalonate pathway. Insulin treatment of dHepaRG™ and HepaRG™ cells resulted in a clear upregulation of HMGCS1 expression.
ACLY is an enzyme which connects carbohydrate metabolism with fatty acid biosynthesis by converting citrate to acetyl-CoA. The RT-qPCR results of dHepaRG™ and HepaRG™ cells show that 1µM insulin caused an upregulation of the gene.
ELOVL6 elongates saturated and monosaturated fatty acids. In dHepaRG™ cells higher insulin concentrations (50nM, 200nM, 1µM) lead to an upregulation of mRNA expression which was also seen in HepaRG™ cells at 200nM and 1µM.

With regard to the degradation of fatty acid we studied two enzymes. ACSL5 is an enzyme of the β-oxidation pathway. In dHepaRG™ cells the expression clearly declined, whereas in HepaRG™ cells insulin leads to a higher expression of ACSL5 mRNA. The enzyme ACADL is involved in β-oxidation of fatty acids as well. The RT-qPCR results of dHepaRG™ cells show that the gene expression decreased with elevated insulin concentrations. In contrast, in HepaRG™ cells gene expression tended to increase under insulin.

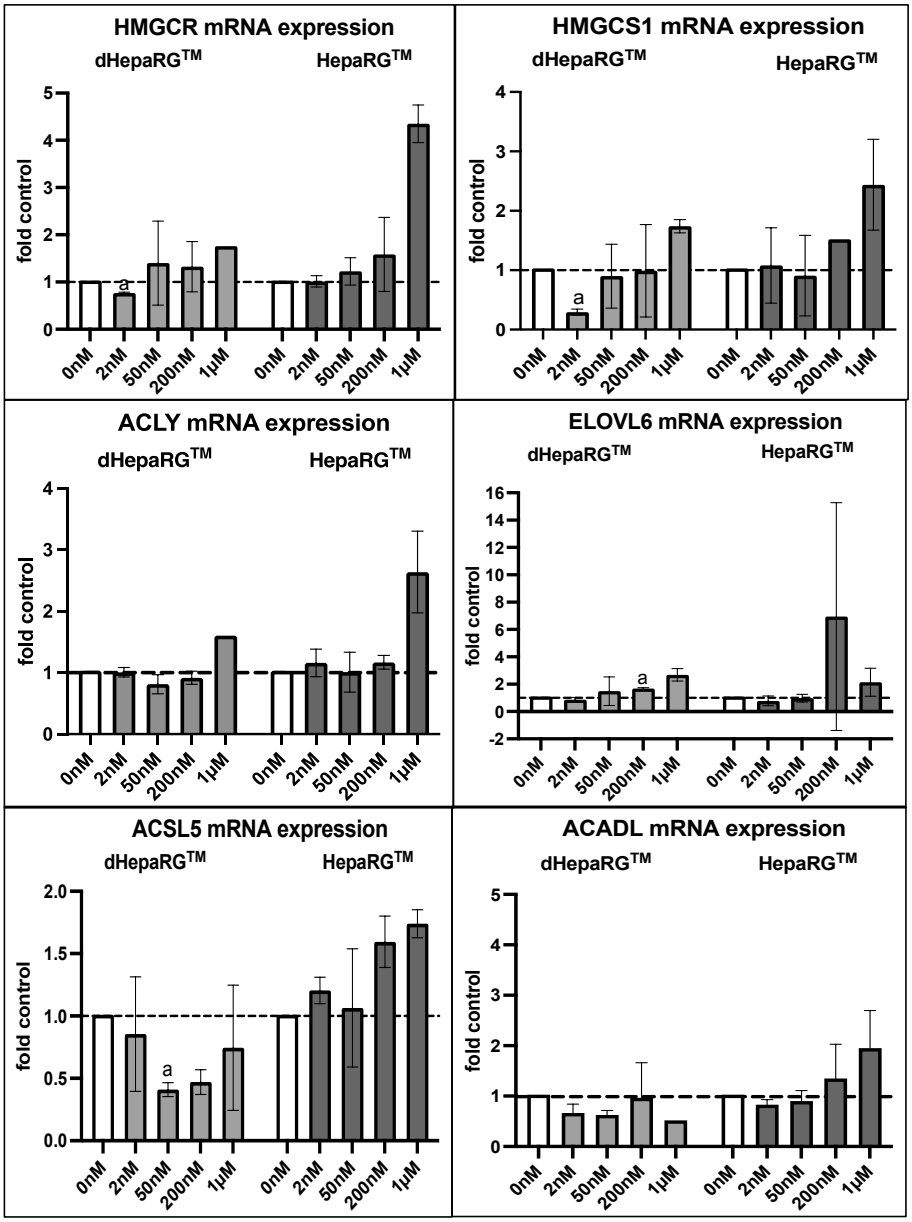

Figure 27. Effect of insulin on mRNA expression of genes in cholesterol/ fatty acid metabolism. dHepaRG™ and HepaRG™ cells were seeded and after 5 days they were starved for 72 hours in serum- and insulin-free medium. Afterwards the cells were treated with 0nM, 2nM, 50nM, 200nM or 1µM insulin for 24 hours. RNA was then extracted and transcribed into cDNA to measure mRNA levels by RT-qPCR. The housekeeping gene β-actin served to normalize expression levels. Symbols: white bars: serum- and insulin free; light grey bars: serum- free and insulin treatment; dark grey bars: serum-free and highest insulin concentration. The data are normalized by expression values obtained at 0nM insulin (control), are based on one or two independent experiments and are expressed as mean ± SEM. The statistical significance of the data was analyzed by the One-Sample t-test. a: $p<0.05$, b: $p<0.01$.

To conclude, the data suggest that insulin supports higher cholesterol/ fatty acid synthesis since both HMGCR and HMGCS1 show an increased mRNA expression in dHepaRG™ and HepaRG™ cells after a 24h of insulin treatment. ACLY and ELOVL6 are overexpressed in dHepaRG™ and HepaRG™ cells, indicating a shift towards enhanced synthesis of fatty acids. This is also supported by the observation that in

dHepaRG™ cells β-oxidation seems to be suppressed as indicated by a decreased expression of ACADL and ACSL5. Only in the dedifferentiated HepaRG™ cells β-oxidation is positively affected by relatively high insulin concentrations.

Enhanced amino acid synthesis may contribute to cancer cell development by sustaining amino acid pools which are used as important building blocks, for epigenetic modifications and bioenergy supply. To investigate the effect of insulin on this pathway the mRNA of the following enzymes was analyzed: ASNS and PHGDH.
ASNS generates asparagine from aspartate. Insulin treatment of dHepaRG™ and HepaRG™ cells showed transcriptional upregulation at higher insulin concentrations. PHGDH is crucial in L-serine biosynthesis. The RT-qPCR results show that insulin increased the mRNA expression in dHepaRG™ and HepaRG™ cell lines.

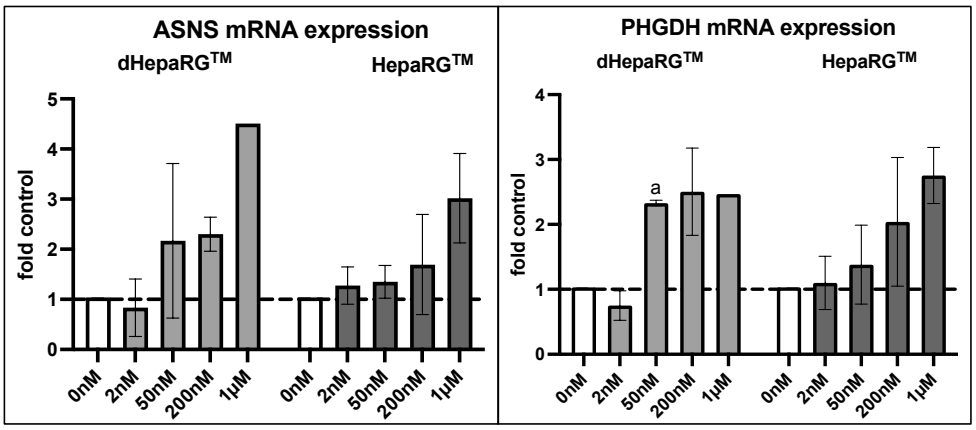

Figure 28. Effect of insulin on mRNA expression of genes in amino acid synthesis.
dHepaRG™ and HepaRG™ cells were seeded and after 5 days they were starved for 72 hours in serum- and insulin-free medium. Afterwards the cells were treated with 0nM, 2nM, 50nM, 200nM or 1µM insulin for 24 hours. RNA was then extracted and transcribed into cDNA to measure mRNA levels by RT-qPCR. The housekeeping gene β-actin served to normalize expression levels. Symbols: white bars: serum- and insulin free; light grey bars: serum- free and insulin treatment; dark grey bars: serum-free and highest insulin concentration. Data evaluation is based on one or two independent experiments and represented as mean ± SEM. The data are normalized by expression values obtained at 0nM insulin (control), are based on one or two independent experiments and are expressed as mean ± SEM. The statistical significance of the data was analyzed by the One-Sample t-test. a: $p<0.05$, b: $p<0.01$.

To conclude, the data indicate that insulin promotes amino acid synthesis both in dHepaRG™ and HepaRG™ cells which is suggested by an mRNA upregulation of ASNS and PHGDH.

V.5 Isotype expression in dHepaRG™ and HepaRG™ cells

In cancer cells regulation of alternative splicing is often disturbed which leads to cancer specific switches in isoenzyme expression patterns. Here, it was studied whether in dHepaRG™ and HepaRG™ cells the expression of isoenzymes is affected by the state of differentiation of the cells and/or by treatment with insulin. Therefore, 4 isoenzyme-pairs were examined, i.e., GLUT1/GLUT2, HK1/HK4, ALDOA/ALDOB and PKLR/PKM2.

Fourteen different glucose transporters with variable affinities for glucose have been identified in mammalian tissues. In liver cells GLUT2 is predominant, while GLUT1 has a very high affinity for glucose and therefore is often expressed in cancer cells (Hay, 2016).

Without insulin treatment the GLUT1:GLUT2 expression ratio was higher in dHepaRG™ than in HepaRG™ cells. Under influence of insulin the ratio remained fairly constant in the differentiated cells but was suppressed in the undifferentiated state. (Figure 29 panel C)

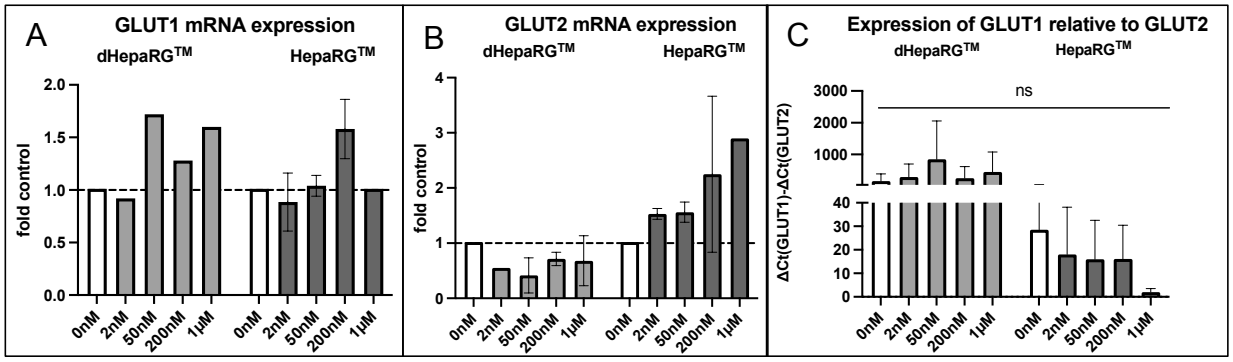

Figure 29. The effect of insulin on mRNA expression of GLUT1 and GLUT2 and the GLUT1:GLUT2 ratio in dHepaRG™ and HepaRG™ cells. Cells were seeded and after 24 hours medium was changed to serum-free medium. After 72 hours of starving, cells were subsequently treated with 0nM, 2nM, 50nM or 1µM insulin for 24 hours. Then mRNA was extracted, transcribed into cDNA and mRNA levels were measured by RT-qPCR. Expression levels were normalized by β-actin. The results are depicted as fold change relative to 0nM (control) in (**A**, **B**) or in (**C**) as ratio of the two isoforms (ΔCt(GLUT1)-ΔCt(GLUT2); $2^{-\Delta\Delta Ct}$). Symbols: white bars: no insulin treatment; light grey bars: treated insulin concentration; dark grey: highest treated insulin concentration. The data derive from one to three independent experiments and are expressed as mean ± SEM. Statistics: Data in **A** and **B** were analyzed by the One-Sample t-test; data in **C** were analyzed by one-way ANOVA: no significance was found.

In humans four genes code for different hexokinase isoenzymes. HK4 is predominant in hepatocytes and often is replaced by HK1 and/or HK2 during the transition from a normal cell to HCC (Pusec *et al.,* 2019)

In untreated controls a higher HK1:HK4 ratio was found in HepaRG™ than in dHepaRG™ cells. The ratio was elevated by insulin towards HK1 in the differentiated state but was unaltered or even suppressed at higher hormone concentrations in HepaRG™ cells (Fig. 30 panel C).

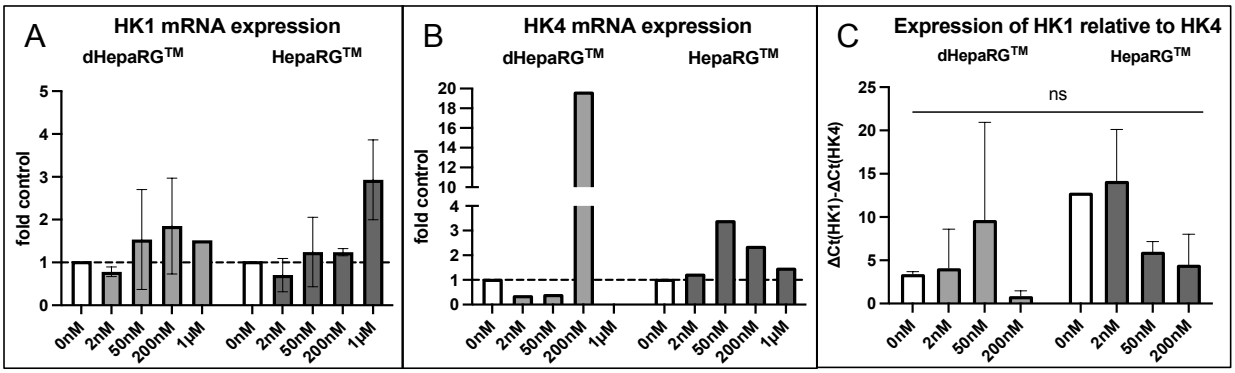

Figure 30. The effect of insulin on mRNA expression of HK1 and HK4 and the ratio of HK1:HK4 in dHepaRG™ and HepaRG™ cells. Cells were seeded and after 24 hours medium was changed to serum-free medium. After 72 hours of starving, cells were subsequently treated with 0nM, 2nM, 50nM or 1µM insulin for 24 hours. Then mRNA was extracted, transcribed into cDNA and mRNA levels were measured by RT-qPCR. Expression levels were normalized by β-actin. The results are depicted as fold change relative to 0nM in (**A**, **B**) or in (**C**) as ratio of the two isoforms (ΔCt(HK1)-ΔCt(HK4); $2^{-\Delta\Delta Ct}$). Symbols: white bars: no insulin treatment; light grey bars: treated insulin concentration; dark grey: highest treated insulin concentration. The data derive from one to three independent experiments and are expressed as mean ± SEM. Statistics: Data in **A** and **B** were analyzed by the One-Sample t-test; data in **C** were analyzed by one-way ANOVA: no significance was found.

ALDOA and ALDOB are glycolytic enzymes cleaving fructose-1,6-bisphosphate to dihydroxyacetone phosphate (DHAP) and glucose-3-phosphate. Three different genes code for three aldolase isoforms. ALDOB is the predominant form in normal differentiated hepatocytes, while HCC tend to express rather ALDOA than ALDOB (Hay, 2016). Without insulin the ratio ALDOA:ALDOB was considerably higher in the dedifferentiated than in the differentiated state of the HepaRG™ cells. dHepaRG™ cells exhibit a slightly higher expression of ALDOA:ALDOB ratios at 50 and 200nM of insulin, whereas in HepaRG™ cells the ratios remained fairly constant (Figure 31 panel C).

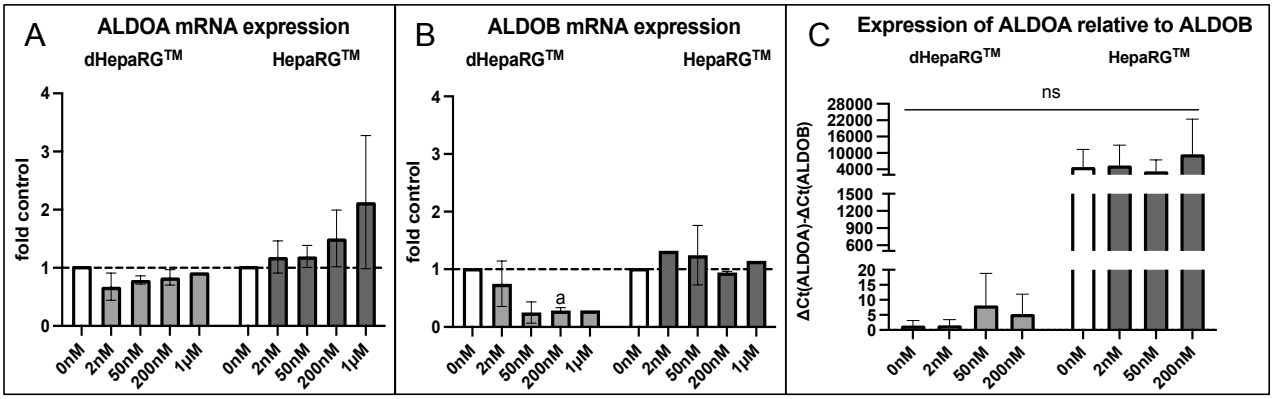

Figure 31. The effect of insulin on mRNA expression of ALDOA and ALDOB and the ALDOA:ALDOB ratio in dHepaRG™ and HepaRG™ cells. Cells were seeded and after 24 hours medium was changed to serum-free medium. After 72 hours of starving, cells were subsequently treated with 0nM, 2nM, 50nM or 1µM insulin for 24 hours. Then mRNA was extracted, transcribed into cDNA and mRNA levels were measured by RT-qPCR. Expression levels were normalized by β-actin. The results are depicted as fold change relative to 0nM in (**A**, **B**) or in (**C**) as ratio of the two isoforms (ΔCt(ALDOA)-ΔCt(ALDOB); $2^{-\Delta\Delta Ct}$). Symbols: white bars: no insulin treatment; light grey bars: treated insulin concentration; dark grey: highest treated insulin concentration. The data derive from one to three independent experiments and are expressed as mean ± SEM. Statistics: Data in **A** and **B** were analyzed by the One-Sample t-test; data in **C** were analyzed by one-way ANOVA. a: $p<0.05$, b: $p<0.01$.

Pyruvate kinase is a key enzyme in glycolysis and catalyzes the last reaction, the formation of pyruvate from phosphoenolpyruvate (PEP). It exists in four isoforms (PKM1, PKM2, PKR and PKL). In normal liver PKL is highly expressed, whereas in liver cancer cells PKM2 often is the predominant form (Hay, 2016). The PKM2:PKLR ratio was higher in untreated HepaRG™ than in dHepaRG™ cells. In the differentiated and dedifferentiated state transcription shifted towards PKM2.

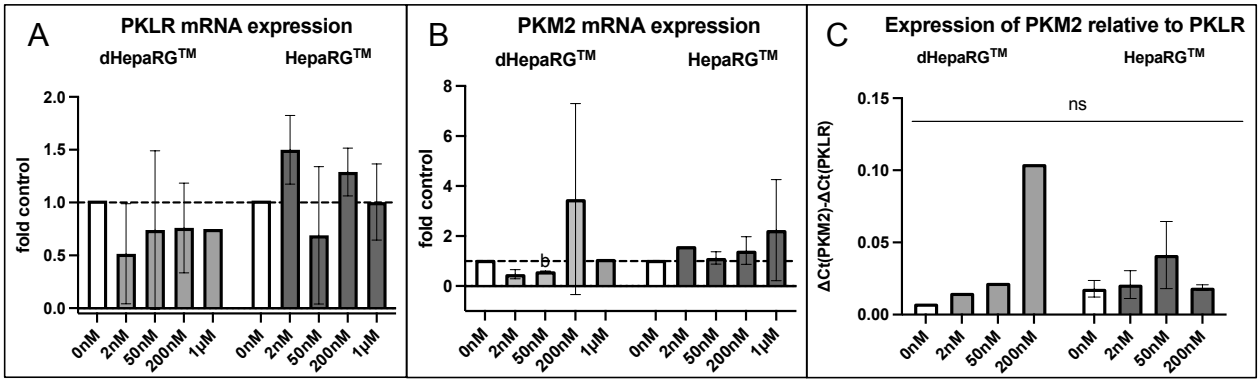

Figure 32. The effect of insulin on mRNA expression of PKLR and PKM2 and the PKM2:PKLR ratio in dHepaRG™ and HepaRG™ cells. Cells were seeded and after 24 hours medium was changed to serum-free medium. After 72 hours of starving, cells were subsequently treated with 0nM, 2nM, 50nM or 1µM insulin for 24 hours. Then mRNA was extracted, transcribed into cDNA and mRNA levels were measured by RT-qPCR. Expression levels were normalized by β-actin. The results are depicted as fold change relative to 0nM in (**A**, **B**) or in (**C**) as ratio of the two isoforms (ΔCt(PKM2)-ΔCt(PKLR); $2^{-\Delta\Delta Ct}$). Symbols: white bars: no insulin treatment; light grey bars: treated insulin concentration; dark grey: highest treated insulin concentration. The data derive from one to three independent experiments and are expressed as mean ± SEM. Statistics: Data in **A** and **B** were analyzed by the One-Sample t-test; data in **C** were analyzed by one-way ANOVA. a: $p<0.05$, b: $p<0.01$.

To conclude, the data indicate that without insulin treatment the dedifferentiated state showed a shift to the isoenzymes generally upregulated in malignancies. Only GLUT1 was expressed at higher levels in the dHepaRG™ than HepaRG™ cells (Kim *et al.,* 2017) In dHepaRG™ cells insulin tended to shift the expression ratios toward the isoenzyme usually being predominant in malignancies.

V.6 Clonogenicity and migration of dHepaRG™ and HepaRG™ cells with InsR-A or InsR-B overexpression

To study the impact of InsR-A and InsR-B overexpression in HepaRG™ cells two cell lines were established, overexpressing either the one or the other IR isoform (HepaRG™ InsR-A or InsR-B) using lentiviral transfection. HepaRG™ EC cell lines functioned as control group, as they were transfected with a vector containing no gene sequence. All three vectors carried a CMV promotor, an IRES gene, a puromycin resistance gene and an eGFP gene. Cells with a successful transduction survived in a medium containing puromycin and fluoresced green, which enabled the elimination of cells no containing the insert.

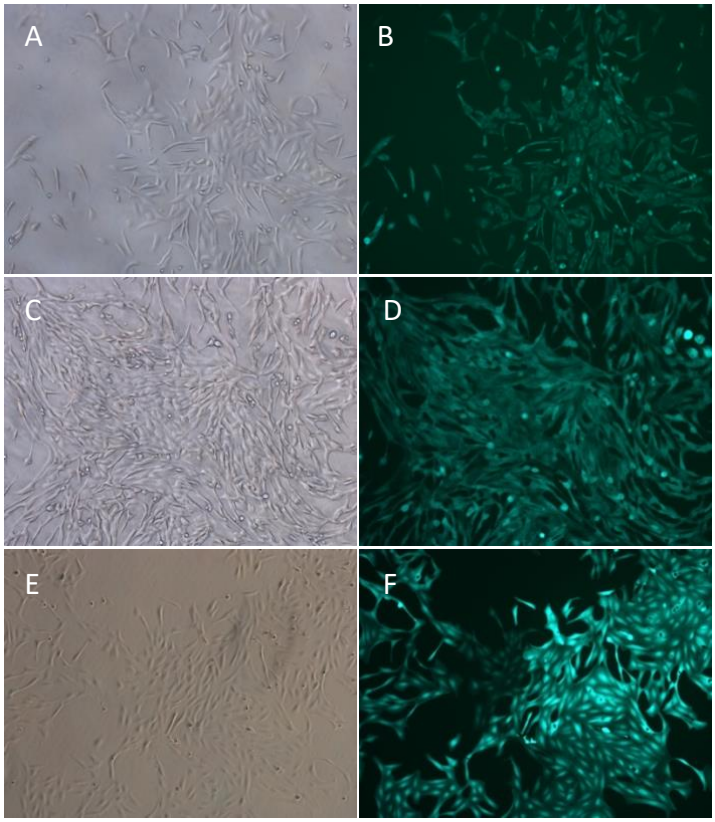

Figure 33. HepaRG™ InsR-A, InsR-B and EC cells visualized with inverse light microscopy or GFP fluorescence. HepaRG™ InsR-A (**A** and **B**), HepaRG™ InsR-B (**C** and **D**), HepaRG™ EC (**E** and **F**) with 10x magnification; left panel: visible light, right panel: GFP fluorescence.

Quantification of overexpression

To verify the successful overexpression of InsR-A and InsR-B in HepaRG™ cells, the mRNA levels of the overexpressing cell lines and the control group (HepaRG™ EC) were measured with RT-qPCR. The data of the control group in Table 17. show that the expression of InsR-B is basically higher than InsR-A.

The fold change of InsR-A and InsR-B expression in both InsR-A and InsR-B overexpressing cell lines compared to the empty control cell line was calculated in Figure 34 panel A. As indicated, InsR-B overexpression was significantly higher than InsR-A overexpression. B and C show the ratios of InsR isoforms in both overexpressing cell lines.

	HepaRG™EC	HepaRG™InsR-A	HepaRG™InsR-B
InsR-A	9,36	6,93	7,97
InsR-B	6,71	7,10	0,34

Table 17. Expression of InsR-A and InsR-B in HepaRG™ EC, InsR-A and InsR-B depicted as ΔCt values normalized with β-actin.

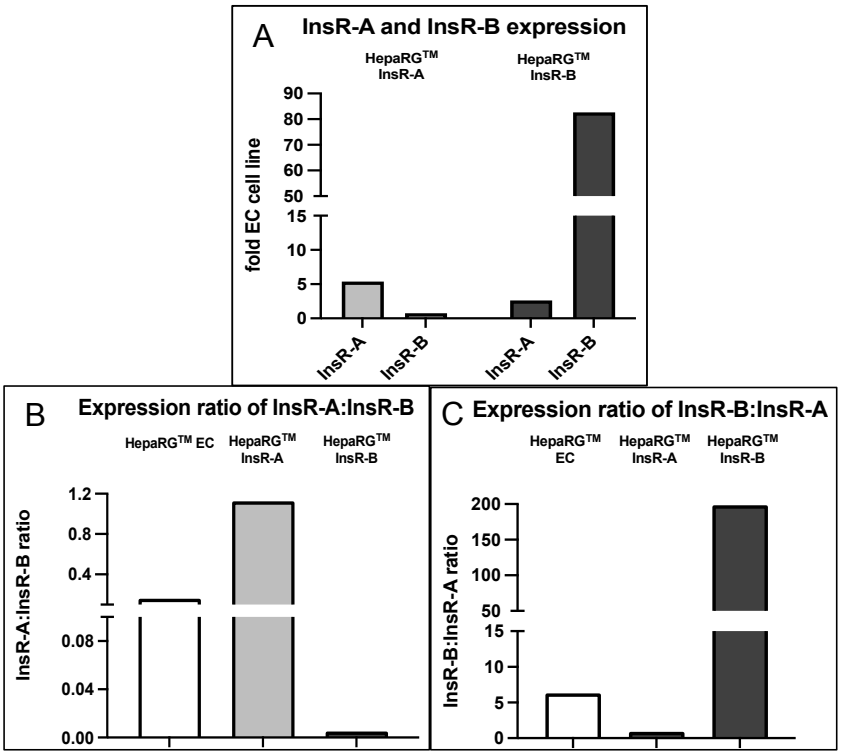

Figure 34. Quantification of InsR-A and InsR-B expression in HepaRG™ InsR-A and HepaRG™ InsR-B cell lines. Cells were cultivated in 6-well plates with 10% FCS medium. At around 90% confluency cells were harvested, mRNA was extracted, transcribed into cDNA and mRNA levels were measured by RT-qPCR. Expression levels were normalized by β-actin. The results are depicted as (**A**) fold change of InsR-A and InsR-B expression in InsR-A and InsR-B overexpression HepaRG™ cell lines relative to empty control HepaRG™ EC cell line and (**B**) as InsR-B:InsR-A ratio (ΔCt(InsR-B)-ΔCt(InsR-A); $2^{-\Delta\Delta Ct}$) and (**C**) as InsR-A:InsR-B ratio (ΔCt(InsR-A)-ΔCt(InsR-B); $2^{-\Delta\Delta Ct}$). The data arise from one experiment.

Clonogenicity Assay

The clonogenicity assay is determining the ability of a single cell to generate a colony at a low cell density, which is a characteristic feature of cancer cells. We asked whether the insulin receptor variants A or B may enhance the expression of this feature of a malignant phenotype.

dHepaRG™ cells, overexpressing the EC, InsR-A or InsR-B failed to form colonies when seeded at low density. Therefore, we used InsR-A and InsR-B overexpressing

HepaRG™ cells. As described in chapter IV.10 HepaRG™ cells were seeded at different low cell densities (1200 or 2000 per well) and were kept in a medium containing 1%, 3% or 10% FCS for 5 weeks.

Concerning the HepaRG™ EC cell line, the number of colonies tended to be elevated at higher FCS concentrations in the growth medium and when the assay was started with 1200 cells per well (Figure 35 panel A1). The colony number and size of HepaRG™ EC cells (starting with 2000 cells per well) was positively affected also by increasing FCS concentrations. The largest colony size was found when seeding 1200 cells per well and applying 1% FCS.

The results show that on average HepaRG™ InsR-B cells were able to form more colonies than HepaRG™ InsR-A cells and the clonogenicity of HepaRG™ InsR-B was elevated by increasing FCS concentrations. In contrast, HepaRG™ InsR-A cells do not form colonies at 3% and 10% FCS when starting with 2000 cells per well. Concerning the colony size per mm^2 HepaRG™ InsR-B colonies were generally larger than HepaRG™ InsR-A colonies.

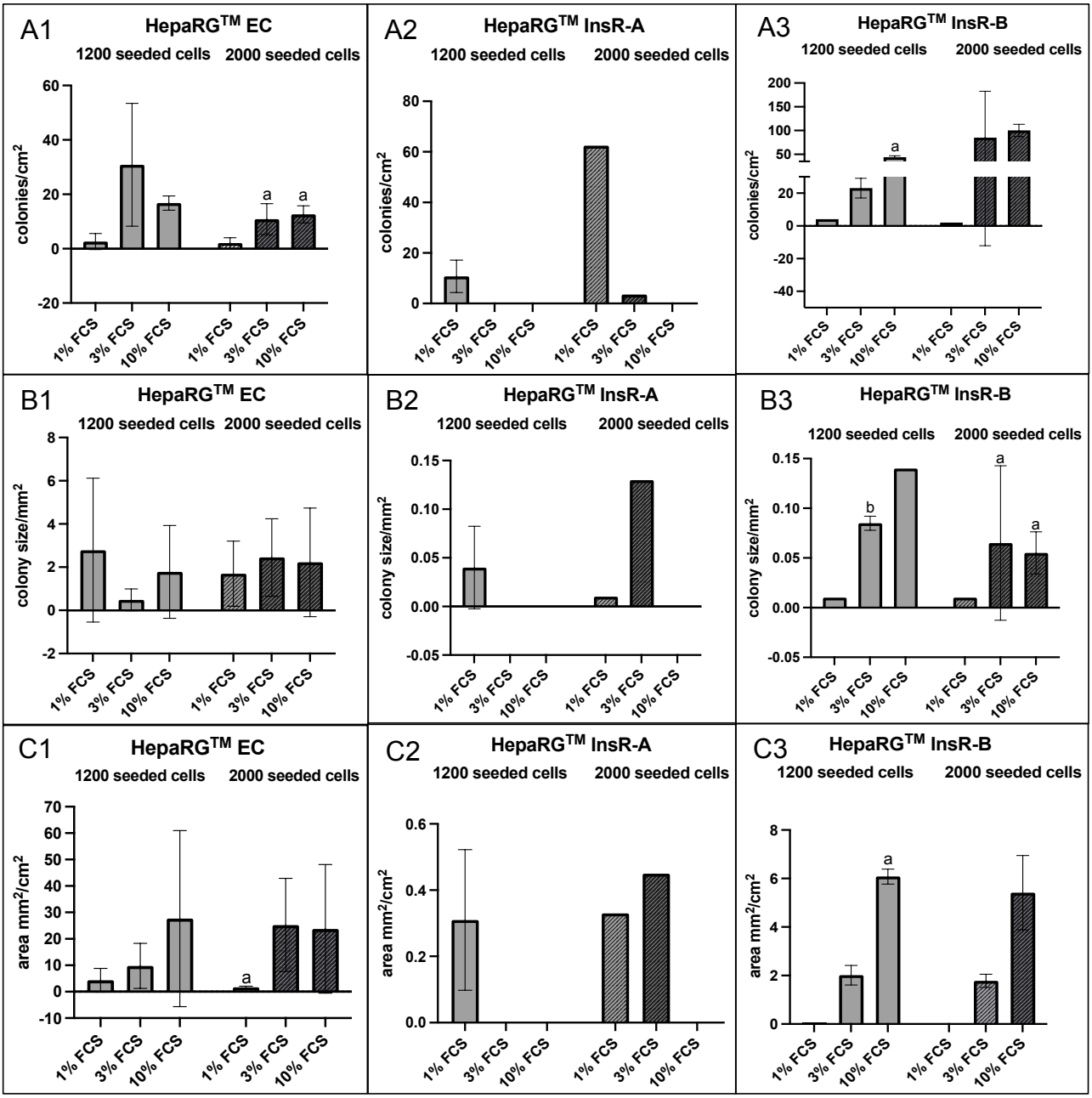

Figure 35. Effect of InsR-A and InsR-B overexpression on number, size and area of colonies formed by HepaRG™ cells. HepaRG™ InsR-A and InsR-B cells were seeded at 1200 and 2000 cells/well (6-well plate). After 24 hours cells were washed with serum free medium, GM with different FCS concentrations was added and cells were kept in the incubator for the next 5 weeks. Medium was changed once a week. Then cells were stained with crystal violet and pictures were taken. Number of colonies per cm^2 (**A1**, **A2**, **A3**), colony size per mm^2 (**B1**, **B2**, **B3**) and total area of colonies in mm^2/cm^2 (**C1**, **C2**, **C3**) were determined by using LUCIA G 4.6 software. The data derive from one to four independent experiments and are expressed as mean ± SEM. The statistical significance of the data was analyzed by the One-sample t-test. a: $p<0.05$, b: $p<0.01$.

To conclude, the data indicate that overexpression of InsR-B in HepaRG™ cells led to more and larger colonies compared to HepaRG™ EC cells. On the other hand, the overexpression of InsR-A did not promote colony formation.

Scratch Assay

For the formation of tumor cell metastasis, migration of cancer cells is required for invasion into surrounding tissues. A scratch assay was performed to determine if the overexpression of InsR-A or InsR-B in dHepaRG™ and HepaRG™ cells and/or the additional treatment with insulin alters the migratory phenotype of the cells. For this purpose, cells were seeded, cultured for one week until a confluent monolayer had formed and were subsequently starved for further 72 hours. Then the cell layer was scratched by a pipette tip followed by an insulin treatment with different insulin concentrations (0nM, 2nM, 50nM, 200nM, 1µM). After 0h, 24h, 28h, and 72h a picture of the scratch was taken under the microscope and the changed scratch area was determined. Since the differentiated dHepaRG™ InsR-A cell line did not grow well and densely these cells were excluded from the experiment.

First, it was studied whether the overexpression of InsrA or InsrB has an impact on the cells without any insulin treatment. The data indicate that HepaRG™ InsR-B cells have an increased migration compared to HeapRG™ InsR-A cells and dHepaRG™ InsR-B.

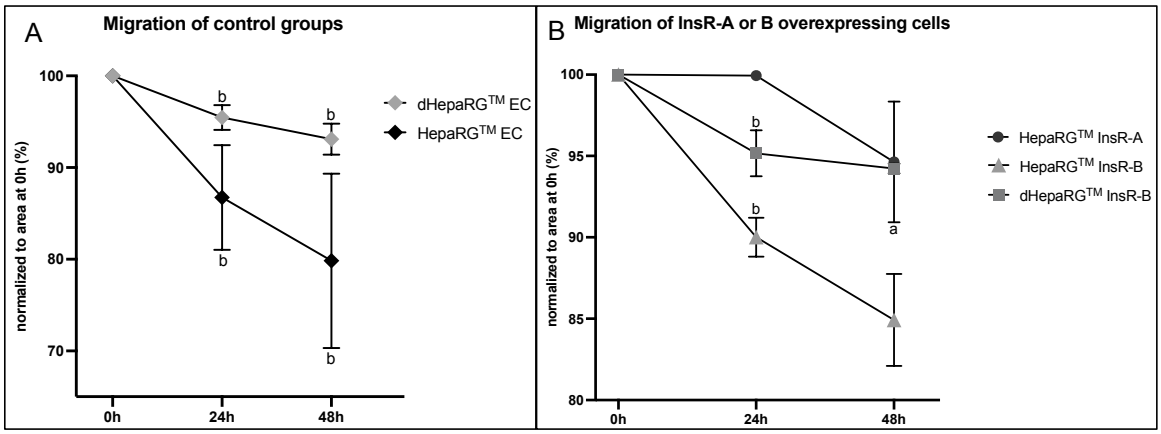

Figure 36. Effect of Insr-A or Insr-B overexpression on the migratory phenotype of dHepaRG™ and HepaRG™ cells. HepaRG™ EC, dHepaRG™ EC, HepaRG™ InsR-A, HepaRG™ InsR-B and dHepaRG™ InsR-B cells were seeded with a density of 2.0 x 10^5 cells per well, incubated for one week and starved for 72h. After scratching the cell layer, pictures of the scratch were taken after 0h, 24h, 28h and 48h, scratch area was measured by Image J program and data were normalized by the scratch area determined at 0h. The data derive from one to 4 independent experiments and are expressed as mean ± SEM. The statistical significance of the data was analyzed by the One-Sample t-test. a: $p<0.05$, b: $p<0.01$.

dHepaRG™ EC and dHepaRG™ InsR-B cells, being treated with various insulin concentrations, did not show considerable changes compared to untreated controls. The ability of HepaRG™ InsR-A cells to migrate also remained quite unchanged by the insulin treatment.

In HepaRG™ EC cells insulin treatment caused an increase in migration, i.e., enhanced reduction of scratch area was observed, starting at 2nM insulin and reaching the highest effect at 1µM insulin. Twenty-four hours after scratching and treatment with 1µM insulin the area was reduced by 20% and after 48 hours by 50%. A similar outcome was observed for HepaRG™ InsR-B cells, particularly after treatment with 1µM of insulin, i.e., insulin caused an area reduction by around 20% after 24 hours of treatment and by 40% after 48 hours.

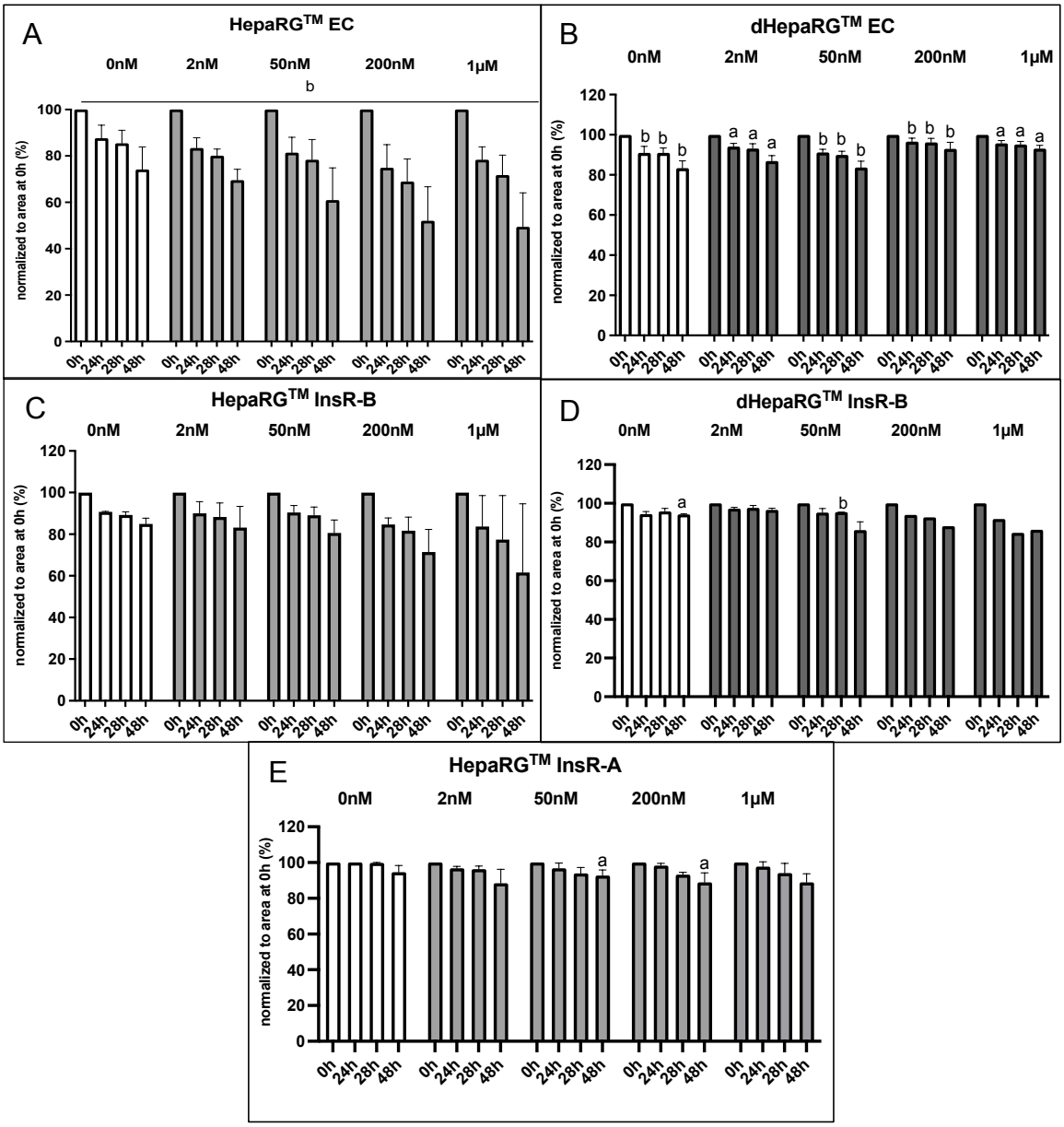

Figure 37. Effect of insulin on the migratory phenotype of InsR-A or InsR-B overexpression HepaRG™ cells. HepaRG™ EC, dHepaRG™ EC, HepaRG™ InsR-A, HepaRG™ InsR-B and dHepaRG™ InsR-B cells were seeded with a density of 2.0 x 10^5 cells per well, incubated for one week and starved for 72h. After scratching the cell layer, insulin treatment with different concentrations (0nM, 2nM, 50nM, 200nM, 1µM) was performed. Pictures of the scratch were taken after 0h, 24h, 28h and 48h, scratch area was measured by Image J program and data were normalized by the scratch area determined at 0h. The data derive from two to four independent experiments and are expressed as

mean ± SEM. The statistical significance of the data was analyzed by the One-Sample t-test. a: $p<0.05$, b: $p<0.01$.

The experiments showed that insulin positively affected the migration of HepaRG™ EC and InsR-B cells but does not influence considerably the differentiated (dHepaRG™) cell types expressing EC and InsR-B. Furthermore, the capability of HepaRG™ InsR-A cells to migrate remained unaffected by insulin.

V.7 PKM2 protein expression after insulin treatment

Published data show that PKM2 may enter the nucleus as a transcription factor which is associated with cell proliferation. The second part of the present work investigated the effect of insulin on protein expression and nuclear translocation of PKM2. For this purpose, dHepaRG™, HepaRG™ and HCC-1.2 cells were treated with different insulin concentrations (0nM, 2nM, 50nM, 200nM, 1µM) for 3h, 6h or 24h as described in chapter IV.8.1. Then, proteins were extracted from cytoplasmic and nuclear fraction (see chapter IV.9.3) and were separated via SDS-PAGE and subjected to western blotting. PKM2 and β-actin (loading control) were detected by immunostaining (Figure 38).

Figure 39 shows the PKM2 levels in the cytoplasmic and nuclear fraction after 3h, 6h or 24h of insulin treatment compared to untreated controls. At the 3h time point PKM2 levels were elevated in the nuclear fraction of dHepaRG™ and HepaRG™ cells at 200nM and 1µM insulin. At 6hrs PKM2 levels were still elevated in the nuclei of dHepaRG™ cells at 1µM insulin and of HepaRG™ cells at 200nM and at 1µM insulin. After 24h insulin treatment of dHepaRG™ and HepaRG™ cells insulin did not impact on the nuclear occurrence of the PKM2 protein. At all time points and insulin concentrations the PKM2 protein levels in the cytoplasmic fraction did not show considerable changes.

In a single experiment on HCC-1.2 cells insulin tended to increase the PKM2 levels in the nucleus and to concomitantly decrease the occurrence of the protein in the cytoplasm.

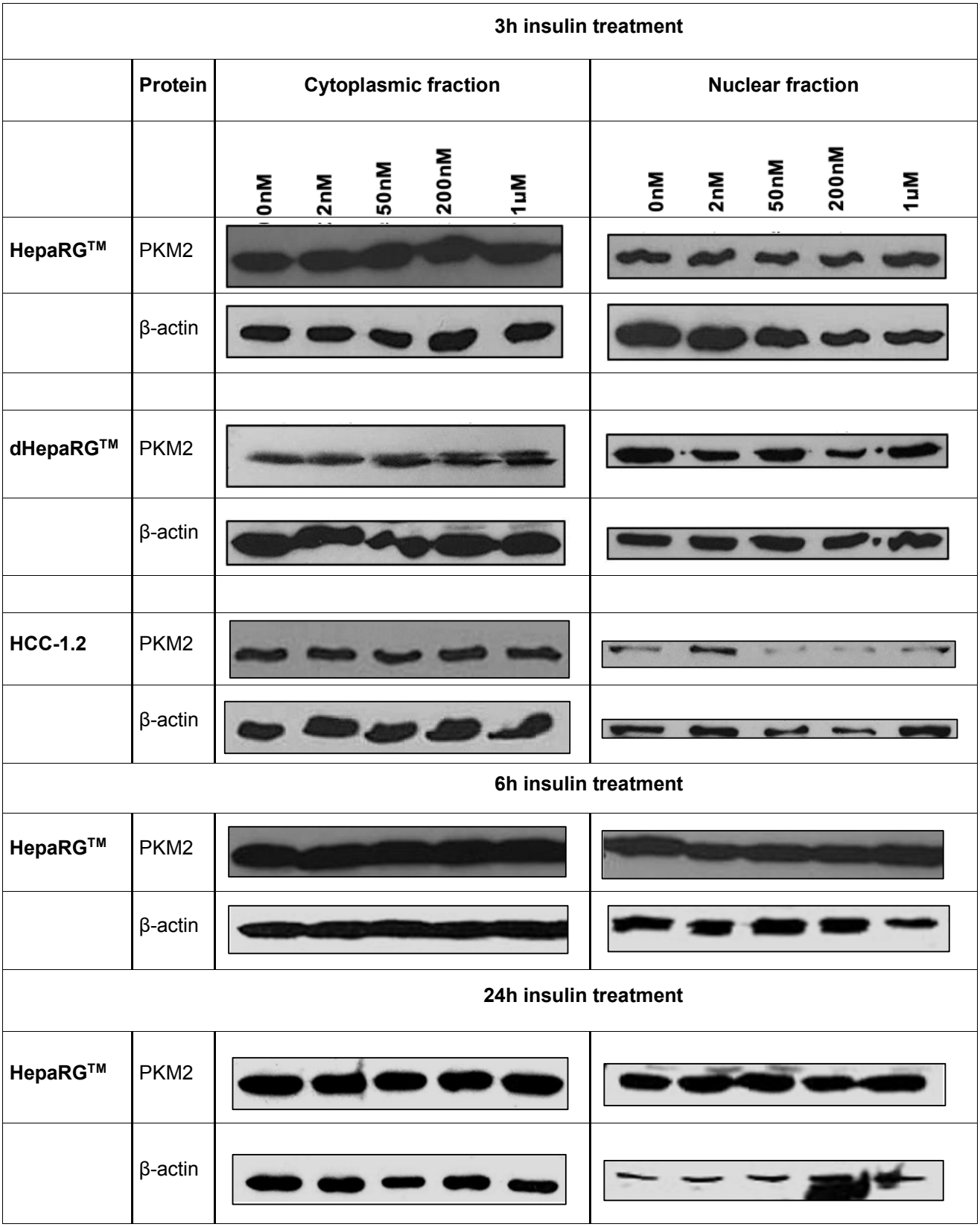

Figure 38. Effect of insulin on PKM2 protein levels in cytoplasmic and nuclear fraction of HepaRG™, dHepaRG™ and HCC-1.2 cell line. Five days after seeding HepaRG™ and dHepaRG™ cells were starved with serum- and insulin-free medium. After 72h cells were treated with 0nM, 2nM, 50nM, 200nM and 1µM insulin. After 3h cytoplasmic and nuclear fraction were extracted, and SDS-PAGE and immunoblotting was performed. The blot was then incubated with antibodies against PKM2 and β-actin as loading control.

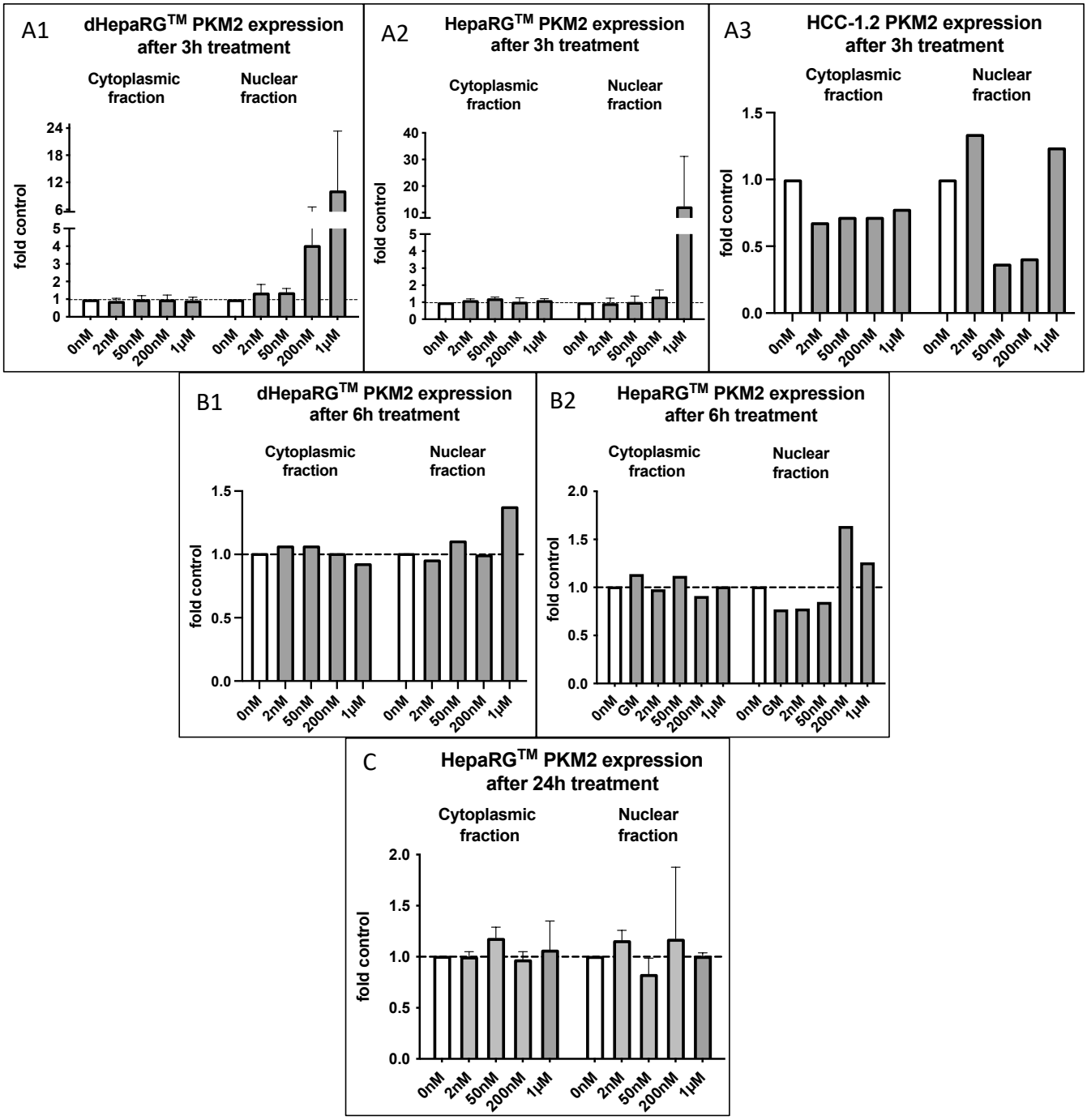

Figure 39. PKM2 protein levels after 3h, 6h, and 24h of insulin treatment. After a 3h, 6h and 24h insulin treatment of dHepaRG™, HepaRG™ and HCC-1.2 cells, PKM2 protein levels were determined by western blots. The protein levels were normalized to β-actin and fold change compared to 0nM insulin (control) was calculated and depicted in the diagram. Symbols: white bars: serum- and insulin free; light grey bars: serum-free and insulin treatment. Data are based on one or two independent experiments and are expressed as mean ± SEM: no significance was found.

To conclude, the data suggest that insulin treatment increased the PKM2 occurrence in the nuclear fraction of dHepaRG™ and HepaRG™ cells.

VI. Discussion

The question about a causal association between conditions leading to hyperinsulinemia and liver cancer development has been the topic of various cancer studies and is still not completely clarified (Vigneri *et al.,* 2020; Arcidiacono *et al.,* 2012; Jee *et al.,* 2005) In unaltered hepatocytes insulin has an impact on the expression of a number of genes which is documented by many publications (Sutherland *et al.,* 2013; O'Brien, *et al.,* 2001; Shahbazi, *et.al.,* 2019*)*. However, this hormone could be involved also in the deregulation of the metabolism and could impact on the malignant phenotype of emerging tumor cells, which is discussed below.

The first aim of this thesis was to find (i) genes which are deregulated in the liver cancer prestages PNL and HCA and (ii) indications that these gene deregulations are due to the effect of insulin. To address this problem, data of whole genome expression analysis of rat PNL and HCA were evaluated. To find out if the deregulated genes in rat samples are also up- or downregulated in human PNL and HCA a literature search was performed. Further, published data were examined for genes which are transcriptionally or post-transcriptionally influenced by insulin. The majority of metabolic genes were found to be under the influence of insulin. The literature search revealed that the hormone has an impact on crucial genes of metabolisms such as glycolysis, pentose-phosphate pathway, amino acid synthesis and fatty acid synthesis. Some of these genes are also deregulated in human or rat PNL and HCA, whereas for human PNL no conclusive data could be found.

In cancer cells metabolism is often disturbed in a way, that survival, proliferation and the formation of metastasis is supported. The Warburg effect is a hallmark of cancer cells, meaning an increased glucose intake and production of lactate via aerobic glycolysis which is an inefficient way of generating energy (Liberti *et al.,* 2016) In liver cancer cells glycolytic metabolites enter the pentose-phosphate pathway instead of the TCA cycle. This shift ensures elevated nucleic acid levels for cell replication and increased NADPH synthesis supporting invasion and angiogenesis (Kowalik *et al.,* 2017). Accordingly, the glycolysis key enzyme HK1[93] is upregulated in cancer prestages; ALDOA (Nissim 2016) as well as TKT and G6PD, both enzymes of the pentose-phosphate pathway, are overexpressed in liver cancer (Kowalik *et al.,* 2017; Lu *et al.,* 2018; Qin *et al.,* 2019). This pathway ensures elevated nucleic acid synthesis and NADPH production which is crucial for liver cancer cells to grow, proliferate and

metastasize (Kowalik *et al.,* 2017). In addition, these four genes are also transcriptionally upregulated by insulin, which supports the assumption that the hormone is involved in the metabolic reprogramming of cancer cells [7, 41, 88, 33]. (Kowalik, *et al.,* 2017; Qin *et al.,* 2019; Sangineto *et al.,* 2020)

Dysregulations in hepatocellular adenoma and carcinoma also affect the lipid metabolism, as documented by upregulation of genes involved in fatty acid biosynthesis, such as, ACACA[93, 94], ACLY[93, 94] and FASN[93, 94] (Sangineto *et al.,* 2020; Hayes & Chayama, 2019; Wang *et al.,* 2015). The enhanced synthesis of fatty acids may serve as important sources of energy, thus supporting cell division and inhibiting cell death (Hayes *et al.,* 2019; Wang *et al.,* 2015). The inhibition of fatty acid synthesis is regarded as promising therapeutic tool against cancer. Inhibition of FASN in HepG2 cells suppresses proliferation and favors apoptosis, exemplifying the importance of fatty acids for liver cancer cells. The expression of ACACA, ACLY and FASN is elevated by insulin which implies that the hormone might promote growth of HCC cells indirectly via enhanced synthesis of fatty acids. (Snaebjornsson *et al.,* 2019; Zhang *et al.,* 2020)

The next aim of this work was to study whether the altered expression of important metabolic genes in HCC may occur early in hepatocarcinogenesis during de-differentiation of hepatocytes (Song *et. al.,* 2022; Zhu *et al.,* 2020). To address the possible impact of de-differentiation dHepaRG™ (differentiated) and HepaRG™ (de-differentiated) cell lines were studied in parallel with the differentiated cells representing normal liver cells and the de-differentiated cells reflecting a phenotype on the pathway to cancer. Basal mRNA expression levels of 21 metabolic genes (from carbohydrate metabolism, pentose-phosphate pathway, cholesterol/ fatty acid synthesis and amino acid synthesis) were measured by RT-qPCR. The data showed that almost all genes (GLUT1, GLUT2, HK4, GYS2, LDHA, LDHB, PKLR, PKM2, ALDOA, ALDOB, G6PD, HMGCR, HMGCS1, ACLY, ACSL5, ACADL, ASNS and PHGDH) were expressed at higher levels in dHepaRG™ cells than in HepaRG™ cells except for a few genes (HK1, TKT, RPIA, HMGCS1 and ACLY) which were equally expressed in both differentiation states.

Our results indicate that de-differentiation is reducing the expression level of metabolic genes. These observations are consistent with the data of Ma et al. who showed that metabolic gene expression patterns changed upon dedifferentiation of thyroid cancer

cells with many genes being downregulated (Ma et al., 2019). In a model of adipogenesis, many metabolic genes were downregulated when cells de-differentiated. In detail, genes of the carbohydrate metabolism (GYS1, and PCK1), the fatty acid metabolism (ACACA, FASN and ELOVL5) and the insulin signaling pathway (FOXO1, IRS1, IRS2) were upregulated during differentiation and showed reduced expression level during dedifferentiation. (Ullah *et al.,* 2013) The data support our results that genes involved in carbohydrate and fatty acid metabolism are expressed lower in the dedifferentiated state, which appears to be a general phenomenon, occurring not only in epithelial cells but also in cells of mesenchymal origin.

The next step was to compare the impact of insulin on mRNA expression of crucial metabolic genes in dHepaRG™ and HepaRG™ cells, representing the differentiated and the de-differentiated state. We chose genes which encode key-enzymes of important metabolic pathways (carbohydrate metabolism, pentose phosphate pathway, cholesterol/ fatty acid synthesis and amino acid synthesis) and which were also subject of our previous literature search. The results showed that insulin impacts on the transcription of crucial metabolic genes in both dHepaRG™ and HepaRG™ cells, affecting all pathways. The following genes showed an elevated transcriptional level due to insulin in dHepaRG™ cells: HK1(glycolysis) and ASNS, PHGHD, and ELOVL6 (amino acid synthesis). There was a weak trend to transcriptional induction for G6PD and TKT (pentose phosphate pathway) and HMGCR and HGMCS1 (cholesterol/ fatty acid synthesis). However, a few genes were downregulated by the hormone in dHepaRG™ cells, i.e., GLUT2, LDHA, PKLR, ALDOA and ALDOB (glycolysis), RPIA (pentose-phosphate pathway) and ACSL5 and ACADL (fatty acid synthesis).
In HepaRG™ cells insulin led to an increased expression of GLUT2, HK1, ALDOA (glycolysis), GYS2 (glycogenesis), G6PD, TKT and RPIA (pentose-phosphate pathway), HMGCR, HMGCS1, ACADL, ACSL5, ELOVL6 (cholesterol/ fatty acid synthesis), and ASNS, PHGDH (amino acid synthesis). Thus, starting from a generally lower basal expression in the de-differentiated state in HepaRG™ cells, genes were probably more prone to be upregulated by insulin than in dHepaRG™ cells. These findings support to some extent the idea that the upregulation of the genes, as observed in rat PNL and HCA and human HCA in section V.1 may be due to the impact

of insulin. This raises the questions on the molecular mechanisms of the higher responsiveness of dedifferentiated liver cells to the metabolic insulin effects.
HCC, further advanced stages of hepatocarcinogenesis, exhibit deregulations of several signaling pathways, which are influenced by insulin under experimental conditions. These deregulations may indicate a changed responsiveness of the HCC cells to the hormone. An example is provided by the mTOR pathway, a regulator of cell proliferation and gene transcription, which is activated by insulin via the IRS1/PI3K/Akt pathway. (Yoon, 2017; Zou *et al.,* 2020; Khamzina *et al.,* 2005; Dif *et al.,* 2006)
For its part, mTOR is an important key player in metabolic signaling of insulin by regulating the transcription factor SREBP that controls the expression of metabolic genes, such as HMGCR, HMGCS, ACACA, FASN, ELOVL, and ALDOC. (Saxton *et al.,* 2018; Takano *et al.,* 2001; Horton *et al.,* 2003). It remains to be studied whether deregulations of insulin-induced pathways occur not only in HCC but also early in hepatocarcinogenesis.

In cancer cells the splicing regulation of gene isoforms is often changed resulting in a cancer specific isoform switch of the transcripts (Vitting-Seerup *et al.,* 2017). Since protein isoforms may have different functions, a deregulation of splicing can lead to altered signaling cascades and promote cancer development (Karakulak *et al.,* 2021). The present thesis examined if (i) the differentiation state impacts on the isoform expression and (ii) insulin is able to induce a switch which is characteristic for HCC cells. For this purpose, dHepaRG™ and HepaRG™ cells were treated with insulin and transcription levels of isoform pairs were evaluated by RT-qPCR. The data of isoform pairs HK1/HK4, ALDOA/ALDOB and PKM2/PKLR reveal that in the dedifferentiated state (HepaRG™) the isoenzyme which is generally upregulated in malignancies was expressed at higher levels leading to shifts towards HK1, ALDOA and PKM2. High expression levels of PKM2 and ALDOA, as compared to their isoforms, were also reported for HCC. (DeWaal *et al.,* 2018; Kim *et al.,* 2017; Lv *et al.,* 2018; Tang *et al.,* 2021; Cheng *et al.,* 2021; Peng *et al.,* 2008) This metabolic profile resembles the so-called Warburg effect, which is associated with higher expressions of PKM2 and ALDOA and a decreased expression of HK4 (GCK) when compared to the respective isoenzymes (Lee *et al.,* 2018; DeWaal *et al.,* 2018). Our results further show an insulin-induced shift towards a cancer specific expression in the dHepaRG™ cell line since the ratios of ALDOA:ALDOB and PKM2:PKLR tended to be elevated. In HepaRG™

cells the ratios of ALDOA:ALDOB, HK1:HK4 and PKM2:PKLR were already high and could not be further elevated by insulin. This may indicate that the isoform switch had been caused already by the dedifferentiated state and was not further inducible. This is not consistent with published data, which indicate that insulin is able to induce this cancer specific PKM2 switch in HepG2 cells (Iqbal *et al.,* 2013). In hepatoma cells expression switches from PKLR towards PKM2 which might be advantageous due to distinct functional characteristics of the isoforms such as the function of PKM2 as transcriptional regulator (Dayton *et al.,* 2016; Gao *et al.,* 2012).

Another frequent isoform switch in carcinogenesis is the shift from Insr-B to Insr-A. InsR-A and InsR-B are the two isoforms of IR, produced by alternative splicing. InsR-B is predominantly expressed in liver and associated with metabolic and differentiating signals. Instead, the InsR-A isoform is prevalent in fetal and cancer tissues such as HCC and is known to play a major role in cell growth, proliferation and survival (Belfiore *et al*., 2017; Benabou *et al.,* 2019; Malaguarnera & Belfiore, 2011).
The present work examined if InsR-A - contrary to InsR-B - might be a key factor in cancer development by pushing cancer cell prestages towards a malignant phenotype. To test this hypothesis two cell lines were established, overexpressing one of the IR isoforms. Cell-biological assays were performed to test the malignant phenotype, i.e. the clonogenicity and the migratory capabilities of the cell lines generated. The formation of a clone from just one cell is a characteristic feature of cancer cells and differentiates them from normal cells. The clonogenicity assay showed that in the absence of insulin-treatment InsR-B overexpression led to the formation of more and larger colonies in contrast to InsR-A overexpression which did not seem to promote colony formation. Similar observations were reported by other groups confirming our data. Massimino, et al. showed that in absence of insulin InsR-B expressing murine fibroblast cells are better protected against apoptosis compared to InsR-A expressing cells. When insulin is bound, both IR isoforms promote cell growth but InsR-A expressing cells show greater effects. In addition, Perks, et al. showed that prostate cancer cells with active InsR-A but silenced InsR-B were inhibited in cell growth due to a disabled response to insulin. These data indicate that InsR-B may support survival pathways which may increase the chance that cells survive at low cell density, increasing the probability for clone formation. (Perks *et al.,* 2016)

In contrast studies showed that changes in InsR-B:InsR-A ratio triggers ligand-independent apoptosis in hepatocytes. Cells expressing only InsR-A take up more glucose than immortalized liver cells expressing only InsR-B. In consequence this might lead to lower apoptosome formation which suppresses apoptosis. (Nevado *et al.,* 2008)

The scratch assay determines the ability of cells to migrate which is a requirement for cancer cells to metastasize. The results reveal that the control cell line and the InsR-B overexpressing cell line show enhanced migration compared to InsR-A overexpressing cells. After insulin treatment InsR-A overexpressing cells remained unaffected whereas migration of HepaRG^{TM} InsR-B and EC positively affected by insulin. In disagreement with our results published data reveal that InsR-A transfected HepG2 cells show increased migration after insulin treatment, whereas InsR-B transfected cells show the opposite effect (Malaguarnera & Belfiore, 2014).Similar observations were made in colon cancer cells (Andres *et al.,* 2013) In addition, overexpression of InsR-A compared to InsR-B was shown to promote migratory and invasive properties of liver cancer cells (Benabou *et al.,* 2019; Wang *et al.,* 2019).

The establishment of HepaRG^{TM} InsR-A and InsR-B cells via lentiviral transduction resulted in a higher overexpression of InsR-B compared to InsR-A. InsR-B is the isoform expressed predominately in mature hepatocytes whereas InsR-A is expressed in undifferentiated cells and cancer cells (Chettouh, *et al.,* 2015; Vella *et al.,* 2018; Massimino *et al.,* 2021). Interestingly, our data disagree since we observed a higher expression of InsR-B in the undifferentiated control group (HepaRG^{TM} EC). Furthermore, Gutmann showed in his master thesis 2020 that InsR-B is predominantly expressed in human HCA and HCC. Based on these studies and the expression data of our control group InsR-B might be the predominant isoform in differentiated as well as undifferentiated liver cells. These observations could explain the advantage of InsR-B overexpressing cells in developing a malignant phenotype.

The present thesis was also interested in the question whether insulin induces the translocation of PKM2 into the cell nucleus. In cancer cells, the PKM2 tetramer may be modified post-translationally to form a dimer which is capable to enter the nucleus. (Zahra *et al.,* 2020). Studies showed that insulin induced the dissociation of the tetramer into the PKM2 dimer form (Iqbal *et al.,* 2013; Prakasam *et al.,* 2018). To examine the impact of insulin on the nuclear PKM2 occurrence, differentiated and

dedifferentiated HepaRG™ cells and HCC-1.2 cells were treated with insulin. Western blot analysis showed that insulin caused elevated the PKM2 levels in the nucleus of dHepaRG™ and HepaRG™ cells and probably also in the HCC-1.2 cell line (Alquaraishi et al., 2019; Liu *et al.,* 2021; Zahra *et al.,* 2020) Xu, et al. (2015) showed that activation of IGF-1/IGF-IR (insulin-like growth factor 1 receptor) induces nuclear transfer of PKM2 and it is known that insulin is able to bind and activate this receptor as well (Taniguchi *et al.,* 2016; Cai *et al.,* 2017) Further, Teng et al. (2016) showed that ERK1/2 is activated by insulin and Yang et al. (2012) revealed that ERK1/2 in turn phosphorylates PKM2 which enables its transfer into the nucleus. Nuclear PKM2 was shown to be an important for the mTOR-induced Warburg effect by directly regulating the expression of genes involved in the cell cycle (cyclin D1, c-Myc) and cell proliferation (Oct-4, HIF-1α). C-Myc, in turn, upregulates transcription of genes involved in glucose metabolism (GLUT1, LDHA, ALDOA, PKM2). Accordingly, a disruption of mTOR pathway or PKM2 suppressed cell proliferation and tumorigenesis (Sun *et al.,* 2011; Wiese *et al.,* 2018; Yang *et al.,* 2013; Dong *et al.,* 2020)

Zhao et al. found that PKM2 stabilizes the transcription factor SREBP-1a and thereby activates lipid synthesis, e.g. genes of cholesterol and fatty acid synthesis, such as HMGCR and FASN, are positively regulated by SREBP-1a (Zhao *et al.,* 2018; Madison et al., 2016). Our results showed an insulin-induced nuclear PKM2 translocation and concomitant upregulation of ALDOA, LDHA, PKM2, FASN and HMGCR in HepaRG™ cells which might be the link between insulin action and metabolic reprogramming of emerging cancer cells.

In summary, the data suggest that insulin may induce a metabolic reprogramming in early stages of hepatocarcinogenesis, which may involve PKM2 translocation to the nucleus. Insulin may also favor the development of a malignant phenotype, as indicated by enhanced clonogenicity and migration. Further research is necessary to characterize thoroughly the effects of insulin in emerging liver tumor cells.

VII. Abbreviations

Abbreviation	Explanation
ACC	acetyl-CoA-carboxylase
Acetyl-CoA	Acetyl-coenzyme A
ACLY	ATP citrate lyase
ADP	Adenosine diphosphate
Akt (PKB)	Proteinkinase B
AldoA	Aldolase A
AP-1	Activator protein-1
ATP	Adenosine triphosphate
bp	base pairs
Cdk	Cyclin dependent kinase
cDNA	complementary DNA
ddH_2O	Double-distilled H_2O
DEPC	Diethyldicarbonate
DMSO	Dimethyl sulfoxid
DNA	Deoxyribonucleic acid
dNTP	Deoxynucleotide triphosphate
EC	Empty control
EGF	Eepidermal growth factor pidermal growth factor
ENO1	Enolase 1
ERK	Extracellular signal-regulated kinase
E2F	E2 factor
$FADH_2$	Flavin adenine dinucleotide
FAS, FASN	Fatty acid synthase
FBP	Fructose-1,6-bisphosphatase
FBS	Fetal bovine serum
FCS	Fetal Calf serum
FOXO	Forkhead box-containing protein, O subfamily
FoxO1	Forkhead box-containing protein, O subfamily 1
GAPDH	Glyceraldehyde-3-phosphate dehydrogenase
GFP	Green Fluorescent Protein
GLUT	Glucose transporter

GM	Growth Medium
GPI	Glucose-6-phosphate isomerase
Grb2	Growth factor receptor-bound protein 2
GSK3	Glycogen synthase kinase 3
G6PC	Glucose-6-phosphatase
G6PD	Glucose-6-phosphate dehydrogenase
HCC	Hepatocellular Carcinoma
HGF	Hepatocyte growth factor
HK	Hexokinase
HMGA1	High mobility group AT-Hook 1 protein
HMGCR	3-hydroxy-3-methylglutaryl-CoA reductase
hnRNP	Heterogenous nuclear ribonucleoprotein
HK1	Hexokinase 1
HTFIR	hepatocyte-specific transcription factor of the insulin receptor gene
IGF-2	Insulin-like growth factor 2
IGFBP	insulin-like growth factor binding protein
IL-6	Interleukin 6
Ins	Insulin gene
$InsP_3$	Inositol 1,4,5-triphosphate
InsR-A, IR-A	Insulin receptor A isoform
InsR-B, IR-B	Insulin receptor B isoform
InsR, IR	Insulin receptor
IRNF-I, IRNF-II	Insulin receptor nuclear factors I and II
IRS-1, IRS-2	Insulin receptor substrate 1,2
HBV	Hepatitis B virus
HCC	Hepatocellular carcinoma
HCV	Hepatitic C virus
HIF-1α	Hypoxia inducible factor-1α
HMGA1	High-mobility group protein A1
LDH	Lactate dehydrogenase
MAPK	Mitogen-activated protein kinase
MCP-1	Monocyte chemoattractant protein

MEK	Mitogen-activated protein kinase kinase
MIF	Migration inhibition factor
MMP-9	Matrix metalloproteinase-9
mRNA	Messenger ribonucleic acid
mTOR	Mammalian target of rapamycin
mTORC1	Mammalian target of rapamycin conplex 1
NADH	Nicotinamide adenine dinucleotide
NADPH	Nicotinamide adenine dinucleotide phosphate
NAFLD	Nonalcoholic fatty liver disease
NFkB	Nuclear factor kB
Oct 4	Octamer binding transcription factor
PEP	Phosphoenolpyruvate
PEPCK	Phosphoenolpyruvate carboxylase
PDC	Pyruvate dehydrogenase complex
PDH	Pyruvate dehydrogenase
PDK4	Pyruvate dehydrogenase kinase 4
PGAM1	Phosphoglycerate mutase 1
PIN1	Peptidyl-prolyl cis-trans isomerase
PI3K	Phosphatidylinositol 3-kinase
PIP2	Phosphatidylinositol-4,5-triphosphate
PIP3	Phosphatidylinositol-3,4,5-triphosphate
PPI	Protein phosphatase I
PPP	Pentose-phosphate pathway
PK	Pyruvate kinase
PKLR	Pyruvate kinase liver and red blood cells
PKL	Pyruvate kinase liver
PKM	Pyruvate kinase muscle
PKR	Pyruvate kinase erythrocytes
pRb	Retinoblastoma protein
RT-qPCR	Real Time Quantitative polymerase chain reaction
Raf	Rapidly accelerated fibrosarcoma
Ras	Rat sarcoma

RNA	Ribonucleic acid
ROS	Reactive oxygen species
RPI	Ribose-5-phosphate isomerase
rpm	Rounds per minute
RT	Room temperature
RTK	Receptor tyrosine kinase family
SCD1	Stearoyl-CoA desaturase
SDS-PAGE	Real time qPCR
SEM	Standard error of the mean
SHC	Src homology 2 domain containing protein
SHGB	Sex hormone-binding globulin
SP1	Spesific protein 1
SREBP	Sterol regulatory element-binding proteins
SRSF1	Serine/arginine-rich splicing factor 1
STAT3	Signal transducer and activator of transcription 3
TF	Tissue factor
TCA	Tricarboxylic acid
TGFα	Transforming growth factor alpha
TGFβ1	Transforming growth factor beta 1
TNFα	Tumor necrosis factor
T2DM	Type-2 diabetes mellitus
UV	Ultra violet
β-cat	β-catenin

VIII. References

Abu Rmilah, A. A., Zhou, W., & Nyberg, S. L. (2020). Hormonal Contribution to Liver Regeneration. *Mayo Clinic Proceedings: Innovations, Quality & Outcomes*, *4*(3), 315–338. https://doi.org/10.1016/j.mayocpiqo.2020.02.001

Alquaraishi, M., Puckett, D.L., Alani, D.S., Humidat, A.S., Frankel, V.D., Danohoe, D.R., Whelan, J., & Bettaieb, A. (2019). Pyruvate Kinase M2: A simple molecule with complex functions. *Free radical biology & medicine, 143,* 176–192. https://doi.org/10.1016/j.freeradbiomed.2019.08.007

Amaya, M. J., Oliveira, A. G., Guimarães, E. S., Casteluber, M. C. F., Carvalho, S. M., Andrade, L. M., Pinto, M. C. X., Mennone, A., Oliveira, C. A., Resende, R. R., Menezes, G. B., Nathanson, M. H., & Leite, M. F. (2013). The insulin receptor translocates to the nucleus to regulate cell proliferation in liver. *Hepatology*, *59*(1), 274–283. https://doi.org/10.1002/hep.26609

Andres, S.F., Simmons, J.G., Mah, A.T., Santoro, A., Landeghem, L.V., & Lund, P.K. (2013). Insulin receptor isoform switching in intestinal stem cells, progenitors, differentiated lineages and tumors: evidence that IR-B limits proliferation. *Journal of Cell Science, 126(24), 5645–5656.* https://doi.org/10.1242/jcs.132985

Arcidiacono, B., Iiritano, S., Nocera, A., Possidente, K., Nevolo, M.T., Ventura, V., Foti, D., Chiefari, E., & Brunetti, A. (2012). Insulin Resistance and Cancer Risk: An Overview of the Pathogenetic Mechanisms. *Journal of Diabetes Research*. https://doi.org/10.1155/2012/789174

Boucher,J., Kleinridders ,A., & Kahn, C.R. (2014). Insulin Receptor Signaling in Normal and in Insulin-Resistand States. *Cold Spring Harbor Perspectives in Biology, 6*(1). PMID: 24384568

Beaufrère, A., & Paradis, V. (2021). Hepatocellular adenomas: review of pathological and molecular features, *Human Pathology, 112,* 128–137. https://doi.org/10.1016/j.humpath.2020.11.016

Belfiore, A., Frasca, F., Pandini, G., Sciacca, L., & Vigneri, R. (2009). Insulin Receptor Isoforms and Insulin Receptor/Insulin-Like Growth Factor Receptor Hybrids in Physiology and Disease. *Endocrine Reviews 30*(6)*,* 586–623. https://doi.org/10.1210/er.2008-0047

Benabou, E., Salamé, Z., Wendum, D., Lequoy M., Tahraoui, S., Merabtene, F., Chrétien, Y., Scatton, O., Rosmorduc, O., Fouassier, L., Fartoux, L., Praz, F., & Desbois-Mouthon, C. (2019). Insulin receptor isoform A favors tumor progression in human hepatocellular carcinoma by increasing stem/progenitor cell features. *Cancer Letters, 450,* 155–168. https://doi.org/10.1016/j.canlet.2019.02.037.

Cai, W., Sakaguchi, M., Kleinridders, A., Gonzalez-Del Pino, G., Dreyfuss, J. M., O'Neill, B. T., Ramirez, A. K., Pan, H., Winnay, J. N., Boucher, J., Eck, M. J., & Kahn, C. R. (2017). Domain-dependent effects of insulin and IGF-1 receptors on signalling and gene expression. *Nature communications*, *8*, 14892. https://doi.org/10.1038/ncomms14892

Chen, H., Wu, Q., Peng, L., Cao, T., Deng, M.L., Liu, Y.W., Huang, J., Hu, Y., Fu, N., Zhou, K.B., Yang, M.L., & Yang, X.F. (2021). *Journal of Nanomaterials.* https://doi.org/10.1155/2021/5164100

Chettouh, H., Lequoy, M., Fartoux, L., Vigouroux, C., & Desbois-Mouthon, C. (2015). Hyperinsulinaemia and insulin signalling in the pathogenesis and the clinical course of hepatocellular carcinoma. *Liver International, 35*(10), 2203–2217. https://doi.org/10.1111/liv.12903

Ciou, S. C., Chou, Y. T., Liu, Y. L., Nieh, Y. C., Lu, J. W., Huang, S. F., Chou, Y. T., Cheng, L. H., Lo, J. F., Chen, M. J., Yang, M. C., Yuh, C. H., & Wang, H. D. (2015). Ribose-5-phosphate isomerase A regulates hepatocarcinogenesis via PP2A and ERK signaling. *International journal of cancer*, *137*(1), 104–115. https://doi.org/10.1002/ijc.29361

Corlu, A., & Loyer, P. (2012). Regulation of the G1/S Transition in Hepatocytes: Involvement of the Cyclin-Dependent Kinase Cdk1 in the DNA Replication. *International Journal of Hepatology*, *2012*, 1–17. https://doi.org/10.1155/2012/689324

Craig, A.J., von Felden, J., Garcia-Lezana, T., Sarcognato, S., & Villanueva, A. (2020). Tumor evolution in hepatocellular carcinoma. *Nature Reviews Gastroenterology &* Hepatology *17,* 139–152. https://doi.org/10.1038/s41575-019-0229-4

Dayton, T.L., Jacks, T., & Vander Heiden, M.G. (2016). PKM2, cancer metabolism, and the road ahead. *EMBO reports, 17*, 1721–1730. https://doi.org/10.15252/embr.201643300

De Matteis, S., Ragusa, A., Marisi, G., De Domenico, S., Gardini, A.C., Bonafè, M., & Giudetti, A.M. (2018). Aberrant Metabolism in Hepatocellular Carcinoma Provides Diagnostic and Therapeutic Opportunities. *Oxidative medicine and cellular longevity,* 7512159. https://doi.org/10.1155/2018/7512159

De Meyts, P. (2008). The insulin receptor: a prototype for dimeric, allosteric membrane receptors? *Trend in Biochemical Sciences, 33*(8), 376-384. https://doi-org.uaccess.univie.ac.at/10.1016/j.tibs.2008.06.003

DeWaal, D., Nogueira, V., Terry, A.R., Patra, K.C., Jeon, S.M., Guzman, G., Au, J., Long, C.P., Antoniewicz, M.R. & Hay, N. (2018). Hexokinase-2 depletion inhibits glycolysis and induces oxidative phosphorylation in hepatocellular carcinoma and sensitizes to metformin. *Nature Communications, 9*(446). https://doi.org/10.1038/s41467-017-02733-4

Dif, N., Euthine, V., Gonnet, E. Laville, M., Vidal, H., & Lefai, E. (2006). Insulin activates human sterol-regulatory-element-binding protein-1c (SREBP-1c) promoter through SRE motifs. *Biochemistry Journal, 400*(1), 179–188. https://doi.org/10.1042/BJ20060499

Dong, Y., Tu, R., Liu, H., & Qing, G. (2020). Regulation of cancer cell metabolism: oncogenic MYC in the driver's seat. *Sig Transduct Target Ther* ,*5(*124). https://doi.org/10.1038/s41392-020-00235-2

Frau, M., Biasi, F., Feo, F., & Pascale, R. M. (2010). Prognostic markers and putative therapeutic targets for hepatocellular carcinoma. *Molecular Aspects of Medicine, 31*(2), 179–193. https://doi.org/10.1016/j.mam.2010.02.007

Gao, X., Wang, H., Yang, J.J., Liu, X., & Liu, Z.R. (2012). Pyruvate kinase M2 regulates gene transcription by acting as a protein kinase. *Molecular Cell, 45*(5), 598–609. https://doi.org/10.1016/j.molcel.2012.01.001

Guo, Y.J., Pan, W.W., Liu, S.B., Shen, Z.F., Xu, Y., & Hu, L.L. (2020). ERK/MAPK signalling pathway and tumorigenesis (Review). *Experimental and Therapeutic Medicine, 19*(3), 1997-2007. https://doi.org/10.3892/etm.2020.8454

Greenbaum, L.E. (2004). Cell cycle regulation and hepatocarcinogenesis. *Cancer Biology & Therapy, 3*(12), 1200-1207. https://doi.org/10.4161/cbt.3.12.1392

Gutmann, M. (2020). *Mechanisms of tumor promotion by insulin: Investigations in models for early and advanced stage hepatocarcinogenesis.* [Master's Thesis, University of Vienna].

Harvey, S. E. & Cheng, C. (2016). Methods for Characterization of Alternative RNA Splicing. *Methods in Molecular Biology, 1402*, 229-241. PMID: 26721495

Hatting, M., Tavares, C.D.J., Sharabi, K., Rines, A.K. & Puigserver, P. (2019). Insulin regulation of gluconeogenesis. *Annals of the New York Academy of Sciences, 1411*(1), 21–35. https://doi.org/10.1111/nyas.13435

Hay, N. (2016). Reprogramming metabolism in cancer: can it be exploited for cancer therapy? *Nature Reviews Cancer, 16,* 635–649. https://doi-org.uaccess.univie.ac.at/10.1038/nrc.2016.77

Hayes, C.N., Zhang, P., & Chayama, K. (2019). The Role of Lipids in Hepatocellular Carcinoma. Hepatocellular Carcinoma. https://www.ncbi.nlm.nih.gov/books/NBK549198/

Horton, J.D., Shah, N.A., Warrington, J.A., Anderson, N.N., Park, S.W., Brown, M.S., & Goldstein, J.L. (2003). Combined analysis of oligonucleotide microarray data from transgenic and knockout mice identifies direct SREBP target genes. *Proc Natl Acad Sci U S A, 100*(21), 12027–12032. doi: 10.1073/pnas.1534923100

Huang, X., Liu, G., Guo, J., & Su, Z. (2018). The PI3K/AKT pathway in obesity and type 2 diabetes. *International Journal of Biological Science, 14*(11), 1483-1496. doi:10.7150/ijbs.27173

Iqbal, M. A., Siddiqui, F.A., Gupta, V., Chattopadhyay, S., Gopinath, P., Kumar, B., Manvati, Chaman, S., N., & Bamezai, R.N.K. (2013). Insulin enhances metabolic capacities of cancer cells by dual regulation of glycolytic enzyme pyruvate kinase M2. *Molecular Cancer, 12*(71). https://doi.org/10.1186/1476-4598-12-72

Jee, S. H., Kim, H. J., & Lee, J. (2005). Obesity, insulin resistance and cancer risk. *Yonsei medical journal*, *46*(4), 449–455. https://doi.org/10.3349/ymj.2005.46.4.449

Karakulak, T., Moch, H., Von Mering, C., & Kahraman, A. (2021). Probing Isoform Switching Events in Various Cancer Types: Lessons From Pan-Cancer Studies. *Frontiers in Molecular Biosciences.* https://doi.org/10.3389/fmolb.2021.726902

Khamzina, L., Veilleux, A., Bergeron, S., & Marette, A. (2005). Increased Activation of the Mammalian Target of Rapamycin Pathway in Liver and Skeletal Muscle of Obese Rats: Possible Involvement in Obesity-Linked Insulin Resistance. *Endocrinology, 146*(3), 1473–1481. https://doi.org/10.1210/en.2004-0921

Khan, M. W., Biswas, D., Ghosh, M., Mandloi, S., Chakrabarti, S., & Chakrabarti P. (2015) mTORC2 controls cancer cell survival by modulating gluconeogenesis. *Cell death discovery* 1(15016). https://doi.org/10.1038/cddiscovery.2015.16

Kim, Y.H., Jeong, D.C., Pak, K., Han, M.E., Kim, J.Y., Kim, H.J., Kim, T.W., Kim, T.H., Hyuan, D.W., & Oh, S.O. (2017). SLC2A2 (GLUT2) as a novel prognostic factor for hepatocellular carcinoma. *Oncotarget, 8*(40), 68381–68392. doi: 10.18632/oncotarget.20266

Kowalik, M.A., Columbano, A., & Perra, A. (2017). Emerging Role of the Pentose Phosphate Pathway in Hepatocellular Carcinoma. *Frontiers in Oncology, 7*(87). https://doi.org/10.3389/fonc.2017.00087

Leclercq, I.A., Da Silva Morais, A., Schroyen, B., Van Hul, N., & Geerts, A. (2007). Insulin resistance in hepatocytes and sinusoidal liver cells: Mechanisms and consequences. *Journal of Hepatology, 47*(1), 142–156. https://doi.org/10.1016/j.jhep.2007.04.002

Lee, N.C.W., Carella, M.A., Papa, S., & Bubici, C. (2018). High Expression of Glycolytic Genes in Cirrhosis Correlates With the Risk of Developing Liver Cancer. *Frontiers in Cell and Developmental Biology, 6.* https://www.frontiersin.org/article/10.3389/fcell.2018.00138

Li, W., Wang, J., Chen, Q.D., Qian, X., Li, Q., Yin, Yu., Shi, Z.M., Wang, Lin., Lin, J., Liu, L.Z., & Jiang, B.H. (2013). Insulin Promotes Glucose Consumption via Regulation of miR-99a/mTOR/PKM2 Pathway. *PLoS ONE, 8*(6). https://doi.org/10.1371/journal.pone.0064924

Li, X., Deng, S., Liu, M., Jin, Y., Zhu, Y., Deng, S., Chen, J., He, C., Qin, Q., Wang C., & Zhao, G. (2018). The responsively decreased PKM2 facilitates the survival of pancreatic cancer cells in hypoglucose. *Cell Death and Disease, 9*(133). https://doi.org/10.1038/s41419-017-0158-5

Li, X., Wang, X., and Gao, P. (2017). Diabetes Mellitus and Risk of Hepatocellular Carcinoma. *Biomed Research International*. https://doi.org/10.1155/2017/5202684

Libbrecht, L., Desmet, V., & Roskams, T. (2005). Preneoplastic lesions in human hepatocarcinogenesis, *Liver international, 25*(1), 16–27. https://doi-org.uaccess.univie.ac.at/10.1111/j.1478-3231.2005.01016.x

Liberti, M.V., & Locasale, J.W. (2016). The Warburg Effect: How Does it Benefit Cancer Cells? *Trends in Biochemical Sciences, 41*(3), 211–218. doi:10.1016/j.tibs.2015.12.001

Liu, J., Zhi, Q., Liu, Y., Wang, Y., Chen, L., Ke, Y., Zeng, L., Wu, X., Yang, X., Guleng, B.,

Liu, H., & Ren, J. (2021). Insulin promotes hepatocarcinoma tumorigenesis by up-regulating PKM2 expression. *Experimental Cell Research, 408*(2). https://doi.org/10.1016/j.yexcr.2021.112872

Livak, K.J., & Schmittgen T.D. (2001). Analysis of Relative Gene Expression Data Using Real-Time Quantitative PCR and the $2^{-\Delta\Delta CT}$ Method. *Methods, 25*(4), 402-408. https://doi.org/10.1006/meth.2001.1262.

Lu, M., Lu, L., Dong, Q., Yu, G., Chen, J., Qin, L., Wang, L., Zhu, W., & Jia, H. (2018). *Acta Biochimica et Biophysica Sinica, 50*(4), 370–380. https://doi.org/10.1093/abbs/gmy009

Luo, W., & Semenza, G.L. (2012). Emerging role of PKM2 in cell metabolism and cancer progression. *Trends Endocrinology & Metabolism, 23*(11). PMID: 22824010

Lv, W.W., Liu, D., Liu, X.C., Feng, T.N., Li, L., Qia, B.Y., & Li, W.X. (2018). Effects of PKM2 on global metabolic changes and prognosis in hepatocellular carcinoma: from gene expression to drug discovery. *BMC Cancer, 18*(1150). https://doi.org/10.1186/s12885 018-5023-0

Ma, B., Jiang, H., Wen, D., Hu, J., Han, L., Liu, W., Xu, W., Shi, X., Wei, W., Liao, T., Wang, Y., Lu, Z., Wang, Y., & Ji, Q. (2019). Transcriptome Analyses Identify a Metabolic Gene Signature Indicative of Dedifferentiation of Papillary Thyroid Cancer. *The Journal of Clinical Endocrinology & Metabolism, 104*(9), 3713–3725. https://doi.org/10.1210/jc.2018-02686

Madison, B.B. (2016). Srebp2: A master regulator of sterol and fatty acid synthesis. *Journal of Lipid Research, 57*(3), 333–335. https://doi.org/10.1194/jlr.C066712

Malaguarnera, R., & Belfiore, A. (2011). The Insulin Receptor: A New Target for Cancer Therapy. *Frontiers in Endocrinology, 2*, 93. https://doi.org/10.3389/fendo.2011.00093

Malaguarnera, R., & Belfiore, A. (2014). The emerging role of insulin and insulin-like growth factor signaling in cancer stem cells. *Frontiers in Endocrinology, 5.* https://www.frontiersin.org/article/10.3389/fendo.2014.00010

Malakar ,P., Chartarifskly, L., Hija, A., Leibowitz, G., Glaser, B., Dor ,Y., & Karni, R. (2016). Insulin receptor alternative splicing is regulated by insulin signaling and modulates beta cell survival. *Sci Rep, 6*(31222). PMID: 27526875

Marion, M.J., Hantz, O., & Durantel, D. (2010). The HepaRG Cell Line: Biological Properties and Relevance as a Tool for Cell Biology, Drug Metabolism, and Virology Sutdies. *Methods in Molecular Biology,* 261-272. https://doi.org/10.1007/978-1-60761-688-7_13

Massimino, M., Sciacca, L., Parrinello, N.L., Scalisi, N.M., Belfiore, A., Vigneri, R., & Vigneri, P. (2021). Insulin Receptor Isoforms Differently Regulate Cell Proliferation and Apoptosis in the Ligand Occupied and Unoccupied State. *International Journal of Molecular Sciences, 22*(16), 8729. https://doi.org/10.3390/ijms22168729

Nault, J.C., Bioulac-Sage, P., & Zucman-Rossi, J. (2013). Hepatocellular Benign Tumors From Molecular Classification to Personalized Clinical Care, *Gastroenterology, 144*(5), 888–902. https://doi.org/10.1053/j.gastro.2013.02.032

Nevado, C., Benito, M., & Valverde, A.M. (2008). Role of Insulin Receptor and Balance in Insulin Receptor Isoforms A and B in Regulation of Apoptosis in Simian Virus 40-immortalized Neonatal Hepatocytes. *Molecular Biology of the Cell, 19*(3). https://doi.org/10.1091/mbc.e07-05-0473

Nissim, H. (2016). Reprogramming glucose metabolism in cancer: can it be exploited for cancer therapy? *Nature Reviews*, 16. doi:10.1038/nrc.2016.77

Nowatari, T., Fukunaga, K., & Ohkohchi, N. (2012). Regulation of Signal Transduction and Role of Platelets in Liver Regeneration. *International Journal of Hepatology*, *2012*, 1–8. https://doi.org/10.1155/2012/542479

O'Brien, R.M., Streeper, R.S., Ayala, J.E., Stadelmaier, B.T., & Hornbuckle, L.A. (2001). Insulin-regulated gene expression. *Biochemchemical Socienty Transactions, 29*(4). 552–558. doi: 10.1042/bst0290552.

Payankaulam, S., Raicu, A.M., & Arnosti, D.N. (2019). Transcriptional Regulation of INSR, the Insulin Receptor Gene. *Genes, 10*(12), 984. PMID: 31795422

Peng, S.Y., Lai, P.L., Pan, H.W., Hsiao, L.P., & Hsu, H.C. (2008). Aberrant expression of the glycolytic enzymes aldolase B and type II hexokinase in hepatocellular carcinoma are predictive markers for advanced stage, early recurrence and poor prognosis. *Oncology Reports, 19*(4), 1045–1053.

Perks, C.M., Zielinska, H.A., Wang, J., Jarrett, C., Frankow, A., Landomery, M.R., Bahl, A., Rhodes, A., Oxley, J., & Holly, J.M.P. (2016). Insulin Receptor Isoform Variations in Prostate Cancer Cells. *Frontiers in Endocrinology, 7,* https://doi.org/10.3389/fendo.2016.00132

Pons, F., Varela, M., & Llovet, J. M. (2005). Staging systems in hepatocellular carcinoma. *HPB: the official journal of the International Hepato Pancreato Biliary Association*, *7*(1), 35–41. https://doi.org/10.1080/13651820410024058

Prakasam, G., Iqbal M.A., Bamezai, R.N.K., & Mazurek, S. (2018). Posttranslational Modifications of Pyruvate Kinase M2: Tweaks that Benefit Cancer. *Frontiers in Oncology, 8*(22). PMID: 29468140

Pusec, C. M., De Jesus, A., Khan, M. W., Terry, A. R., Ludvik, A. E., Xu, K., Giancola, N., Pervaiz, H., Daviau Smith, E., Ding, X., Harrison, S., Chandel, N. S., Becker, T. C., Hay, N., Ardehali, H., Cordoba-Chacon, J., & Layden, B. T. (2019). Hepatic HKDC1 Expression Contributes to Liver Metabolism. *Endocrinology*, *160*(2), 313–330. https://doi.org/10.1210/en.2018-00887

Qaid, M.M., & Abdelrahman, M.M. (2016). Role of insulin and other related hormones in energy metabolism. *Cogent Food & Agriculture*, *2*(1). DOI: 10.1080/23311932.2016.1267691

Qin, Z., Xiang, C., Zhong, F., Liu, Y., Dong, Q., Li, K., Shi, W., Ding, C., Qin, L., & He, F. (2019). Transketolase (TKT) activity and nuclear localization promote hepatocellular carcinoma in a metabolic and non-metabolic manner. *Journal of Experimental & Clinical Cancer Research, 38*(154). https://doi.org/10.1186/s13046-019-1131-1

Sagmeister, S., Eisenbauer, M., Pirker, C., Mohr, T., Holzmann, K., Zwickl, H., Bichler, C., Kandioler, D., Wrba, F., Mikulits, W., Gerner, C., Shehata, M., Majdic, O., Streubel, B., Berger, W., Micksche, M., Zatloukal, K., Schulte-Hermann, R., & Grasl-Kraupp, B. (2008). New cellular tools reveal complex epithelial-mesenchymal interactions in hepatocarcinogenesis. *British Journal of Cancer, 99*(1), 151–159. https://doi.org/10.1038/sj.bjc.6604440

Sangineto, M., Villani, R., Cavallone, F., Romano, A., Loizzi, D., & Serviddio, G. (2020). Lipid Metabolism in Development and Progression of Hepatocellular Carcinoma. *Cancers, 12*(6), 1419. https://doi.org/10.3390/cancers12061419

Saxton, R.A., & Sabatini, D.M. (2018). mTOR Signaling in Growth, Metabolism, and Disease. *Cell, 168*(6), 960–976. https://doi.org/10.1016/j.cell.2017.02.004

Schwarz, P. (2021). *Effect of insulin on malignant phenotype and metabolic gene expression in hepatoma cell line.* [Master's Thesis, University of Vienna].

Schulze, RJ., Schott, MB., Casey, CA., Tuma, PL., & McNiven, MA. (2019). The cell biology of the hepatocyte: A membrane trafficking machine. *Journal of Cell Biology 218*(7), 2096–2112. https://doi.org/10.1083/jcb.201903090

Shahbazi, M., Cundiff, P., Zhou, W., Lee, P., Patel, A., D'Souza, S.L., Abbasi, F., Quertermous, T., Knowles, J.W. (2019). The role of insulin as a key regulator of seeding, proliferation, and mRNA transcription of human pluripotent stem cells. *Stem Cell Research & Therapy, 10*(1), 228. doi: 10.1186/s13287-019-1319-5.

Singh, M.K., Da, B.K., Choudhary, S., Gupta, D., & Patil, U.K. (2018). Diabetes and hepatocellular carcinoma: A pathophysiological link and pharmacological management. *Biomedicine & Pharmacotherapy, 106, 991-1002.* https://doi.org/10.1016/j.biopha.2018.06.095

Snaebjornsson, M.T., Janaki-Raman, S., & Schulze, A. (2019). Greasing the Wheels of the

Cancer Machine: The Role of Lipid Metabolism in Cancer. *Cell Metabolism.* https://doi.org/10.1016/J.CMET.2019.11.010

Song, J., Zhou, H., Gu, D., & Xu, Y. (2022). Hepatocellular Carcinoma Differentiation: Research Progress in Mechanism and Treatment. *Frontiers in Oncology, 11*. https://www.frontiersin.org/article/10.3389/fonc.2021.790358

Song, S. H., McIntyre, S. S., Shah, H., Veldhuis, J. D., Hayes, P. C., & Butler, P. C. (2000). Direct measurement of pulsatile insulin secretion from the portal vein in human subjects. *Journal of Clinical Endocrinology and Metabolism, 85*(12), 4491–4499. https://doi.org/10.1210/jc.85.12.4491

Sun, Q., Chen, X., Ma, J., Zhang, H. et al. (2011). Mammalian target of rapamycin upregulation of pyruvate kinase isoenzyme type M2 is critical for aerobic glycolysis and tumor growth. *Proc Natl Acad Sci USA, 108*(10), 4129–4134. https://doi.org/10.1073/pnas.1014769108

Sutherland, C., O'Brien, R.M., Granner, D.K. (2013). Insulin Action Gene Regulation. *Madame Curie Bioscience Database.* https://www.ncbi.nlm.nih.gov/books/NBK6471/

Takano, A., Usui, A., Haruta, T., Kawahara, J., Uno, T., Iwata, M., & Kobayashi, M. (2001). Mammalian Target of Rapamycin Pathway Regulates Insulin Signaling via Subcellular Redistribution of Insulin Receptor Substrate 1 and Integrates Nutritional Signals and Metabolic Signals of Insulin. *Molecular Cell Biology, 21*(15), 5050–5062. https://doi.org/10.1128/MCB.21.15.5050-5062.2001

Taub, R. (2004). Liver regeneration: from myth to mechanism. *Nature Reviews Molecular Cell Biology, 5,* 836-857. https://doi-org.uaccess.univie.ac.at/10.1038/nrm1489

Tang, Y., Yang, X., Feng, K., Hu, C., & Li, S. (2021). High expression of aldolase A is associated with tumor poor prognosis in hepatocellular carcinoma. *Journal of Gastrointestinal Oncology, 12*(1), 174–183. https://doi.org/10.21037/jgo-20-534

Taniguchi, C.M., Emanuelli, B., & Kahn, C.R. (2006). Critical nodes in signalling pathways: insights into insulin action. *Nature Reviews Molecular Cell Biology, 7,* 85–96. https://doi.org/10.1038/nrm1837

Teng, J.A., Wu, S.G., Chen, J.X., Li, Q., Peng, F., Zhu, Z., Qin, J., & Hu, Z.Y. (2016). The Activation of ERK1/2 and JNK MAPK Signaling by Insulin/IGF-1 Is Responsible for the Development of Colon Cancer with Type 2 Diabetes Mellitus. *PLoS ONE.* https://doi.org/10.1371/journal.pone.0149822

Tenen, T.G., Chai, L., & Tan, J.L. (2021). Metabolic alterations and vulnerabilities in hepatocellular carcinoma. *Gastroenterology Report, 9*(1), 1-13. https://doi.org/10.1093/gastro/goaa066

Theriault, M. (2016). Innate Immune Recognition of Candida Albicans in Zebrafish. *Honors College, 420*. https://digitalcommons.library.umaine.edu/honors/420

Titchenell, P., Chu, Q., Monks, B., & Birnbaum, M.J. (2015). Hepatic insulin signaling is dispensable for suppression of glucose output by insulin in vivo. *Nature Communications, 6*(7078). https://doi.org/10.1038/ncomms8078

Tokarz, V. L., MacDonald, P. E., & Klip, A. (2018). The cell biology of systemic insulin function. *Journal of Cell Biology, 217*(7), 1–17. https://doi.org/10.1083/jcb.201802095

Ullah, M., Stich, S., Häupl, T., Eucker, J., Sittinger, M., & Ringe, J. (2013). Reverse Differentiation as a Gene Filtering Tool in Genome Expression Profiling of Adipogensis for Fat Marker Gene Selection and Their Analysis. *PLoS ONE, 8*(7). https://doi.org/10.1371/journal.pone.0069754

Vakilian, M., Tahamtani, Y., & Ghaedi, K. (2019). A review on insulin trafficking and exocytosis. *Gene, 706,* 52-61. https://doi.org/10.1016/j.gene.2019.04.063

Vargas, E., Yoj, N.V., Supulveda, M.A.C. (2021). Biochemistry, Insulin Metabolic Effects. *StatPearls.* https://www.ncbi.nlm.nih.gov/books/NBK525983/

Vella, V., Milluzzo, A., Scalisi, N.M., Vigneri, P., & Sciacca, L. (2018). Insulin Receptor Isoforms in Cancer. *International Journal of Molecular Sciences, 19*(11), 3615. https://doi.org/10.3390/ijms19113615

Vigneri, R., Sciacca, L., Vigneri, P. (2020). Rethinking the Relationship between Insulin and Cancer. *Trends in Endocrinology & Metabolism*, *31*(8), 551–560. https://doi.org/10.1016/j.tem.2020.05.004

Vitting-Seerup, K., & Sandelin, A. (2017). The Landscape of Isoform Switches in Human Cancers. *Molecular Cancer Research, 15*(9), 1206–1220. https://doi.org/10.1158/1541-7786.MCR-16-0459

Wang, C., Su, K., Zhang, Y., Zhang, W., Zhao, Q., Chu, D., & Guo, R. (2019). IR-A/IGF-1R mediated signals promote epithelial-mesenchymal transition of endometrial carcinoma cells by activating PI3K/AKT and ERK pathways. *Cancer Biology & Therapy, 20*(3), 295–306. https://doi.org/10.1080/15384047.2018.1529096

Wang, M., Han, J., Xing, H., Zhang, H., Li, Z., Liang, L., Li, C., Dai, S., Wu, M., Shen, F., & Yang T. (2016). Dysregulated fatty acid metabolism in hepatocellular carcinoma. *Hepatic oncology, 3*(4), 241-251. https://doi.org/10.2217/hep-2016-0012

Wang, M.D., Wu, Han, Fu, G.B., Zhang, H.L., Zhou, X., Tang, L., Dong, L.W., Qin, C.J., Huang, S., Zhao, L.H., Zeng, M., Wu, M.C, Yan, H.X., & Wang, H.Y. (2015). Acetyl-coenzyme A carboxylase alpha promotion of glucose-mediated fatty acid synthesis enhances survival of hepatocellular carcinoma in mice and patients. *American Association for the Study of Liver Diseases, 63*(4), 1272–1286. https://doi.org/10.1002/hep.28415

Wiese, E. K., & Hitosugi, T. (2018). Tyrosine Kinase Signaling in Cancer Metabolism: PKM2 Paradox in the Warburg Effect. *Frontiers in cell and developmental biology*, *6*, 79. https://doi.org/10.3389/fcell.2018.00079

Wilcox, G. (2005). Insulin and Insulin Resistance. *Clinical Biochemistry Review 26*(2), 19-39. PMID: 16278749

Westermeier, F., Sáez T., Arroyo P., Toledo F., Gutiérrez J., Sanhueza C., Pardo F., Leiva A., & Sobrevia, L. (2015). Insulin receptor isoforms: an integrated view focused on gestational diabetes mellitus. *Diabetes/Metabolism Research and Reviews 32*(4), 350-365. https://doi.org/10.1002/dmrr.2729

Wong, N., De Melo, J., & Tang D. (2013). PKM2, a Central Point of Regulation in Cancer Metabolism. *International Journal of Cell Biology*. https://doi.org/10.1155/2013/242513

Xu, Q., Liu, L-Z., Yin, Y., He, Y., Li, Q., Qian, X., You, Y., Lu, Z., Peiper, S.C., Shu, Y., & Jiang, B-H. (2015). Regulatory circuit of PKM2/NF-κB/mir-148a/152-modulated tumor angiogenesis and cancer progression. *Oncogene, 34,* 5482–5493. https://doi.org/10.1038/onc.2015.6

Yamada, K., & Noguchi, T. (1999). Nutrient and hormonal regulation of pyruvate kinase gene expression. *Biochemical Journal, 337, 1-11.* PMID: 9854017

Yang, J., Wang, L., & Jia, R., (2020). Role of de novo cholesterol synthesis enzymes in cancer. *Journal of Cancer, 11*(7), 1761–1767. https://doi.org/10.7150/jca.38598

Yang, J., Wang, C., Zhao, F., Luo, X., Qin, M., Arunachalam, E., Ge, Z., Wang, N., Deng, X., Jin, G., Cong, W., & Qin, W. (2017). Loss of FBP1 facilitates aggressive features of hepatocellular carcinoma cells through the Warburg effect. *Carcinogenesis 38*(2), 134-143. https://doi.org/10.1093/carcin/bgw109

Yang, W., & Lu, Z. (2013). Nuclear PKM2 regulates the Warburg effect. *Cell Cycle, 12*(19), 3154-3158. PMID: 24013426

Yang, W., Zheng, Y., Xia, Y., Ji, H., Chen, X., Guo, F., Lyssiotis, C. A., Aldape, K., Cantley, L. C., & Lu, Z. (2012). ERK1/2-dependent phosphorylation and nuclear translocation of PKM2 promotes the Warburg effect. *Nature cell biology*, *14*(12), 1295–1304. https://doi.org/10.1038/ncb2629

Ye, J., Coulouris, G., Zaretskaya, I., Cutcutache, I., Rozen, S., & Madden, T. L. (2012). Primer-BLAST: a tool to design target-specific primers for polymerase chain reaction. *BMC Bioinformatics*, *13*, 134. https://doi.org/10.1186/1471-2105-13-134

Yoon, M.S. (2017). The Role of Mammalian Target of Rapamycin (mTOR) in Insulin Signaling. *Nutrients, 9*(11), 1176. doi: 10.3390/nu9111176

Yu, L., Chen, X., Sun, X., Wang, L., & Chen, S. (2017). The Glycolytic Switch in Tumors: How Many Players Are Involved?. *Journal of Cancer*, *8*(17), 3430–3440. https://doi.org/10.7150/jca.21125

Zahra, K., Dey, T.K., Ashish, A., Mishra, S.P., & Pandey, U. (2020). Pyruvate Kinase K2 and Cancer: The Role of PKM2 in Promoting Tumorigenesis. *Frontiers in Oncology.* https://doi.org/10.3389/fonc.2020.00159

Zhang, W., Juan, H., Tang, Y., Yang, Y., & Hu, H. (2020). Inhibition of fatty acid synthase (FASN) affects the proliferation and apoptosis of HepG2 hepatoma carcinoma cells via the β-catenin/C-myc signaling pathway. *Annals of Hepatology, 19*(4), 411–416. https://doi.org/10.1016/j.aohep.2020.03.005

Zhang, Z., Deng, X., Liu, Y., Sun, L., & Chen, F. (2019). PKM2, function and expression and regulation. *Cell & Bioscience, 9*(52). https://doi.org/10.1186/s13578-019-0317-8

Zhao, R., Li, L., & Yang, J. (2016). PKM2 affects the development of hepatocellular carcinoma. *International Journal of Clinical and Experimental Medicine, 9(6),* 9744-9751.

Zhao, Y., Zhao, L., Yang, H., Li, J., Min, X., Yang, F., Liua, J., & Huang, G. (2018). Pyruvate kinase M2 interacts with nuclear sterol regulatory element-binding protein 1a and thereby activates lipogenesis and cell proliferation in hepatocellular carcinoma. *Journal of biological chemistry, 293(*17), 6623–6634. https://doi.org/10.1074/jbc.RA117.000100

Zhu, W.W., Lu, M., Wang, X.Y., Zhou, X., Gao, C., & Qin, L.X. (2020). The fuel and engine: The roles of reprogrammed metabolism in metastasis of primary liver cancer. *Genes & Diseases, 7*(3), 299–307. https://doi.org/10.1016/j.gendis.2020.01.016

Zou, Z., Tao, T., Li, H., & Zhu, X. (2020). mTOR signaling pathway and mTOR inhibitors in cancer: progress and challenges. *Cell & Bioscience, 10*(31). https://doi.org/10.1186/s13578-020-00396-1

IX. List of figures

X. List of tables

XI. Appendix

Zusammenfassung

Die Entstehung des hepatozellulären Karzinoms (HCC), wird durch Hyperinsulinämie begünstigt, was eine wichtige Rolle des Insulins bei der Hepatokarzinogenese nahe legt. In der vorliegenden Arbeit wurde der Effekt des Hormons als auch die Rolle der Insulinrezeptor-Splicevarianten A und B bei der Entwicklung des malignen Phänotyps untersucht.

Die Expression von Insulin-regulierten Genen wurde mittels whole-genome Genexpressionsanalysen in HCC-Vorstufen der Ratte erhoben und mit publizierten Genexpressionsdaten von humanen HCC-Vorstufen verglichen. Als Zellkultur Modelle dienten differenzierte (dHepaRG™) und nicht-differenzierte (HepaRG™) Zellen, die mit Insulin behandelt wurden. Mittels lentiviralem Gentransfer wurden Insulinrezeptor A- und B-überkexprimierende Zelllinien hergestellt. Der Hormon-Effekt auf die Expression metabolischer Gene wurde durch RT-qPCR und auf den malignen Phänotyp durch Kolonieformations- und Zellmigrations-Tests erfasst. Der Western Blot diente dem Nachweis der Translokation der Pyruvatkinase M2 (PKM2) in den Zellkern.

Die Genexpressionsmuster in HCC-Vorstufen der Ratte und des Menschen zeigten eine Überexpression vieler Insulin-regulierter Gene im Kohlenhydrat-, Cholesterol-, Fettsäure und Aminosäure-Stoffwechsels und Pentosephosphatweg. Im Zellmodell induzierte Insulin viele dieser Gene vor allem in HepaRG™ und induzierte teilweise die Expression krebsspezifischer Isoenzyme in dHepaRG™ Zellen. Eine Überexpression des Insulinrezeptor-B führte zur erhöhten Koloniebildung und Migration der Zellen, während der Insulinrezeptor-A keinen Effekt zeigte. Die Insulinbehandlung führte auch zu verstärkter nukleärer PKM2 Translokation in dHepaRG™ und HepaRG™, was die erhöhte Expression einiger metabolischer Gene erklären könnte.

Die Ergebnisse zeigen, dass Insulin durch seine regulatorische Wirkung auf die Expression metabolischer Gene und die vermehrte nukleäre PKM2-Translokation zur Entwicklung eines HCC beitragen könnte. Die Ausprägung eines malignen Phänotyps könnte über den Insulinrezeptor B vermittelt werden.

Legend: + increased

- decreased

/ no information available

Table 18.
The table was created in cooperation with Schwarz Paula (2021).

GENE	PROTEIN	UNALTERED HEPATOCYTES					
		Effect of insulin on mRNA expression	**Posttranscriptional effects of insulin**	**Information on experiments**	**Rat PNL (Preneoplastic Lesions)**	**Rat HCA (Hepatocallular Adenoma)**	**Human HCA**
ACACA	Acetyl-coenzyme A carboxylase alpha	+	/	insulin enhanced promotor activity of Acetyl-CoA Carboxylase gene in HepG2 cells [1]	unchanged	+	+ [94]
ACADL / LCAD	Acyl-CoA dehydrogenase, long chain	/		ACADL knockout leads to defect in insulin signal transduction in mice [2]	unchanged	unchanged	/
ACADM	Acyl-Coenzyme A dehydrogenase, medium chain	+	/	higher ACADM mRNA expression in liver of diabetic mice [3]	-	-	+ [93]
ACLY	ATP citrate lyase/ synthase	+	/	Increased expression in liver of SREBP overexpressing mice [4]	unchanged	unchanged	+ [94]

ACSL5	acyl-CoA synthetase long-chain family member 5	+	/	ACSL5 gene expression is induced by insulin in cultured hepatocytes and in liver of insulin treated diabetic mice [5] Insulin increased expression in primary rat hepatocytes mediated by SREBP [6]	-	-	/
ALDOA	Aldolase A	+	/	Insulin increases gene transcription in HepG2 cells [7]	+	+	/
ASNS	Asparagine Synthetase	+	/	Insulin promotes gene expression in Foa cells (rat hepatoma cell line) [8]	+	+	/
ATF3	Activating Transcription Factor 3	+	/	Insulin promotes gene expression in Fao cells (rat hepatoma cell line) [8]	+	+	/
CAV1	Caveolin 1 (Membrane microdomain) 1	+	/	Promotor has an Sp-1 and Ap-1 binding site. Sp-1 is a transcription factor in the liver. AP-1 mediates insulins effect. [9 10 11]	-	unchanged	/
CCNB1	Cyclin B1	+	/	Akt activates coactivator p300 which activates CCNB1 expression [12] Decreased in liver of insulin deficient, streptozotozin induced rats. [13]	+	+	-[94 95]

CCND1	Cyclin D1	/	/	metformin (insulin sentisizer) supresses insulin induced hepatic CCND1 expression in obese/diabetic mice [14]	+	+	-[94]
CD36	CD36 Antigen / Collagen Type I Receptor / Thrombospondin Receptor)	+	/	Insulin directly increases CD36 expression in liver [15]	+	+	/
CDK2	Cyclin-dependent kinase 2	+	/	Sp-1 and Ap-1 transcription factor binding sites in promoter [16]	unchanged	-	/
CDK4	Cyclin-dependent kinase 4	/	/	Insulin activates cyclin D1-CDK4 which supresses hepatic glucose production [17]	unchanged	unchanged	/
CPEB1	Cytoplasmic polyadenylation element-binding protein 1	/	/	CPEB1-knockout mice have increased expression of PTEN and STAT3 and decreased insulin signaling to protein kinase B (Akt) in the livers of mice [18]	unchanged	+	/
CPT1A	Carnitine palmitoyltransferase I	-	/	The mRNA levels of *CPT1A* are reduced by insulin in the liver of rats [19 20]	-	-	/
DDR1	Discoidin domain receptor tyrosine kinase 1	+	/	DDR1 is upregulated by IGF-1, IGF-2 and insulin through the PI3K/AKT/miR-199a-5p circuit [21]	+	+	/

EGLN3/PHD3	Alpha-ketoglutarate-dependent hydroxylase 3 / Hypoxia-Inducible Factor Prolyl Hydroxylase 3	/		PHD3 depletion leads to impaired insulin signalling in hepatocytes [22]	+	+	/
ELOVL6	elongation of long-chain fatty acids family member 6	+	/	ELOVL-6 is a target of SREBP-1 transcription factor in hepatocytes. Knochdown of SREBP-1 in mouse liver supressed ELOVL-6 mRNA [23]	+	+	/
ENO1	Enolase	+	/	FOXO-1 decreases the mRNA levels encoding enolase (ENO) in mice livers [24]	unchanged	unchanged	/
ENPP1	Ectonucleotide pyrophosphatase /phospho-diesterase 1	-	/	Insulin reduces ENPP1 expression in rat hepatocytes and HepG2 hepatoma cells [25]	unchanged	unchanged	/
FAM3B/PANDER	Family with sequence similarity 3, member B	/		Hepatic expression of FAM3B is increased under obese state. FAM3B induced insulin resistance in hepatocytes and human HepG2 cells. [26] Reduced expression in liver of obese and diabetic mice, overexpression in liver resulted in increased insulin sensitivity [27]	-	unchanged	/

FASN	Fatty acid synthetase	+	/	increased in primary rat hepatocytes after insulin administration [28] In liver, insulin activates FASN mRNA expression and gene transcription [29]	unchanged	+	+ [94]
FBP1	Fructose-1,6-biphosphatase-1	-	/	FPB1 gene expression increases in Insulin resistant liver of rats [30]	-	-	+[93 94]
FOXA2 =HNF3beta	Forkhead Box A2	/		Foxa2 is inactive in insulin-resistant mice [31]	unchanged	unchanged	/
G6PC	Glucose-6-phosphatase	-	/	Insulin disturbs G6PC gene expression in hepatocytes [32]	-	-	/
G6PD	Glucose-6-phosphate dehydrogenase	+	/	Insulin induces G6PD gene expression in hepatocytes of rats [33]	+	+	/
GAPDH	Glyceraldehyde-3-phosphate dehydrogenase	+	/	Insulin increases mRNA levels of GAPDH in hepatoma cells. Insulin response elements (IRE)are in the upstream regulatory region of GAPDH gene [34]	unchanged	unchanged	/
GHR	Growth hormone receptor	+	/	Insulin increases mRNA expression in Huh7 cells [35]	-	-	+[93]
GK	Glycerolkinase	/		Increased glycerol kinase activity in liver of Bar Habor mice after after insulin treatment [36]	-	-	+[94]
GPAM	Glycerol-3-phosphate acyltransferase, mitochondrial	+	/	Reduced in hepatocytes of transgenic mice model with constitutive active FoxO1[37]	unchanged	unchanged	/

GPI	Glucose-6-phosphate isomerase	+	/	Reduced in hepatocytes of transgenic mice model with constitutive active FoxO1[37]	unchanged	unchanged	+[94]
GPLD1 / GPI-PLD	glucosylphosphatidylinositol specific phospholipase D1	-	/	Increased mRNA levels in the liver of diabetic mice[38]	-	-	+[94]
GSK3A	Glycogen synthase kinase 3 alpha	/		Insulin inhibits GSK3 activity in liver[39]	-	unchanged	/
GSK3B	glycogen synthase kinase 3 beta	/		Insulin inhibits GSK3 activity in liver[39]	unchanged	unchanged	/
GYS2	Glycogen synthase	/		Insulin increased GYS2 activity in rhesus monkeys[40]	-	-	+[93]
HK1	Hexokinase 1, 2, 3,	+	/	eleveted Akt activation leads to Increased HK1 expression in liver of mice [41]	+	+	/
HK4/GCK	Hexokinase 4/Glucokinase	+	/	Insulin-dependent downstream promoter regulates expression in the liver[42]	unchanged	unchanged	-[94]
HMGCR	3-hydroxy-3-methylglutaryl-Coenzyme A reductase / HMG-CoA Reductase	+	/	Insulin increases the rate of transcription of hepatic HMGCR[43]	+	+	+[94]
HMGCS1	Hydroxymethylglutaryl-CoA synthase (cytosolic)	+	/	Increased after insulin treatment in the liver of mice[44]	-	-	/
IDE	Insulin degrading enzyme	/		After insulin treatment of liver of DIE knock-out mice IR levels and insulin stimulated phosporylation are reduced.[45]	unchanged	unchanged	/

IGF1	Insulin-like growth factor 1	+	/	Studys in diabetic rats showed that deficiency of insulin causes IGF-1 gene downregulation [46]	-	-	+[93]
IGF1R	Insulin-like growth factor 1 receptor	/		IGF1R is not expressed in healthy mature hepatocytes. Response to IGF1 are mediated by extra-hepatocyte actions [47]	unchanged	unchanged	/
IGF2	Insulin-like growth factor 2	/		Correlation between increased PI3K and MAPK activation and increased IGF2 levels in liver of mice [48]	unchanged	unchanged	+[93]
IGF2BP3	insulin-like growth factor 2 mRNA binding protein 1-3	/		A positive feedback loop may exist between the IGF/PI3K/MAPK/mTOR pathway and IGF2BP3 expression in cancer cells [49]	-	-	/
IGFBP1	Insulin-like growth factor 1 binding protein 1	-	/	Insulin is an inhibitor of IGFBP1 gene expression [50]	unchanged	unchanged	/
IGFBP3	Insulin-like growth factor 1 binding protein 3	+	/	Insulin stimulates IGFBP3 gene transcripotion in rat liver cells[51]	+	+	/
INSIG1	INS induced gene 1	-	/	INSIG1 mRNA is reduced by insulin in the liver of rats [52]	-	-	/
INSIG2	INS induced gene 2	-	/	INSIG2 mRNA is reduced by insulin in the liver of rats [52]	unchanged	-	+[94]

INSR	Insulin Receptor	-	/	In liver cells FOXO acts as transcription factor for the INSR gene. Reduction of INSR gene expression after in vitro insulin treatment. [53]	unchanged	-	/
IRS2	INS receptor substrate 2	-	/	Insulin represses IRS2 gene expression through the phsophatidylinositol 3-kinase/Akt pathway [54]	-	-	/
LDHB	Lactat dehydrogenase A-D	+	/	Higher expression in fetal rat livers treated with insulin [55]	-	+	/
LEP	Leptin	/		Leptin improves hepatic insulin sensitivity and glucose metabolism in diabetic ob/ob mice [56]	unchanged	unchanged	/
LEPR	Leptin receptor	-	/	Insulin downregulates LEPR transcription in liver of mice [57]	-	-	/
MFSD2	Major facilitator superfamily domain-containing protein 2	-	/	Decreased after insulin treatment in the liver of glucose clamped mice [58]	-	-	/
NCK1	NCK adaptor protein 1	/		Improved insulin signalling in liver of obese mice lacking Nck1 [59]	unchanged	-	/

NCOA5	Nuclear receptor coactivator 5	/		Impaired insulin signalling in liver of NCOA5 haplo-insufficient (single allele knock-out) mice (decreased phosphorylation of IR beta chain, IRS1 and Akt) [60]	-	unchanged	/
NR1H4; FXR	Farnesoid X receptor / nuclear bile acid receptor	+	/	FXR expression is decreased in livers of streptozotocin-induced diabetic rats. Insulin supplementation normalizes the expression [61]	unchanged	unchanged	/
NUCKS1	Nuclear ubiquitous casein and cyclin-dependent kinases substrate	/		NUCKS is a transcriptional regulator of the insulin signaling components (e.g. IR). knock out mice show decreased insulin signaling [62]	unchanged	unchanged	-[95]
PCK1	Phosphoenolpyruvate carboxykinase (cytocolic)	-	/	Insulin supresses PCK1 gene expression in rat primary hepatocytes [63]	-	-	-[94]
PDK2	Pyruvatedehydrogenase Kinase 2	-	/	Insulin represses expression of PDK2 via phosphorylation of transcription factor FOXO through Akt/PI3K signaling.[64]	unchanged	unchanged	/

PDK4	Pyruvatedehydrogenase Kinase 4	-	/	Insulin represses expression of PDK4 via phosphorylation of transcription factor FOXO through Akt/PI3K signaling. [65] Reduced in liver of transgenic mice model with constitutive active FoxO1 [66]	-	-	+[93]
PFKL	Phosphofructokinase L, M, P	+	/	In liver of mice insulin upregulates PFKL gene expression [67]	unchanged	unchanged	/
PGAM1	Phosphoglycerate mutase 1	+	/	mTOR enhances expression [68]	unchanged	unchanged	/
PGK1	Phosphoglyceratkinase 1, 2	/		Insulin stimulates PGK1 activity in HEK293T cells [69]	unchanged	unchanged	/
PHGDH	phosphoglycerate dehydrogenase	+	/	Insulin activates ATF4 in mouse lymphocytes, ATF4 activates PHGDH expression [70 71]	+	+	-[94]
PKLR	Pyruvate kinase (liver and RBC)	+	/	Insulin treatment of diabetic rats results in an increase of PKL transcription and mRNA level. [72]	-	unchanged	-[94 95]
PRKCI	PKC-i	/	/	Overexpression in primary Zucker lean rat hepatocytes impaired insulin signal transduction and insulin regulated gene expression [73]	+	+	/

RPIA	Ribose-5-phosphate isomerase A	+	/	Reduced in liver of transgenic mice model with constitutive active FoxO1 [74]	unchanged	unchanged	/
RPS6KB1	Ribosomal protein S6 kinase 1	/		Increased activating phosphorylation in liver of insulin resistant Zucker rats [75]	unchanged	unchanged	/
SCD1	Stearoyl-CoA desaturase (Δ-9-desaturase)	+	/	Studies in human liver showed an activation of the SCD1 promoter by insulin via Akt/PI3K/mTOR pathway which targets the insulin response element (IRE) on the SCD1 promoter [76] increased in primary rat hepatocytes after insulin administration [77]	+	+	+ [94]
Serpin B1a	Serpin B1a	-	/	Foxo1 promotes serpin B1a expression in hepatic insulin resistance [78]	+	+	/
SERPINA12	Serine (or cysteine) peptidase inhibitor / clade A (alpha-1 antiproteinase, antitrypsin), member 12 / vaspin	+	/	Serpina12 mRNA expression in liver is induced after insulin injection in fasting mice. [79]	unchanged	unchanged	/
SLC25a22	mitochondrial glutamate carrier	-	/	Gene transcription is downregulated by insulin in liver of mice [80]	-	unchanged	+ [93]

SLC2A2	GLUT2	-	/	GLUT2 gene expression in primary rat hepatocytes is downregulated by insulin via an unknown mechanism [81]	unchanged	unchanged	/
SLC2A4	GLUT-4	-		Reduced mRNA levels in liver of diet induced obese rats (a following high fat diet showed increased insulin levels) [82]	-	unchanged	/
SLC2A8	GLUT-8 (Glucosetransporter type 8)	-	/	Down regulation in liver of streptozotocin induced diabetic mice [83]	unchanged	-	/
SORT1	Sortilin 1 / NTSR 3	-	/	Insulin treatment induces expression of ATF3 in Fao cells [84] SORT1 expression is repressed by ATF3 [85]	+	+	/
SREBF1 =SREBP	sterol regulatory element binding transcription factor 1	+	/	Insulin increases SREBP-1c mRNA in the livers of rats with streptozotocin-induced diabetes [86]	-	-	+[93]
ST3GAL5	ST3 beta-galactoside alpha-2,3-sialyltransferase 5	/		ST3GAL5 knock-out mice showed enhanced insulin sensitivity in liver [87]	+	+	/
TKT	Transketolase	+	/	Reduced in liver of transgenic mice model with constitutive active FoxO1 [88]	+	+	/

TXNIP	thioredoxin interacting protein	/		TXNIP knock-out mice show enhanced insulin-mediated suppression of glucose production in hepatocytes [89]	unchanged	unchanged	+[93]
UGP2	UTP glucose-1-phosphate uridylyltransferase 2 / UDP-Glucose- Pyrophosphorylase	-	/	Increased in IRS1 knock-out mice with a liver specific IRS2 knock-out [90]	+	unchanged	+[93]
USF1	Upstream stimulatory factor	/		Increased protein levels in liver of refeed rats [91]	-	-	/
YBX1	Nuclease-sensitive element-binding protein	/		Akt phosphorylates YBX1 [92]	unchanged	unchanged	/

References of table 18

1 Zhao, L.F., Iwasaki, Y., Zhe, W., Nishiyama, M., Taguchi, T., Tsugita, M., Kambayashi, M., Hashimoto, K., & Terada, Y. (2010). Hormonal regulation of acetyl-CoA carboxylase isoenzyme gene transcription. *Endocrine Journal, 57*(4), 317–24. PMID: 20139635.

2 Zhang, Do., Liu, Z.X., Choi, C.S., Tian, L., Kibbey, R., Dong, J., Cline, G.W., Wood, P.A.,
& Shulman, G.I. (2007). Mitochondrial dysfunction due to long-chain Acyl-CoA dehydrogenase deficiency causes hepatic steatosis and hepatic insulin resistance. *Proceeding of the National Academy of Sciences, 104*(43), 17075–17080. https://doi.org/10.1073/pnas.0707060104

3 Kurtz, D.M., Tian, L., Gower, B.A., Nagy, T.R., Pinkert, C.A., & Wood, P.A. (2000). Transgenic studies of fatty acid oxidation gene expression in nonobese mice. *Journal of Lipid Research, 41*(12), 2063–2070. PMID: 11108740

4 Horton, J. D., Goldstein, J. L. & Brown, M. S. (2002). SREBPs: activators of the complete program of cholesterol and fatty acid synthesis in the liver. *The Journal of clinical investigation, 109*(9), 1125–1131. doi:10.1172/JCI15593

5 Mashek, D.G., & Bu, S.Y. (2010). Hepatic long-chain acyl-CoA synthetase 5 mediates fatty acid channeling between anabolic and catabolic pathways. *Journal of Lipid Research, 51*(11), 3270–3280. *PMID: 20798351*

6 Achouri, Y., Hegarty, B.D., Allanic, D., Bécard, D., Hainault, I., Ferrè, P., & Foufelle, F. (2005). Long chain fatty acyl-CoA synthetase 5 expression is induced by insulin and glucose: involvement of sterol regulatory element-binding protein-1c. *Biochimie, 87*(112), 1149–1155, doi:10.1016/j.biochi.2005.04.015

7 Zelzer, E., Levy, Y., Kahana, C., Shilo, B.Z., Rubinstein, M., & Cohen, B. (1998). Insulin induces transcription of target genes through the hypoxia-inducible factor HIF-1alpha/ARNT. *The EMBO journal, 17*(17), 5085–5094, doi:10.1093/emboj/17.17.5085

8 Du, K. & Ding, J. (2009). Insulin regulates TRB3 and other stress-responsive gene expression through induction of C/EBPbeta. *Molecular Endocrinology 23*(4), 475–485, doi:10.1210/me.2008-028

9 Chen, W., Chen, Y., Qin, L., Li, A., Zhao, X., Wang, Y., Xiao, S., & Mo, D. (2011). Transcription factor Sp1 is essential for the regulation of the porcine caveolin-1 gene. *DNA and Cell Biology 30*(7), 491–497, doi:10.1089/dna.2010.1202

10 Samson, S. L. & Wong, N. C. (2002) Role of Sp1 in insulin regulation of gene expression. *Journal of Molecular Endocrinology, 29*, 265–279, doi:10.1677/jme.0.0290265

11 Ayala, J.E., Boustead, J.N., Chapman, S.C., Svitek, C.A., Oeser, J.K., Robey, R.B., & O'Brien, R.M. (2004). *Journal of Molecular Endocrinology, 33*(1), 263–280, doi: 10.1677/jme.0.0330263

12 Wasner, M., Tschöp, K., Spiesbach, K., Haugwitz, U., Johne, C., Mössner, J., Mantovani, R., & Engeland, K. (2003). Cyclin B1 transcription is enhanced by the p300 coactivator and regulated during cell cycle by CHR-dependent repression mechanism. *FEBS Letters, 536*(1-3), 66–70. https://doi.org/10.1016/S00145793(03)00028-02

13 Tseng, J. H., Ouyang, C. H., Lin, K. J. & Yeh, T. S. (2011). Significance of insulin signaling in liver regeneration triggered by portal vein ligation. *The Journal of Surgical Research 166*, 77-86, doi:10.1016/j.jss.2009.06.043

14 Luo, C., Liang, J., Sharabi, K., Hatting, M., Perry, E.A., Tavares, C.D.J., Goyal, L., Srivastava, A., Bilodeau, M., Zhu, A.X., Sicinski, P., & Puigserver, P. (2020).

Obesity/Type 2 Diabates-Associated Liver Tumors Are Sensitive to Cyclin D1 Deficiency. *Cancer Research, 80*(16), 3215–3221. https://doi.org/10.1158/0008-5472.CAN-20-0106

15 Steneberg, P., Sykaras, A.G., Backlund, F., Straseviciene, J., Söderström, I., & Edlund, H. (2015). Hyperinsulinemia Enhances Hepatic Expression of the Fatty Acid Transporter Cd36 and Provokes Hepatosteatosis and Hepatic Insulin Resistance. *The Journal of Biological Chemistry, 290*(31), 19034-19043, doi:10.1074/jbc.M115.640292

16 Shiffman, D., Brooks, E.E., Brooks, A.R., Chan, C.S., Milner, P.G. (1996). Characterization of the Human Cyclin-dependent Kinase 2 Gene Promoter Analysis and Gene Structure. Journal of Biological Chemistry, 271(21), 12199–12204. https://doi.org/10.1074/jbc.271.21.12199

17 Lee, Y., Dominy, J.E., Choi, Y.J., Jurczak, M., Tolliday, N., Caporez, J.P., Chim, H., Lim, J.H., Ruan, H.B., Yang, X., Vazques, F., Sicinski, P., Shulman, G.I., & Puigserver, P. (2014). Cyclin D1-CDK4 Controls Glucose Metabolism Independently of Cell Cycle Progression. *Nature, 510*(7506), 547–551. https://doi.org/10.1038/nature13267

18 Chen, Y., Tsai, Y.H., & Tseng, S.H. (2016). Regulation of the Expression of Cytoplasmic Polyadenylation Element Binding Proteins for the Treatment of Cancer. *Anticancer Research, 36*(11), 5673–5680. https://ar.iiarjournals.org/content/36/11/5673

19 Park, E.A., Mynatt, R.L., Cook, G.A., & Kashfi, K. (1995). Insulin regulates enzyme activity, malonyl-CoA sensitivity and mRNA abundance of hepatic carnitine palmitoyltransferase-I. *The Biochemical Journal, 310*(3). 853–858. https://doi.org/10.1042/bj3100853

20 Schlaepfer, I.R., & Joshia, M. (2020). CPT1A-mediated Fat Oxidation, Mechanisms, and Therapeutic Potential. *Endocrinology, 161*(2). https://doi.org/10.1210/endocr/bqz046

21 Belfiore, A., Malaguarnera, R., Nicolosi, M.L., Lappano, R., Ragusa, M., Morrione, A., & Vella, V. (2018). A novel functional crosstalk between DDR1 and the IGF axis and its relevance for breast cancer. *Cell Adhesion & Migration, 12*(4). 305–314. https://doi.org/10.1080/19336918.2018.1445953

22 Yano, H., Sakai, M., Matsukawa, T., Yagi, T., Naganuma, T., Mitsushima, M., Iida, S., Inaba, Y., Inoue, H., Unoki-Kubota, H., Kaburagi, Y., Asahara, S., Kido, Y., Minami, S., Kasuga, M., & Matsumoto, M. (2018). PHD3 regulates glucose metabolism by suppressing stress-induced signalling and optimizing gluconeogenesis and insulin singalling in hepatocytes. *Scientific Reports, 8.* 14290. https://doi.org/10.1038/s41598-018-32575-z

23 Kumadaki, S., Matsuzaka, T., Kato, T., Yahagi, N., Yamamoto, T., Okada, S., Kobayashi, K., Takahashi, A., Yatoh, S., Suzuki, H., Yamada, N., & Shimano, H. (2008). Mouse Elovl-6 promoter is an SREBP target. *Biochemical and Biophysical Research Communications, 368*(2). 261–266. https://doi.org/10.1016/j.bbrc.2008.01.075

24 Rodríguez-Enríquez, S., Marin-Hernández, A., Gallarado-Pérez, J.C., Pacheco-Velázquez, S. C., Belmont-Díaz, J.A., Robledo-Cadena, D.X., Vargas-Navarro, J.L., Corona de la Peña, N.A., Saavedra, E., Moreno-Sánchez, R. (2019). Transcriptional Regulation of Energy Metabolism in Cancer Cells. *Cells, 8*(10). 1225. DOI:10.3390/cells8101225

25 Ma, H., Wang, P., Jin, D., Jia, T., Mao, H., Zhang, J., & Zhao, S. (2018). The hepatic ectonucleotide pyrophosphatase/phosphodiesterase 1 gene mRNA

abundance is reduced by insulin and induced by dexamethasone. Brazilian Journal of Medical and Biological Research, 51(4). 1414–1431. https://doi.org/10.1590/1414-431X20176980

26 Zhang, X., Yang, W., Wang, J., Meng, Y., Guan, Y., & Yang, J. (2018). FAM3 gene familiy: A promising therapeutical target for NAFDL and type 2 diabetes. *Metabolism, 81.* 71–82. https://doi.org/10.1016/j.metabol.2017.12.001

27 Wang, C., Chi, Y., Li, J., Miao, Y., Li, S., Su, W., Jia, S., Chen, Z., Du, S., Zhang, X., Zhou, Y., Wu, W., Zhu, M., Wang, Z., Yang, H., Xu, G., Wang, S., Yang, J., Guan, Y.(2014). FAM3A activates PI3K p110alpha/Akt signaling to ameliorate hepatic gluconeogenesis and lipogenesis. *Hepatology, 59*. 1779–1790. doi:10.1002/hep.26945

28 Düve,I K., Yecies, J.L., Menon, S., Raman, P., Lipovsky, Al., Souza, A.L., Triantafellow, E., Ma, Q., Gorski, R., Cleaver, S., Vander Heiden, M.G., MacKeigan, J.P., Finan, P.M., Clish, C.B., Murphy, L.O., Manning, B.D. (2010) Activation of a metabolic gene regulatory network downstream of mTOR complex 1. *Molecular cell, 39*. 171–183. doi:10.1016/j.molcel.2010.06.022

29 Radenne, A., Akpa, M., Martel, C., Sawadogo, S., Mauvoisin, D., & Mounier, C. (2008). Hepatic regulation of fatty acid synthase by insulin and T3: evidence for T3 genomic and nongenomic actions. *American Journal of physiology. Endocrinology and metabolism, 295*(4). 884–894. https://doi.org/10.1152/ajpendo.90438.2008

30 González-Santiago, A.E., Vargas-Guerrero, B., García-López, P.M., Martínez Ayala, A.L., Domínguez-Rosales, J.A., & Gurrola-Díaz, C.M. (2017). Lupinus albus Conglutin Gamma Modifies the Gene Expressions of Enzymes Involved in Glucose Hepatic Production In Vivo. *Plant Foods for Human Nutrition, 72*(2). 134–140. https://doi.org/10.1007/s11130-016-0597-7

31 Wolfrum, C., Asilmaz, E., Luca, E., Friedman, J. M. & Stoffel, M. (2004). Foxa2 regulates lipid metabolism and ketogenesis in the liver during fasting and in diabetes. *Nature 432*(7020), 1027–1032. doi:10.1038/nature03047

32 Salgado, M.C., Metón, I., Egea, M., & Baanante, I.V. (2004). Transcriptional regulation of glucose-6-phosphatase catalytic subunit promoter by insulin and glucose in the carnivorous fish, Sparus aurata. Journal of Molecular Endocrinology, 33(3). 783–795. https://doi.org/10.1677/jme.1.01552

33 Wagle, A., Jivraj, S., Garlock, G.L., & Stapleton, S.R. (1998). Insulin regulation of glucose-6-phosphate dehydrogenase gene expression is rapamycin-sensitive and requires phospatidylinositol 3-kinase. *The Journal of biological chemistry, 273*(24). 14968–14974. https://doi.org/10.1074/jbc.273.24.14968

34 Zhang, J.Y., Zhang, F., Hong, C.Q., Giuliano, A.E., Cui, X.J., Zhou, G.J., Zhang, G.J., & Cui, Y.K. (2015). Critical protein GAPDH and its regulatory mechanisms in cancer cells. *CancerBiology & Medicine. 12*(1). 10–22. https://doi.org/10.7497/j.issn.2095-3941.2014.0019

35 Leung, K.C., Doyle, N., Ballesteros, M., Waters, M.J., & Ho, K.K.Y. (2000). Insulin Regulation of Human Hepatic Growth Hormone Receptors: Divergent Effects on Biosynthesis and Surface Translocation. *The Journal of Clinical Endocrinology & Metabolism 85*(12). 4712–4720. https://doi.org/10.1210/jcem.85.12.7017

36 Koschinsky, T., Gries, F. A. & Herberg, L. (1971). Regulation of glycerol kinase by insulin in isolated fat cells and liver of Bar Harbor obese mice. *Diabetologia 7*, 316-322, doi:10.1007/BF01219464

37 Zhang, W., Patil, S., Chauhan, B., Guo, S., Powell, D.R., Le, J., Klostas, A., Matika, R., Xiao, X., Franks, R., Heidenreich, K.A., Sajan, M.P., Farese, R.V., Stolz, D.B., Tso, P., Koo, S.H., Montminy, M., & Unterman, T.G. (2006). FoxO1 regulates multiple metabolic pathways in the liver: effects on gluconeogenic, glycolytic, and lipogenic gene expression. *The Journal of Biological Chemistry 281*(15), 10105-10117. doi:10.1074/jbc.M600272200

38 Masuda, S., Fujishima, Y., Maeda, N., Tsugawa-Shimizu, Y., Nakamura, Y., Tanaka, Y., Obata, Y., Fukuda, S., Nagao, H., Kita, S., Nishizawa, H., & Shimomura, I. (2019). Impact of glycosylphosphatidylinositol-specific phospholipase D on hepatic diacylglycerol accumulation, steatosis, and insulin resistance in diet-induced obesity. *American Journal of Physiology-Endocrinology and Metabolism, 316*(2). 239–250. https://doi.org/10.1152/ajpendo.00319.2018

39 Lipina, C., Huang, X., Finlay, D., McManus, E.J., Alessi, D.R., & Suterland, C. (2005). Analysis of hepatic gene transcription in mice expressing insulin-insensitive GSK3. *Biochemical Journal 392*(3), 633–639. doi:10.1042/BJ20051046

40 Ortmeyer, H. K., Bodkin, N. L. & Hansen, B. C. (1997). Insulin regulates liver glycogen synthase and glycogen phosphorylase activity reciprocally in rhesus monkeys. *The American Journal of Physiology 272*, 133–138, doi:10.1152/ajpendo.1997.272.1.E133

41 He, X., Li, M., Yu, H., Liu, G., Wang, N., Yin, C., Narla, G., Tao, Y., Cheng, S., & Yin, H. (2020). Loss of hepatic aldolase B activates Akt and promotes hepatocellular carcinogenesis by destabilizing the Aldob/Akt/PP2A protein complex. *PLoS Biology, 18*. doi:10.1371/journal.pbio.3000803

42 Wilson, D.F., & Matschinsky, F.M. (2019). The Central Role of Glucokinase in Glucose Homeostasis: A Perspective 50 Years After Demonstrating the Presence of the Enzyme in Islets of Langerhans. *Frontiers in Physiology, 10*(148). doi: 10.3389/fphys.2019.00148

43 Chambers, C.M., & Ness, G.C. (2008). Feedback and Hormonal Regulation of Hepatic 3-Hydroxy-3-Methylglutaryl Coenzyme A Reductase: The Concept of Cholesterol Buffering Capacity. *Proceedings of the Society for Experimental Biology and Medicine. Society for Experimental Biology and Medicine, 224*(1). 8–19. https://doi.org/10.1046/j.1525-1373.2000.22359.x

44 Batista, T. M., Garcia-Martin, R., Cai, W., Konishi, M., O'Neill, B.T., Sakaguchi, M., Kim, J.H., Jung, D.Y., Kim, J.K., & Kahn, C.R. (2019). Multi-dimensional Transcriptional Remodeling by Physiological Insulin In Vivo. *Cell Reports 26*(12), 3429-3443, doi:10.1016/j.celrep.2019.02.081

45 Villa-Perez, P., Merino, B., Fernández-Díaz, C.M., Cidad, P., Lobatón, C.D., Moreno, A., Muturi, H.T., Ghadieh, H.E., Najjar, S.M., Leissring, M.A., Cózar-Castellano, I., & Perdomo, G. (2018). Liver-specific ablation of insulin-degrading enzyme causes hepatic insulin resistance and glucose intolerance, without affecting insulin clearance in mice. *Metabolism: clinical and experimental 88*, 1–11. doi:10.1016/j.metabol.2018.08.001

46 Li, J.B., Wang, C.Y., Chen, J.W., Feng, Z.Q., & Ma, H.T. (2004). Expression of liver insulin-like growth factor 1 gene and its serum level in rats with diabetes. *World Journal of Gastroenterology, 10*(2). 255–259. https://doi.org/10.3748/wjg.v10.i2.255

47 Kineman, R. D., Del Rio-Moreno, M. & Sarmento-Cabral, A. (2018). 40 YEARS of IGF1: Understanding the tissue-specific roles of IGF1/IGF1R in regulating

metabolism using the Cre/loxP system. *Journal of Molecular Endocrinology 61*(1)*,* 187–198. doi:10.1530/JME-18-0076

48 Wang, M. J., Chen, F., Liu, Q.G., Liu, C.C., Yao, H., Yu, B., Zhang, H.B., Yan, H.X., Ye, Y., Chen, T., Wangensteen, K.J., Wang, X., Hu, Y.P., & He, Z.Y. (2018) Insulin-like growth factor 2 is a key mitogen driving liver repopulation in mice. *Cell Death & Disease 9*, 26. doi:10.1038/s41419-017-0186-1

49 Mancarella, C. & Scotlandi, K. (2019). IGF2BP3 From Physiology to Cancer: Novel Discoveries, Unsolved Issues, and Future Perspectives. *Frontiers in Cell and Developmental Biology 7*, 363. doi:10.3389/fcell.2019.00363

50 Ross, R.J., Rodriguez-Arnao, J., Donaghy, A., Bentham, J., Clark, A., Holly, J., Williams, R., & Gimson, A. (1994). *Expression of IGFBP-1 in normal and cirrhotic human livers. 141*(1). 377–82. https://doi.org/10.1677/joe.0.1410377

51 Villafuerte, B. C., Zhang, W. N. & Phillips, L. S. (1996). Insulin and insulin-like growth factor-I regulate hepatic insulin-like growth factor binding protein-3 by different mechanisms. *Molecular Endocrinolgy 10*(6), 622–630, doi:10.1210/mend.10.6.8776722

52 Boden, G., Salehi, S., Cheung, P., Homko, C., Song, W., Loveland-Jones, C., & Jayarajan, S. (2013). Comparison of In Vivo Effects of Insulin on SREBP-1c Activation and INSIG-1/2 in Rat Liver and Human and Rat Adipose Tissue. *Obesity (Silver Spring), 21*(6). 1208–1214. https://doi.org/10.1002/oby.20134

53 Payankaulam, S., Raicu, A.M., & Arnosti, D.N. (2019). Transcriptional Regulation of INSR, the Insulin Receptor Gene. *Genes, 10*(12). https://doi.org/10.3390/genes10120984

54 Hirashima, Y., Tsuruzoe, K., Kodama, S., Igata, M., Toyonaga, T., Ueki, K., Kahn, C.R., & Araki, E.(2003). Insulin down-regulates insulin receptor substrate-2 expression through the phosphatidylinositol 3-kinase/Akt pathway. *Journal of Endocrinology, 179*(2). 253–266. https://doi.org/10.1677/joe.0.1790253

55 Rozance, P. J., Jones, A.K., Bourque, S.L., D'Allessandro, A:, Hay Jr, W.W., Brown, L.D., & Wesolowski, S.R. (2020). Effects of chronic hyperinsulinemia on metabolic pathways and insulin signaling in the fetal liver. American journal of physiology. Endocrinology and metabolism 319, E721-E733, doi:10.1152/ajpendo.00323.2020

56 Lam, N.T., Lewis, J.T., Cheung, A.T., Luk, C.T., Tse, J., Wang, J., Bryer-Ash, M., Kolls, & J.K., Kieffer, T.J. (2004). Leptin Increases Hepatic Insulin Sensitivity and Protein Tyrosine Phosphatase 1B Expression. *Molecular Endocrinology 18*(6). 1333–1345. https://doi.org/10.1210/me.2002-0193

57 Thorn, S.R., Ehrhardt, R.A., Butler, W.R., Quirk, S.M., & Boisclair, Y.R.(2008). *Endocrine Physiology and Metabolism, 295*(5). 1455–1462. https://doi.org/10.1152/ajpregu.90546.2008

58 Batista, T.M., Garcia-Martin, R., Cai, W., Jung, D.Y., Kim, J.K., & Kahn, R. (2019). Multi-dimensional Transcriptional Remodeling by Physiological Insulin In Vivo. *Cell Reports, 26*, 3429–3443. https://doi.org/10.1016/j.celrep.2019.02.081

59 Latreille, M., Laberge, M. K., Bourret, G., Yamani, L. & Larose, L. (2011). Deletion of Nck1 attenuates hepatic ER stress signaling and improves glucose tolerance and insulin signaling in liver of obese mice. *American journal of physiology. Endocrinology and metabolism 300,* 423–434, doi:10.1152/ajpendo.00088.2010

60 Gao, S., Li, A., Liu, F., Chen, F., Williams, M., Zhang, C., Kelley, Z., Wu, C.L., Luo, R., & Xiao, H. (2013). NCOA5 haploinsufficiency results in glucose

intolerance and subsequent hepatocellular carcinoma. *Cancer cell 24*(6)*,* 725–737, doi:10.1016/j.ccr.2013.11.005

61 Duran-Sandoval, D., Mautino, G., Martin, G., Percevault, F., Barbier, O., Fruchart, J.C., Kuipers, F., & Staels, B. (2004). Glucose Regulates the Expression of the Farnesoid X Receptor in Liver. *Diabetes 53*(4), 890–898. https://doi.org/10.2337/diabetes.53.4.890

62 Qiu, B., Shi, X., Wong, E.T., Lim, J., Bezzi, M., Low, D., Zhou, Q., Akincilar, S.C., Lakshmanan, M., Swa, H.L.F., Tham, J.M.L., Gunaratne, J., Cheng, K.K.Y., Hong, W., Lam, K.S.L., Ikawa, M., Guccione, E., Xu, A., Han, W., & Tergaonkar, V. (2014). NUCKS Is a Positive Transcriptional Regulator of Insulin Signaling. *Cell Reports, 7*(6). 1876–1886. https://doi.org/10.1016/j.celrep.2014.05.030.

63 Zhang, Y., Li, R., Chen, W., Li, Y., & Chen, G. (2011). Retinoids induced Pck1 expression and attenuated insulin-mediated suppression of its expression via activation of retinoic acid receptor in primary rat hepatocytes. *Molecular and Cellular Biochemistry, 355*(1). https://doi.org/10.1007/s11010-011-0831-4

64 Jeong, J. Y., Jeoung, N. H., Park, K. G., & Lee, I. K. (2012). Transcriptional regulation of pyruvate dehydrogenase kinase. *Diabetes & metabolism journal*, *36*(5), 328–335. https://doi.org/10.4093/dmj.2012.36.5.328

65 Jeong, J. Y., Jeoung, N. H., Park, K. G., & Lee, I. K. (2012). Transcriptional regulation of pyruvate dehydrogenase kinase. *Diabetes & metabolism journal*, *36*(5), 328–335. https://doi.org/10.4093/dmj.2012.36.5.328

66 Zhang, W., Patil, S., Chauhan, B., Guo, S., Powell, D.R., Le, J., Klostas, A., Matika, R., Xiao, X., Franks, R., Heidenreich, K.A., Sajan, M.P., Farese, R.V., Stolz, D.B., Tso, P., Koo, S.H., Montminy, M., & Unterman, T.G. (2006). FoxO1 regulates multiple metabolic pathways in the liver: effects on gluconeogenic, glycolytic, and lipogenic gene expression. *The Journal of Biological Chemistry 281*(15), 10105-10117. doi:10.1074/jbc.M600272200

67 Ausina, P., Da Silva, D., Majerowicz, D., Zancan, P., & Sola-Penna, M. (2018). Insulin specifically regulates expression of liver and muscle phosphofructokinase isoforms. *Biomedicine & Pharmacotherpy, 103,* 228–233. https://doi.org/10.1016/j.biopha.2018.04.033

68 Sun, Q., Li, S., Wang, Y., Peng, H., Zhang, X., Zheng, Y., Li, C., Li, L., Chen, R., Chen, X., Bai, W., Jiang, X., Liu, L., Wei, F., Wang, B., Zhang, Y., Li, H., Ren, X., & Zhang, H. (2018). Phosphoglyceric acid mutase-1 contributes to oncogenic mTOR-mediated tumor growth and confers non-small cell lung cancer patients with poor prognosis. *Cell Death and Differentiation 25*, 1160–1173. doi:10.1038/s41418-017-0034-y

69 Wang, S., Jiang, B., Zhang, T., Liu, L., Wang, Y., Wang, Y., Chen, X., Lin, H., Zhou, L., Xia, Y., Chen, L., Yang, C., Xiong, Y., Ye, D., & Guan, K.L. (2015). Insulin and mTOR Pathway Regulate HDAC3-Mediated Deacetylation and Activation of PGK1. *PLoS Biology 13*(9). doi:10.1371/journal.pbio.1002243

70 Adams, C. M. (2007). Role of the transcription factor ATF4 in the anabolic actions of insulin and the anti-anabolic actions of glucocorticoids. *The Journal of Biological Chemistry 282*(23), 16744–16753. doi:10.1074/jbc.M610510200

71 Zhao, X., Fu, J., Du, J. & Xu, W. (2020). The Role of D-3-Phosphoglycerate Dehydrogenase in Cancer. *International Journal of Biological Sciences 16*(9), 1495–1506, doi:10.7150/ijbs.41051

72 Matsuda, T., Noguchi T., Takenaka, M., Yamada, K., & Tanaka, T. (1990). Regulation of L-Type Pyruvate Kinase Gene Expression by Dietary Fructose in Normal and Diabetic Rats. *The Journal of Biochemistry, 107*(4)*,* 655–660.

https://www.jstage.jst.go.jp/article/biochemistry1922/107/4/107_4_655/_article/-char/en

73 Chen, W., Goff, M. R., Kuang, H. & Chen, G. (2015). Higher protein kinase C zeta in fatty rat liver and its effect on insulin actions in primary hepatocytes. *PloS One 10*(3). doi:10.1371/journal.pone.0121890

74 Zhang, W., Patil, S., Chauhan, B., Guo, S., Powell, D.R., Le, J., Klostas, A., Matika, R., Xiao, X., Franks, R., Heidenreich, K.A., Sajan, M.P., Farese, R.V., Stolz, D.B., Tso, P., Koo, S.H., Montminy, M., & Unterman, T.G. (2006). FoxO1 regulates multiple metabolic pathways in the liver: effects on gluconeogenic, glycolytic, and lipogenic gene expression. *The Journal of Biological Chemistry 281*(15), 10105-10117. doi:10.1074/jbc.M600272200

75 Zheng, Y., Zhang, W., Pendleton, E., Leng, S., Wu, J., Chen, R., & Sun X.J. (2009). Improved insulin sensitivity by calorie restriction is associated with reduction of ERK and p70S6K activities in the liver of obese Zucker rats. *The Journal of Endocrinology 203*(3), 337–347. doi:10.1677/JOE-09-0181

76 Mounier, C., & Mauvoisin, D. (2011). Hormonal and nutritional regulation of SCD1 gene expression. *Biochemie, 93*(1), 78–86. https://doi.org/10.1016/j.biochi.2010.08.001

77 Düvel, K., Yecies, J.L., Menon, S., Raman, P., Lipovsky, A.I., Souza, A.L., Triantafellow, E., Ma, Q., Gorski, R., Cleaver, S., Heiden, M.G.V., MacKeigan, J.P., Finan, P.M., Clish, C.B., O Murphy, L., & Manning, B.D. (2010). Activation of a metabolic gene regulatory network downstream of mTOR complex 1. *Molecular Cell 39*(2), 171–183, doi:10.1016/j.molcel.2010.06.022

78 El Ouaamari, A., O-Sullivan, I., Shirakawa, J., Basile, G., Zhang, W., Roger, S., Thomou, T., Xu, S., Qiang, G., Liew, C. W., Kulkarni, R. N., & Unterman, T. G. (2019). Forkhead box protein O1 (FoxO1) regulates hepatic serine protease inhibitor B1 (serpinB1) expression in a non-cell-autonomous fashion. *The Journal of biological chemistry*, *294*(3), 1059–1069. https://doi.org/10.1074/jbc.RA118.006031

79 Aibara, D., Matsuo, K., Yamano, S., & Matsusue, K. (2019). Insulin induces expression of the hepatic vaspin gene. *Endocrine Journal, 67*(1), 9–14. https://doi.org/10.1507/endocrj.EJ19-0276

80 Batista, T.M., Garcia-Martin, R., Cai, W., Jung, D.Y., Kim, J.K., & Kahn, R. (2019). Multi-dimensional Transcriptional Remodeling by Physiological Insulin In Vivo. *Cell Reports, 26*, 3429–3443. https://doi.org/10.1016/j.celrep.2019.02.081

81 Postic, C., Burcelin, R., Rencurel, F., Pegorier, J. P., Loizeau, M., Girard, J., & Leturque, A. (1993). Evidence for a transient inhibitory effect of insulin on GLUT2 expression in the liver: studies in vivo and in vitro. *The Biochemical journal*, *293*(1), 119–124. https://doi.org/10.1042/bj2930119

82 Hoffler, U., Hobbie, K., Wilson, R., Bai, R., Rahman, A., Malarkey, D., Travlos, G., & Ghanayem, B.I. (2009). Diet-induced obesity is associated with hyperleptinemia, hyperinsulinemia, hepatic steatosis, and glomerulopathy in C57Bl/6J mice. *Endocrine 36*(2), 311–325. doi:10.1007/s12020-009-9224-9

83 Gorovits, N., Cui, L., Busik, J.V., Ranalletta, M., Hauguel de-Mouzon, S., Charron, M.J. (2003). Regulation of hepatic GLUT8 Expression in Normal and Diabetic Models. *Endocrinology 144*(5), 1703–1711. doi:10.1210/en.2002-220968

84 Du, K. & Ding, J. (2009). Insulin regulates TRB3 and other stress-responsive gene expression through induction of C/EBPbeta. *Molecular Endocrinology 23*(4), 475–485, doi:10.1210/me.2008-028

85 Ai, D., Baez, J.M., Jiang, H., Conlon, D.M., Hernandez-Ono, A., Frank-Kamenetsky, M., Milstein, S., Fitzgerald, K., Murphy, A.J., Woo, C.W., Strong, A., Ginsberg, H.N., Tabas, I., Rader, D.J., & Tall, A.R. (2012) Activation of ER stress and mTORC1 suppresses hepatic sortilin-1 levels in obese mice. *The Journal of Clinical Investigation 122*(5), 1677–1687. doi:10.1172/JCI61248

86 Shimomura, I., Bashmakov, Y., Ikemoto, S., Horton, J. D., Brown, M. S., & Goldstein, J. L. (1999). Insulin selectively increases SREBP-1c mRNA in the livers of rats with streptozotocin-induced diabetes. *Proceedings of the National Academy of Sciences of the United States of America*, *96*(24), 13656–13661. https://doi.org/10.1073/pnas.96.24.13656

87 Yamashita, T., Hashiramoto, A., Haluzik, M., Mizukami, H., Beck, S., Norton, A., Kono, M., Tsuji, S., Daniotti, J.L., Wert, N., Sandhoff, R., Sandhoff, K., & Proia, R.L. (2003). Enhanced insulin sensitivity in mice lacking ganglioside GM3. *Proceedings of the National Academy of Sciences of the United States of America 100*(6), 3445–3449. doi:10.1073/pnas.0635898100

88 Zhang, W., Patil, S., Chauhan, B., Guo, S., Powell, D.R., Le, J., Klostas, A., Matika, R., Xiao, X., Franks, R., Heidenreich, K.A., Sajan, M.P., Farese, R.V., Stolz, D.B., Tso, P., Koo, S.H., Montminy, M., & Unterman, T.G. (2006). FoxO1 regulates multiple metabolic pathways in the liver: effects on gluconeogenic, glycolytic, and lipogenic gene expression. *The Journal of Biological Chemistry 281*(15), 10105-10117. doi:10.1074/jbc.M600272200

89 Chutkow, W. A., Patwari, P., Yoshioka, J. & Lee, R. T. Thioredoxin-interacting protein (Txnip) is a critical regulator of hepatic glucose production. *The Journal of Biological Chemistry 283*(4), 2397–2406, doi:10.1074/jbc.M708169200

90 Dong, X., Park, S., Copps, K., Yi, X., & White, M.F. (2006). Irs1 and Irs2 signaling is essential for hepatic glucose homeostasis and systemic growth. *The Journal of Clinical Investigation 116*(1), 101–114, doi:10.1172/JCI25735

91 Wang, D. & Sul, H. S. (1995). Upstream stimulatory factors bind to insulin response sequence of the fatty acid synthase promoter. USF1 is regulated. *The Journal of Biological Chemistry 270*(48), 28716–28722. doi:10.1074/jbc.270.48.28716

92 Sutherland, B. W., Kucab, J., Wu, J., Lee, C., Cheang, M.C.U., Yorifa, E., Turbin, D., Dedhar, S., Nelson, C., Pollak, M., Grimes, H.L., Miller, K., Badve, S., Huntsman, D., Blake-Gilks, C., Chen, M., Pallen, C.J., & Dunn, S.E. (2005). Akt phosphorylates the Y-box binding protein 1 at Ser102 located in the cold shock domain and affects the anchorage- independent growth of breast cancer cells. *Oncogene 24*(26), 4281–4292, doi:10.1038/sj.onc.1208590

93 Skawran, B., Steinemann, D., Weigmann, A., Flemming, P., Becker, T., Flik, J., Kreipe, H., Schlegelberger, B., & Wilkens, L. (2008). Gene expression profiling in hepatocellular carcinoma: upregulation of genes in amplified chromosome regions. *Modern Pathology, 21***,** 505–516. https://doi.org/10.1038/modpathol.3800998

94 Rebouissou, S., Imbeaud, S., Balabaud, C., Boulanger, V., Bertrand-Michel, J., Tercé, F., Auffray, C., Bioulac-Sage, P., Zucman-Rossi, J. (2007). HNF1alpha inactivation promotes lipogenesis in human hepatocellular adenoma independently of SREBP-1 and carbohydrate-response element-binding protein (ChREBP) activation. *Journal of Biological Chemistry, 282*(19), 14437–14446. https://doi.org/10.1074/jbc.M610725200

95 Pilati, C., Letouzé, E., Nault, J.C., Imbeaud, S., Boulai, A., Calderaro, J., Poussin, K., Franconi, A., Couchy, G., Morcrette, G., Mallet, M., Taouji, S., Balabaud, C., Terris, B., Canal, F., Paradis, V., Scoazec, J.Y., De Muret, A., Guettier, C., Bioulac-Sage, P., Chevet, E., Calvo, F., & Zucman-Rossi, J. (2014). Genomic Profiling of Hepatocellular Adenomas Reveals Recurrent FRK-Activating Mutations and the Mechanisms of Malignant Transformation. *Cancer Cell, 25*(4)*,* 428–441. https://doi.org/10.1016/j.ccr.2014.03.005